ABSTRACT

MARCHIN, RENÉE MICHELLE. Using a Physiological Approach to Improve Predictions of Climate Change Effects on Temperate Forests. (Under the direction of Dr. William A. Hoffmann.)

Evidence of climate change on Earth is unequivocal. Around the globe, air temperatures and ocean heat content are increasing, the extent of snow and ice is decreasing, sea levels are rising, and extreme climate events are more frequent. Temperature in the eastern US is expected to increase by 2–6 °C by 2100 and drought is projected to become more frequent and severe, yet it is uncertain how terrestrial ecosystems will respond to these climate changes.

This dissertation used a physiological approach to analyze plant species responses to increased temperature and drought in North Carolina. I utilized an experimental warming site in the understory of a temperate deciduous forest (Duke Forest, NC), where air temperature inside large open-top chambers was increased from 1.6–5.3 °C above ambient. Warming of 5 °C extended the growing season of four tree species by 20–28 days. Nonlinear responses of budburst phenology and failure to fully track warmer temperatures suggests that current high rates of phenological change are unsustainable and will decrease with warming throughout the coming century. Warming advanced flowering by 6–25 days in three of seven study species, but warming delayed flowering of *Tipularia discolor* by 10 days and had no effect on three species that flower in early spring. Warming of 2 °C inhibited reproduction of *Chimaphila maculata* and *T. discolor*, suggesting temperature thresholds that could severely limit the distribution of these species in the future.

Experimental warming negatively affected growth of the terrestrial orchid *T. discolor*, which is leafless in summer and acquires carbon primarily in winter. Like many plant

species, the optimum temperature for photosynthesis in *T. discolor* is higher than the maximum temperature throughout most of its growing season, and therefore growth should increase with warming. Warming of 4.4 °C resulted in nearly 60% less growth than under ambient conditions, however, likely due to restrictions in stomatal conductance (g_s). Leaf-to-air vapor pressure deficit (VPD) over 1.3 kPa restricted g_s of *T. discolor* to 10–40% of maximum conductance. Sensitivity of orchid stomata to VPD was higher than for most species in mesic ecosystems. These results highlight the need to account for changes in VPD when estimating temperature responses of plants under future warming scenarios.

Mean VPD was increased by 0.16–0.96 kPa inside the chambers as a consequence of heating. I used miniature sap flow gauges to measure the effect of atmospheric drying on transpiration and g_s of four common deciduous trees (*Acer rubrum*, *Carya tomentosa*, *Quercus alba*, *Quercus rubra*) throughout the growing season. Experimental warming for 3 years resulted in growth increases in *C. tomentosa* and *Q. alba* but not the other two species. Warming and increased VPD significantly decreased midday leaf water potential while increasing midday transpiration and daily water use, indicating that future climate change will increase the potential for temperature-induced drought stress.

I measured the physiology of transgenic black cottonwood (*Populus trichocarpa*) trees growing at two sites in NC: a cooler mountain site and a warmer piedmont site that experienced frequent water stress. Two low-lignin genotypes had significantly lower mean leaf water potential, g_s, transpiration, hydraulic conductivity, and leaf-specific whole-plant hydraulic conductance relative to the wild-type. The water transport capacity of vascular tissues in transgenic genotypes was severely impaired. Stunted growth of low-lignin trees at the piedmont site was caused by restricted carbon gain due to water stress and lower

biochemical and biophysical photosynthetic processes. Despite the fact that transgenic trees did not maintain lower lignin content at the mountain site, the genetic transformation resulted in a total water savings of roughly 1 kg tree^{-1} day^{-1} without sacrificing productivity.

Using a Physiological Approach to Improve Predictions of Climate Change Effects on Temperate Forests

by
Renée M. Marchin

A dissertation submitted to the Graduate Faculty of
North Carolina State University
in partial fulfillment of the
requirements for the degree of
Doctor of Philosophy

Plant Biology

Raleigh, North Carolina

2013

APPROVED BY:

_____	_____
William A. Hoffmann Committee Chair	Rob R. Dunn
_____	_____
John S. King	Jenny Xiang

BIOGRAPHY

Renée M. Marchin was born in Shawnee, Kansas in 1981 to parents Joseph and Denise Marchin. She graduated from high school in 1999 as one of the top students in her graduating class. Renée earned a B.S. in Environmental Science in 2003 from Texas Christian University in Ft. Worth, Texas and graduated *magna cum laude* with honors. During her undergraduate studies, she spent one semester studying environmental issues at the Biosphere II Center in Oracle, Arizona. Her friends joked that she left Texas "normal" but came back a hippie (this was probably mostly due to the fact that she became a vegetarian while she was gone). At the Biosphere, she learned to value "sustainable" living, and these ideas drove her along her future career path.

After graduation, Renée went to work for an environmental laboratory, Pace Analytical Services, Inc. in Lenexa, KS. She spent a year collecting and analyzing soil and water samples for pollutants by day, while reading biographies of environmental leaders by night. These people were her personal heroes, although she realized that her role in saving the environment would probably not be on the crusading front (she just could not see herself living for months in a tree or staring down the guns of seal poachers). Instead, she decided to begin her work as a research scientist.

Renée chose to study plant ecophysiology in graduate school, because she was interested in how climate change would affect terrestrial ecosystems. Renée earned a M.A. in Botany in 2003 from the University of Kansas in Lawrence, KS, where she worked with Dr. Joy Ward on a project investigating the potential of *Fraxinus americana* (white ash)

populations to adapt to climate change. She compared growth, survival, and physiological differences among 44 populations of 30-year-old trees growing in a common garden. Among populations originating within a narrow latitudinal band along an east–west gradient of decreasing precipitation, those from the drier western edge of the species range were best adapted to the dry climate of the common garden site. This suggests that eastern populations may not perform well under the hotter and drier climate conditions expected in the future.

Renée went to work for the Bureau of Land Management in northern California in 2006 after obtaining her Master's degree. In the intermountain west, the alteration of landscape disturbances by human activities has increased conifer encroachment and limited the presence of *Populus tremuloides* (quaking aspen) stands. She worked in conjunction with the Aspen Delineation Project and three BLM offices (Surprise, Alturas, Eagle Lake Field Offices) to monitor seedling regeneration and ungulate browse of aspen stands within a number of restoration projects on public lands. Restoration efforts of degraded aspen stands involved conifer removal, prescribed burning, and fencing.

Renée continued her work with research projects related to land management in 2006 when she became a research specialist under the direction of Dr. Bill Hoffmann at North Carolina State University in Raleigh, North Carolina. She examined whether differences in shade tolerance can explain rarity within the genus *Amorpha*. One species of *Amorpha* (*A. georgiana*) is listed as endangered in NC, and the land managers at Fort Bragg are involved in maintaining viable *Amorpha* populations. In another project, her lab group discovered that hydraulic failure and dieback of temperate forest tree species was associated with high wood density during extreme drought.

In 2009, Renée started her Ph.D. research at NC State University. Renée was awarded an EPA-STAR graduate fellowship in 2010 for her research proposal, "Assessing the hydrological costs of carbon sequestration in managed forests and biofuel plantations". After graduation from NC State University in 2013, Renée will move to Australia for a postdoc position with Dr. Mark Adams at the University of Sydney, where she will study how Australian plants cope with high radiation loads in the virtual absence of water.

ACKNOWLEDGEMENTS

First and foremost I would like to thank my advisor, Dr. Bill Hoffmann, for being a great mentor over the past seven years. How many advisors can conjure up equations off the top of their head? Or come up with the perfect wording for a paragraph in five minutes that you have been working on yourself for a month? Mine could! He has taught me a number of new skills over the years, including how to build a hydraulic conductivity apparatus out of an empty two liter soda bottle and some scrap tubing. I am eternally thankful that his door was always open whenever I needed help with a problem. I am also lucky that he gave me the freedom to pursue my own personal research interests.

Dr. Rob Dunn, my decision to enroll in graduate school for my Ph.D. is largely due to your willingness to include other researchers in your warming experiment. Much of the improvement in my oral and written communication skills can be attributed to your advice and excellent example. Dr. John King, it is through my work with your lab group that I have finally begun to learn something about forestry! As a tree physiologist, it was a field that I am thankful to have studied. Dr. Jenny Xiang, thank you for teaching me about plant taxonomy and systematics, as well as serving on my committee.

There are a number of other colleagues (past and present) of the Plant Biology department at NC State that I would like to thank. Dr. Sybil Gotsch, Dr. Erika Geiger, Dr. Wade Wall, and Dr. Jenny Schafer: I couldn't think of greater role models than you! Thanks for being great Brazilian tour guides, for identifying strange plants, for research advice, and most of all, for friendship over the years. The remainder of the Hoffmann lab group,

including Pam Abit, On Lee Lau, Alice Wines, Sam Swatling-Holcomb, Steph Hollingsworth, Michael Just, and Brad Breslow, I thank you for being the greatest group of co-workers that I have ever had the pleasure of conspiring with! I've enjoyed spending time outside work with all of you; there is probably no greater compliment than that. Steph Mixson, I'm glad that you and I served together as President and Vice President (respectively) of the Plant Biology Graduate Student Association. It was a great experience! I would also like to thank those individuals in the Dunn and King labs that I have collaborated with for my various dissertation chapters – Lauren Nichols, Aletta Davis, and Anna Stout. Without you emailing me various pieces of environmental data, field site information, and data collected in previous years, my dissertation could never have been completed.

Lastly, I would like to thank my family and friends. My family has always been there to support and love me, despite the fact that I live halfway across the country. Jill and Jason Braman, my family away from home – thank you for listening to all the trials of graduate school, for laughing and crying with me, for letting me sleep in your spare bed, and for all of the fun that we have had over the years. Laura Bostic, I couldn't have survived graduate school without all of our weekly lunches and our attempts at accountability of each other's monthly goals. Not to mention your very capable field assistance during our hot summer of sapflow measurements! Matt Clopper, thank you for believing in me and for being there to take care of me when I've been too busy to do it myself. I never say it enough, so thank you everyone!

TABLE OF CONTENTS

LIST OF TABLES

LIST OF FIGURES

CHAPTER 1

Climate change in the 21st century

1.1 Introduction

We live in an era of climate change caused in large part by the burning of fossil fuels. Many people in the United States continue to attribute global warming to natural causes, while others simply do not understand which side of the debate is correct. A recent Gallup poll indicated that only 34% of Americans believe that rising global temperatures are a result of human activities, whereas 47% think rising temperature is a result of natural causes (Ray & Pugliese, 2011). For comparison, 76% of people in developed Asia believe in anthropogenic climate change and 12% believe climate change has natural causes (Ray & Pugliese, 2011). When strangers learn that I am a climate change biologist, the first question that I am often asked is, "Is climate change really occurring?" I find this disheartening, because our nation must first accept responsibility for climate change before any significant changes to our policies will be made.

Most people prefer to think that the consequences of climate change are a problem that the next generation, and not OUR generation, will have to solve. But the truth is that we are already seeing the effects of climate change on Earth. The worst consequences of warming may occur decades after a given level of atmospheric greenhouse gases is reached.

Although today's oil and gas prices are at record highs, global energy demand continues to increase with world population growth and economic development. A major challenge for our society will be to provide energy and water to future generations. As atmospheric carbon dioxide (CO_2) concentrations continue to increase, global action is needed to minimize the negative impacts of climate change and avoid putting the future of our civilization at risk.

I have dedicated my career to the study of climate change issues in the US. This dissertation describes potential changes in the phenology and physiology of temperate forest species in response to experimental warming in North Carolina. I also provide two case studies of climate change impacts on plant species in the southeastern US (an orchid, *Tipularia discolor*, and a tree, *Populus trichocarpa*). It is important for us to take steps to mitigate these potential impacts of climate change, because continuing to live our lives under a business-as-usual scenario will have disastrous impacts on natural ecosystems.

"*It is not necessary to change. Survival is not mandatory.*"

– William Edwards Deming

1.2 Climate Change in the Past

Current atmospheric CO_2 concentrations and global temperatures are not at their historic highs and have fluctuated greatly over geologic time (Figure 1.1). Over the last 65 million years, Earth's climate has shifted from extremes of expansive warmth with ice-free poles to extremes of cold with massive continental ice sheets and polar ice caps (Zachos *et al*., 2001). This knowledge of past climate fluctuations was obtained from measurement of oxygen and

carbon isotope concentrations of benthic foraminifera in deep-sea sediment cores. Air bubbles and dust particles trapped in ice cores also provide information about past climate changes, although these records only extend back 800,000 years before the present (Petit *et al*., 1999; Lambert *et al*., 2008). Here I review some of the major climate changes over geologic time, because a better understanding of these large swings in Earth's climate may help to provide insight into how future climate change will progress.

During the late Paleocene epoch, 55 million years ago, there was a large shift in Earth's climate that was in some ways analogous to present-day climate change. The climate had been slowly warming when there was an influx of 1500-4500 billion metric tons of carbon to the ocean and atmosphere over perhaps 1000 years (Zachos *et al*., 2005). The same amount of carbon is projected to enter the climate system by the end of the 21st century, if human use of fossil fuels continues at the current pace (Mathez, 2009). During the **Paleocene-Eocene Thermal Maximum** (PETM), as it has become known, global mean surface temperature rose 5–9 °C as atmospheric CO_2 content increased and the oceans acidified (Bowen *et al*., 2006). The source of the carbon is unknown, but because the sudden release was preceded by warming, there is the alarming possibility that a warming climate may reach a threshold that triggers a much more dramatic shift (Mathez, 2009). The climate throughout the PETM remained warm for around 120,000 years. The return to cooler conditions occurred over a period of about 40,000 years, as the rate of silicate weathering increased, which drew down atmospheric CO_2 and increased the bicarbonate content of the ocean. This timescale may represent the natural recovery time of the global carbon cycle to short-term perturbations (Mathez, 2009).

The PETM is only one example of a dramatic shift in Earth's climate. Large, abrupt climate changes have occurred repeatedly in the past, when the Earth has been forced across some threshold (Alley *et al*., 2003). One of the most dramatic perturbations to the Earth system was the rapid onset of **Antarctic glaciation** near the Eocene/Oligocene boundary, 34 million years ago (Figure 1.1). This phenomenon was preceded by a 17-million-year cooling trend, where deep-sea temperature declined by 7 °C (Zachos *et al*., 2001). The leading explanation for the rapid glaciation is that the associated sea-level fall increased silicate weathering and orbital forcing (see below) inhibited warm Antarctic summers, which triggered a chain of carbon cycle responses (Merico *et al*., 2008). Among those responses was a decrease in global atmospheric CO_2 concentration from approximately 1000–2000 ppm at the end of the Eocene to lower levels in the early Oligocene (Merico *et al*., 2008).

Over the past 15 million years, the climate of Earth has been gradually cooling (Figures 1.1, 1.2). Climate records from the Pliocene (5.3 million to 1.8 million years ago) and Pleistocene (1.8 million to 11,600 years ago) epochs are fairly complete (Figure 1.2). From about 5 to 3 million years ago, the mean global temperature was 2–3 °C warmer than today (Mathez, 2009). Ice covered eastern Antarctica but there was no ice cap in the Northern Hemisphere, and sea level was 15–25 meters higher than today (Mathez, 2009). Beginning about 3 million years ago, an ice cap became established in the Northern Hemisphere for the first time in nearly 200 million years.

During this long period of gradual cooling, the ice sheets periodically advanced and retreated in a continuous cycling pattern. Known as the **Ice Ages**, these cycles occurred with regularity at approximately 41,000-year intervals from about 2.7 million to 1 million years

ago (Lisiecki & Raymo, 2005; Figure 1.2). After that, the cycles started to become less frequent, with long glacial periods that lasted on average about 80,000–90,000 years alternating with shorter interglacial periods that lasted about 10,000 years (Figure 1.2). The difference in temperature at the surface of the Earth between glacial–interglacial cycles ranges from 5–12 °C (Petit *et al*., 1999; Alley *et al*., 2003). Throughout the past 420,000 years, atmospheric CO_2 concentration ranged from 170−300 ppm, and periods of higher atmospheric CO_2 and methane correlate well with periods of warmer Antarctic air temperature (Petit *et al*., 1999).

The high regularity of these ice-age cycles are caused by changes in Earth's orbit around the sun, or *orbital forcings*, as theorized by the Serbian mathematician Milankovitch (Mathez, 2009). Orbital forcings strongly influence climate by changing the amount and seasonality of solar radiation received at different locations on Earth. There are three orbital perturbations with five periods (Zachos *et al*., 2001): eccentricity (at 400,000 and 100,000 years), obliquity (41,000 years), and precession (23,000 and 19,000 years). Eccentricity refers to the shape of the Earth's orbit about the sun, which varies from near circular to elliptical, and has only a weak effect on insolation. Obliquity refers to the tilt of the Earth's axis relative to the solar plane varying between 22.1° and 24.5°, where a high angle of tilt increases the seasonal contrast of both hemispheres (i.e. as obliquity increases, winters will be colder and summers will be hotter), most effectively at high latitudes. Precession refers to the wobble of the axis of rotation of Earth, just as a spinning top may slowly rotate around a second axis. Precession increases the seasonal contrast in one hemisphere while decreasing it in the other, which controls the duration of the seasons.

The ice sheets were most recently at their maximum extension (i.e. the **Last Glacial Maximum**) from 26,500 to 19,000 years ago, and sea levels were about 130 meters lower than today (Clark *et al*., 2009). The retreat of the glaciers around 20,000–19,000 years ago was caused by an increase in northern summer insolation (Clark *et al*., 2009). The **Younger Dryas** (12,900–11,600 years ago) was a brief return to glacial conditions marked by extremely rapid climate transitions, where temperature changes of 7 °C occurred over a period of a few decades or less (Mathez, 2009). This abrupt shift was more rapid than any climate change experienced since the rise of human civilization. One theory to account for the rapid climate change is that Lake Agassiz, an enormous lake covering part of Canada, burst its ice dam to release a vast amount of freshwater into the North Atlantic (Broecker & Denton, 1990). This influx prevented the increase in salinity and density that is necessary to drive circulation of deep ocean currents in the North Atlantic. The Younger Dryas ended when the freshwater input dwindled, thus restoring flow to the global ocean conveyer system and allowing the Gulf Stream to deliver warm surface water from the tropics.

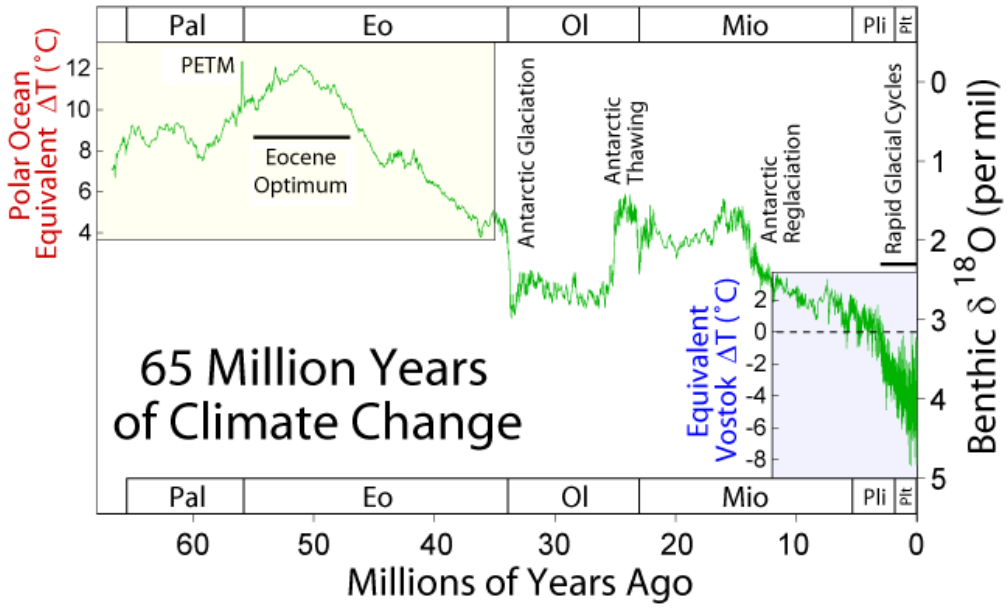

Figure 1.1 Climate changes over the last 65 million years, as obtained from oxygen isotope measurements of benthic foraminifera (Zachos *et al*., 2001). Figure created by: RA Rohde, Global Warming Art.

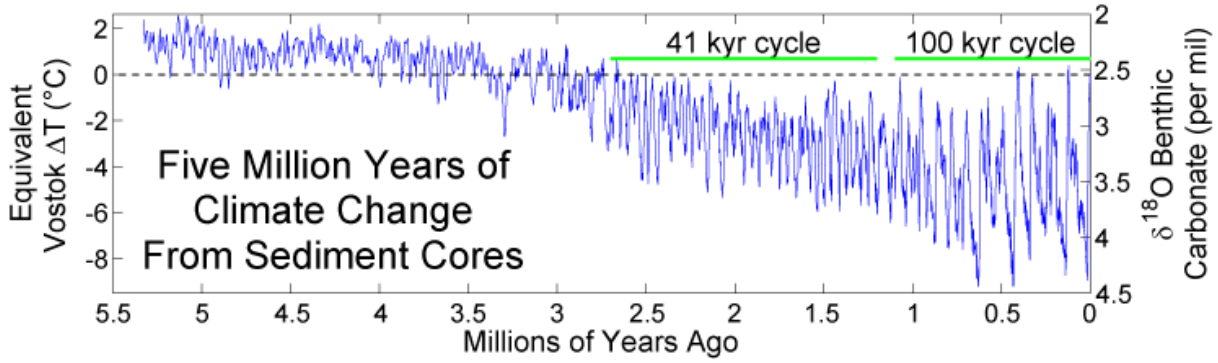

Figure 1.2 Climate changes over the last 5 million years, as obtained from oxygen isotope measurements of benthic foraminifera (Lisiecki & Raymo, 2005). The temperature scale approximates temperature variations at Lake Vostok (Petit *et al*., 1999), while the horizontal dotted line indicates modern temperatures (circa 1950). Figure created by: RA Rohde, Global Warming Art.

1.3 Observations of Global Climate Change

Over the past 650,000 years, global atmospheric CO_2 concentration has remained below 300 ppm (IPCC, 2007). Human activities, primarily through fossil fuel use and land-use change, have caused the atmospheric CO_2 concentration on Earth to increase from a pre-industrial value of about 280 ppm to 396 ppm in 2013. Evidence of climate change has been documented around the globe, including increases in global temperature and ocean heat content, decreases in the extent of snow/ice, and sea-level rise. Long-term changes in extreme climate events have also been observed, such as increases in the frequency and intensity of drought, increases in the number of heavy precipitation events, and more intense cyclone activity (IPCC, 2007).

Surface air temperature has been approximately constant throughout the last two millennia, until global temperatures began steadily increasing in the 20th century (Figure 1.3). From 1850 to 2005, global temperature increased by 0.76 °C, and within the last 50 years, the decadal rate of warming has almost doubled from 0.07 to 0.13 °C per decade (IPCC, 2007; Gautier, 2008; Figure 1.4). This rate of warming is very rapid and can only be fully reproduced when human forcings are included in global climate model simulations (Crowley, 2000; Figure 1.4). Nights have warmed more than days, an observation that is consistent with greenhouse gas buildup as the cause of global warming (Mathez, 2009). A widespread reduction in the number of frost days has been observed in mid-latitudes, and summer heat waves have occurred more frequently, particularly in Europe (Gautier, 2008). The summer of 2003 in Europe was the hottest since at least 1500, and the unanticipated heat wave is said to have killed 22,000−45,000 people in a 2-week period (Patz *et al*., 2005).

The oceans have been warming at a lower rate than land surfaces and are estimated to have warmed down to a depth of 3000 m by an average of 0.037 °C per decade from 1955 to 1998 (Mathez, 2009). Surface air temperatures in the Arctic have warmed by 2 °C since the mid-1960's, which is faster than warming over the rest of the globe (Overland *et al*., 2012). As a consequence, late summer ice cover in the Arctic Ocean has been decreasing at a rate of 3% per decade since the 1980's (Gautier, 2008). In 2012, Arctic sea ice extent declined to a record minimum of 49% below the 1979–2000 average (Perovich *et al*., 2013). Due to increases in melting snow/ice and to thermal expansion of the ocean, global sea levels rose about 20 cm during the 20^{th} century (IPCC, 2007). The world's oceans are not only warming and rising, but also becoming more acidic. As a result of uptake of atmospheric CO_2 by the oceans, there was a 30% increase in the concentration of H^+ in ocean surface waters during the 1900's (IPCC, 2007).

Warmer climates are expected to enhance the hydrologic cycle by increasing precipitation and evaporation (Jackson *et al*., 2001; Karl *et al*., 2009). Global mean precipitation has increased by 7.4 ± 2.6% per °C from 1987 to 2006 (Mathez, 2009), and atmospheric water vapor content has also increased since the 1980's (IPCC, 2007). In the US, precipitation has increased by an average of 5% over the past 50 years (Karl *et al*., 2009). The majority of global evaporation comes from the oceans (86%) and from 1987–2006, global ocean evaporation increased by 1.3% per decade (Wentz *et al*., 2007). Ocean evaporation depends heavily on non-atmospheric processes such as ocean heat flux, but terrestrial evaporation is controlled by completely different processes (Ohmura & Wild, 2002). Rates of evapotranspiration over land depend on meteorological conditions, such as

atmospheric demand and water availability, as well as land cover conditions. Evapotranspiration is one of the most difficult climate system variables to observe, and therefore global estimates of evapotranspiration have a high degree of uncertainty (Jung *et al*., 2010).

There has recently been a debate in the literature, termed the "pan evaporation paradox", over whether global terrestrial evaporation is increasing (as expected in a wetter, warmer world) or decreasing. The debate began with a report of decreased pan evaporation (i.e. the rate of evaporation from an open pan of water installed in the field) over the past 50 years at multiple sites around the globe (Peterson *et al*., 1995) and was further corroborated by research at other sites (Liu *et al*., 2004; Fu *et al*., 2009). The "paradox" refers to the deviation of observation from expectation and is further confused by the inconsistent instrumentation and methods for measurement of pan evaporation (Fu *et al*., 2009). A recent review of the paradox concluded that the overall decreasing trend in pan evaporation is not universal around the globe, as several climate stations have reported significant increases in pan evaporation (Fu *et al*., 2009). Despite the intriguing controversy surrounding the pan evaporation paradox, the trend in actual evaporation is ultimately more important (Ohmura & Wild, 2002).

The most comprehensive synthesis of global trends in terrestrial evapotranspiration combined *in situ* measurements, meteorology, and remote sensing information to conclude that global annual land evapotranspiration increased on average by 7.1 ± 1.0 mm yr^{-1} per decade from 1982 to 1997 (Jung *et al*., 2010). Coincident with an El Niño event in 1998, however, this global evapotranspiration increase seems to have ceased. The change is driven

primarily by moisture limitation in the Southern Hemisphere, particularly Africa and Australia (Jung *et al*., 2010). It is hard to evaluate whether this is natural climate variability or a climate-change signal in which land evapotranspiration becomes more and more supply limited in the long-term (Jung *et al*., 2010). The answer to this question has serious implications for the future behavior of terrestrial ecosystems. If global evapotranspiration has already reached its maximum limit, terrestrial productivity may decrease in the future, leading to accelerated land-surface warming and an intensified regional land–atmosphere feedback (Jung *et al*., 2010).

On a global scale, the world is indeed becoming warmer and wetter. Some of the most severe impacts of climate change may not result from these shifts in mean climate conditions over time, however, but from changes in extreme climate events (Katz & Brown, 1992; Jentsch *et al*., 2007). Very strong hurricanes (Category 4 and 5) increased in frequency after 1970, although the total number of hurricanes has remained essentially constant (Webster *et al*., 2005). Higher atmospheric moisture results in more intense precipitation events and flooding, but the rainfall events are shorter and more infrequent, causing the incidence of drought to increase (IPCC, 2007; Figure 1.5). The global total land area that can be classified as very dry (i.e. a Palmer Drought Severity Index < –3.0) increased from 12 to 30% since 1972 (Dai *et al*., 2004b). Recent large-scale and severe droughts occurred in Europe in 2003 (Ciais *et al*., 2005), western North America for the last decade (Cook *et al*., 2004; Allen *et al*., 2010), the Sahel region of Africa from the 1960's to the present (Dai *et al*., 2004a), Amazonia in 2005 (Marengo *et al*., 2008), and Australia in 2002–2003 (Nicholls, 2004). Reports of widespread tree mortality appear to be on the rise globally (Zeppel *et al*.,

2011), with large-scale tree dieback occurring on all wooded continents (van Mantgem *et al*., 2009; Allen *et al*., 2010). Drought-induced declines in productivity were observed recently in European temperate forests (Ciais *et al*., 2005) and the Amazon rainforest (Phillips *et al*., 2009).

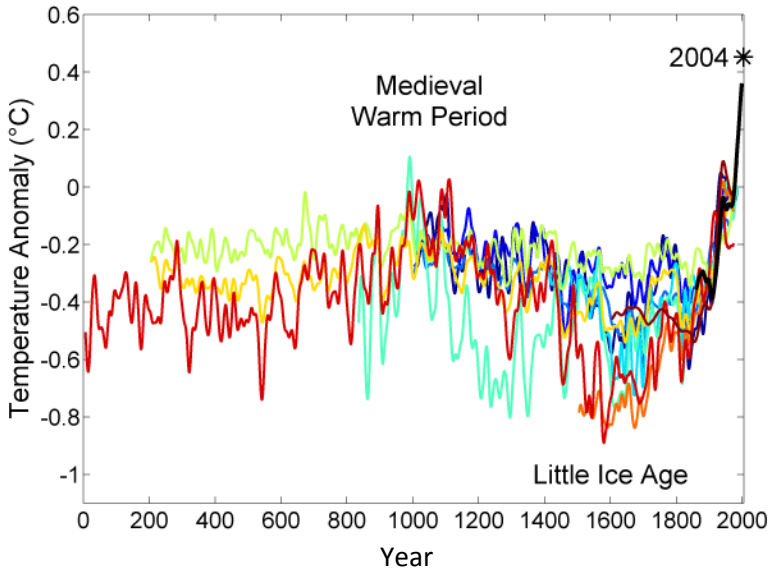

Figure 1.3 Mean temperature changes during the last 2000 years as reconstructed from tree rings, ice cores, and corals (colored lines) and black (instrumental record). Figure created by: RA Rohde, Global Warming Art.

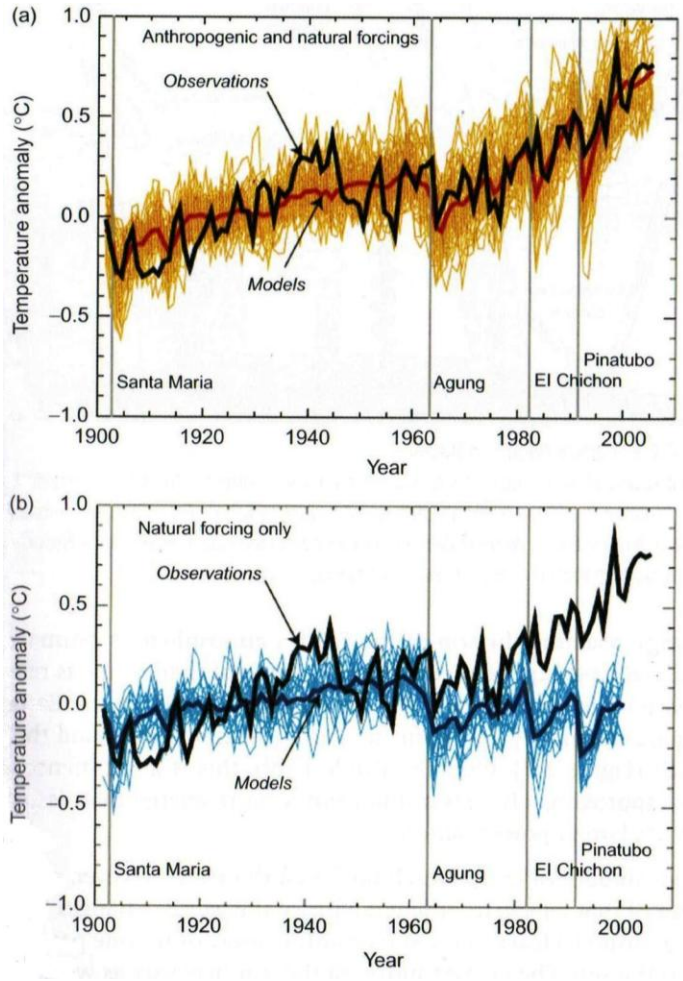

Figure 1.4 (a) Mean temperature projections from global climate model (GCM) simulations (colored lines) show that the actual temperature record (black line) can only be fully reproduced when human forcings, primarily burning of fossil fuels and deforestation, are included in the GCM simulations. (b) Models solely driven by natural forcings, such as solar variability and volcanic events, do not replicate observed temperature changes. Figure from: (IPCC, 2007).

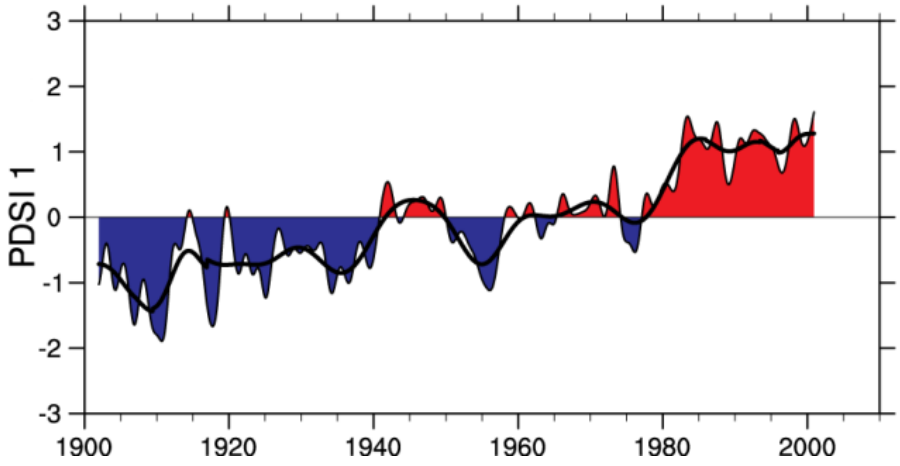

Figure 1.5 The change in globally averaged Palmer Drought Severity Index from 1900–2002. The PDSI is a measure of soil moisture based on precipitation and temperature records. Red is drier and blue is wetter than average; the black line is the 10-year running average. Figure created by: UCAR. Figure data from: (Dai *et al*., 2004b; IPCC, 2007).

1.4 Future Climate Predictions and Uncertainties

Today's most complex global climate models (GCMs) predict future climate change by incorporating the coupled circulation of the atmosphere and ocean with other important features of the climate system, such as land surfaces, ice, and snow. Model simulations of future changes in global temperature are thought to be realistic, primarily because the models accurately simulate temperature changes over the past 100 years (Crowley, 2000; Figure 1.4). The models predict that global temperature will increase by 1.8−4.5 °C by 2100 (IPCC, 2007; Figure 1.6), depending on future rates of greenhouse gas emissions. This is an important caveat, as there is more uncertainty associated with predicting future global CO_2 concentration than future global temperature (Mathez, 2009).

Greenhouse gas emission projections are generated based on assumptions regarding a number of unknown factors, such as world population growth, socioeconomic development, technological changes, and future global energy usage (Gautier, 2008). The IPCC has defined three emissions scenarios to cover a wide range of future possibilities (Figure 1.6), from high emissions (A2) to moderate emissions (A1B) to low emissions (B1). Based on scenario A2, a recent synthesis of 11 global climate–carbon cycle models found that atmospheric CO_2 concentration in 2100 is predicted to range from 730−1020 ppm (Friedlingstein *et al.*, 2006). This atmospheric CO_2 concentration is higher than at any time in at least the past 800,000 years, and the current rate of CO_2 increase is 100 times faster than the mean rate of CO_2 change during past glacial–interglacial cycles (1.4 ppm yr^{-1} from 1960–2005 vs. 0.01−0.02 ppm yr^{-1}, respectively; Mathez, 2009).

The nature of the relationship between the atmosphere, land, and ocean is currently changing (Alley *et al*., 2003; IPCC, 2007), and there is large uncertainty in how the climate system of Earth will respond. In the words of climate scientist Wallace Broecker, "The climate system is an angry beast, and we are poking it with sticks." All global biogeochemical processes will be operating beyond the bounds of natural atmospheric composition, and it is unclear if these processes will continue to operate in the same manner now as they have in the past. Even the most sophisticated climate models have inherent uncertainties, because there are feedbacks in the climate system that are simply unpredictable at present. Feedback mechanisms can have positive or negative effects on global warming (i.e. enhance a disturbance and cause additional warming above the direct effect of increasing greenhouse gases, or dampen a disturbance and stabilize climate, respectively) and continue to operate until a new equilibrium in climate has been achieved.

Some of the key sources of remaining uncertainty in climate change predictions include: the interactions and feedbacks between clouds and radiative energy transfer, the interactions between the atmosphere and the oceans, the dynamics of ocean circulation, the stability of the large ice sheets on Greenland and Antarctica, and the role of aerosols in the climate system (Gautier, 2008). These topics are important priorities for future research on climate change, but they are outside the scope of the present discussion. Instead, I shall concentrate on a more relevant topic to this dissertation – the uncertainty between future climate change and the global carbon cycle.

The Carbon Cycle

Most carbon on the Earth's surface (>99.9%) is sequestered in sedimentary rocks or in the ocean (50×10^6 metric GtC, 39×10^3 GtC, respectively; Kump *et al*., 2010). The total carbon contained in other surface reservoirs, such as soil, living biomass, and the atmosphere, is less than 4×10^3 GtC (Kump *et al*., 2010). A close long-term balance has existed between the rock reservoir and the surface reservoirs for millions of years, where the formation of carbonate and organic-carbon rocks is balanced by the release of carbon from subduction, thermal decomposition in the deep Earth, and volcanic eruptions (Mathez, 2009). The natural processes that sequester carbon into the rock reservoir, however, operate much more slowly than the rate at which we are liberating CO_2 through the burning of fossil fuels.

Over timescales of decades to millennia, the ocean is the primary regulator of CO_2 in the atmosphere. Ocean uptake of carbon is expected to continue to increase throughout the 21st century (Friedlingstein *et al*., 2006; Figure 1.7). It is uncertain, however, if carbon uptake by terrestrial plant ecosystems will increase or decrease over the next 100 years (Friedlingstein *et al*., 2006; Figure 1.7). Factors complicating the estimation of future global carbon uptake by land surfaces include uncertainties of changes in land use, regional climate patterns affecting productivity of plant ecosystems, and climate–carbon cycle feedbacks.

Carbon dioxide emissions from land use change were estimated to be approximately 25% of total CO_2 emissions during the 1990's (1.6 ± 1.1 GtC yr^{-1} vs. 6.4 ± 0.4 GtC yr^{-1}, respectively; IPCC, 2007), largely due to deforestation in the tropics. Such estimates are highly variable, because there is high uncertainty in the annual land area affected by different types of land use change (Houghton & Goodale, 2004). Forests of the northern mid-latitudes

are currently a carbon sink, accumulating anywhere from 0.03−2.1 GtC yr^{-1} during the 1990's (Houghton & Goodale, 2004). It is unclear whether this carbon sink is driven by forest regrowth following harvest, enhanced growth due to changing environmental conditions, or some combination of both factors.

Elevated CO_2 should enhance the productivity of plants on a global scale (Ward & Kelly, 2004), but future increases in plant growth rate may be limited by the local availability of water, nutrients, or co-occurring pollutants (King *et al*., 2005). Changes in water availability depend critically upon uncertain regional aspects of climate change projections and are therefore a dominant source of uncertainty (Friedlingstein *et al*., 2006). Furthermore, the rate of respiration by plants is typically assumed to increase with temperature, but there is an ongoing debate about the extent of acclimation of respiration to higher temperatures (Knorr, 2000). Climate models predict that there will be a positive feedback between the climate and global carbon cycle, where future climate change will increase the fraction of anthropogenic CO_2 emissions that remain in the atmosphere (Friedlingstein *et al*., 2006). By 2100, this additional CO_2 gain ranges between 20−200 ppm and corresponds to an additional warming of 0.1−1.5 °C (Friedlingstein *et al*., 2006).

Distinguishing between the two explanations for the terrestrial carbon sink in the northern mid-latitudes (regrowth vs. enhanced growth of forests) is necessary for predicting whether terrestrial carbon uptake can be expected to continue in the future (Houghton & Goodale, 2004). Although uncertainty persists in how the global carbon cycle will operate in a warmer, more CO_2-rich world, the natural processes of that cycle are clearly incapable of absorbing all 7.2 ± 0.3 GtC yr^{-1} that are now being injected into the atmosphere (IPCC,

2007). Even if greenhouse gas emissions were to stop at their present level, Earth's surface temperature would continue to rise for several decades due to inertia in the climate system (Gautier, 2008) and would not drop significantly for at least 1000 years (Solomon *et al*., 2009).

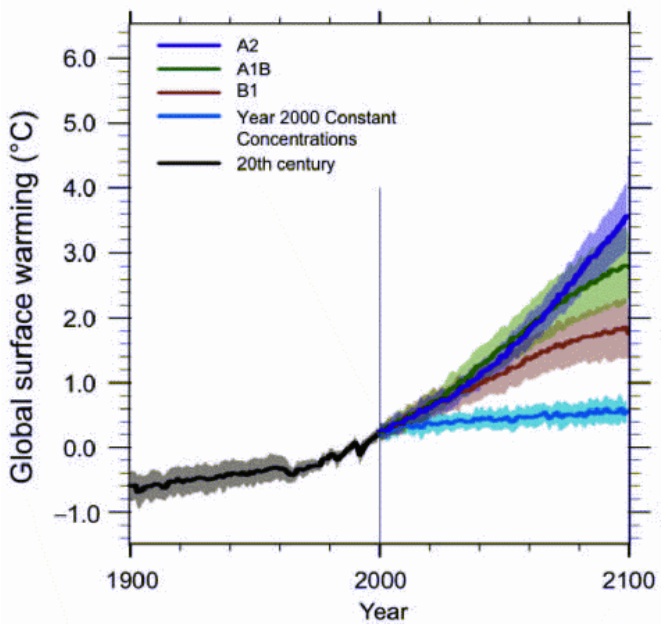

Figure 1.6 Global temperature projections to the year 2100, predicted by 23 climate models. The heavy line is the mean, and the shading refers to the ±1 standard deviation. Emission scenario A2 represents high growth, A1B represents moderate growth, and B1 represents low growth. Figure from: (IPCC, 2007).

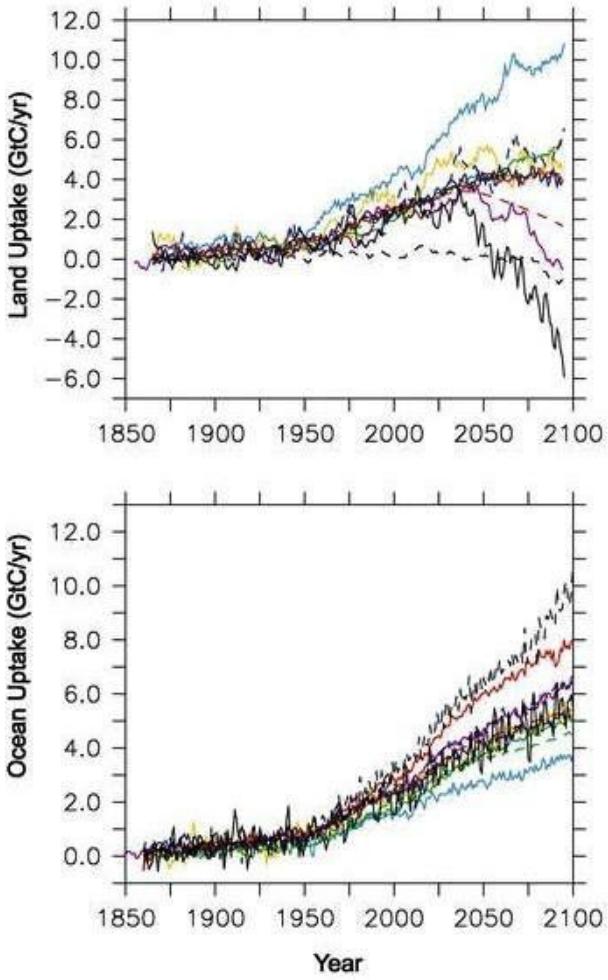

Figure 1.7 Global land carbon fluxes (GtC yr^{-1}) and ocean carbon fluxes (GtC yr^{-1}) as simulated by HadCM3LC (solid black), IPSL-CM2C (solid red), IPSL-CM4-LOOP (solid yellow), CSM-1 (solid green), MPI (solid dark blue), LLNL (solid light blue), FRCGC (solid purple), UMD (dash black), UVic-2.7 (dash red), CLIMBER (dash green), and BERN-CC (dash blue). Figure from: (Friedlingstein *et al*., 2006).

1.5 The Physiological Approach

Early studies in the field of plant ecophysiology demonstrated that stomata provide a major resistance to the passage of water through vegetation (Jarvis, 1976). More than a third of the CO_2 in the atmosphere is exchanged annually with the terrestrial biosphere through stomata (Farquhar *et al*., 1993; Ciais *et al*., 1997). The need to better quantify the global response of terrestrial ecosystems to climate change has driven the development of fully integrated dynamic global vegetation models (DGVMs) over the past two decades. These models are designed to fit in the framework of existing global climate and land models (Levis *et al*., 2004) and combine natural vegetation dynamics with land–atmosphere carbon and water exchanges to predict how natural ecosystems will respond to future climate change (Sitch *et al*., 2003).

In most DGVMs, vegetation within a grid cell is classified according to plant functional type (PFT), such as tropical broadleaf deciduous, temperate needleleaf evergreen, or herbaceous (Table 1.1). These PFTs are used instead of species to generalize plant structure and function to the global scale, where the concept of an *average* individual is used to increase computational efficiency (Levis *et al*., 2004). The fundamental entity for a woody PFT in the Lund–Potsdam–Jena DGVM (LPJ), for example, is an individual tree defined by its average crown area, leaf mass, sapwood mass, heartwood mass, and fine root mass, which are constrained by biomass allometric equations (Sitch *et al*., 2003). Each PFT is further described by physiological and bioclimatic limits (e.g. minimum canopy conductance, fire resistance, leaf longevity, minimum temperature for survival, minimum degree-day sum for establishment, etc.; Table 1.1) which determine whether it can survive under the climatic

conditions of a grid cell at a particular time in the simulation. Thus, a set of processes operating at the individual plant level can be scaled up to the 'population' level based on fractional coverage of PFTs in a grid cell (Sitch *et al*., 2003).

The current PFT classification system is rather simple and requires further development, particularly in the area of plant responses to drought. Water stress effects on plants are represented by only simplistic responses of stomatal conductance and/or gas exchange, despite a relatively good mechanistic understanding of how plants move water and a large body of observations on the relationship between leaf water status and stomatal conductance (R.A. Fisher, National Center for Atmospheric Research, 2011 April 4). Arguably the most advanced DGVM incorporation of plant hydraulic traits is by Hickler *et al.* (2006), who included the concept of soil-to-leaf plant water supply limiting evapotranspiration if the rate of supply is less than atmospheric demand. This relatively simple advance has not been adopted and highly simplistic representations of water stress on plants remain the norm in land surface models (R.A. Fisher, National Center for Atmospheric Research, 2011 April 4). A better understanding of plant physiology, ecological processes, and ecosystem dynamics can be used to improve the current PFT classification system.

A physiological approach has already led to some interesting discoveries that could potentially improve the accuracy of DGVM predictions. Climate-induced trembling aspen forest mortality in western North America was found to be caused by hydraulic failure of roots and branches, with no depletion in carbohydrate reserves prior to death (Anderegg *et al*., 2012). Warmer temperatures are also implicated as a cause of drought stress in this species, as elevated growth temperature was found to alter hydraulic traits of seedlings via

increased whole plant conductance and vulnerability to cavitation in leaves (Way *et al*., 2012). During drought-induced mortality of piñon pine, however, no hydraulic changes were observed at higher temperatures (Adams et al., 2009b). Instead, the earlier death of piñon pine trees was associated with higher respiration rates in trees growing under warmer conditions, possibly driving trees below their zero-carbon assimilation point (Adams et al., 2009a). Species differences, which are currently neglected in DGVMs, may be locally important in driving community responses to increased temperature and drought.

This dissertation uses a physiological approach to examine potential climate change effects on plant species in North Carolina, USA. Species responses to increased temperature and drought were analyzed separately at different sites. To test the response of species to increased temperature, I used an experimental warming site in the understory of a temperate deciduous forest (Duke Forest, Hillsborough, NC), where air temperature inside large, open-top chambers was increased from 1.6–5.3 °C above ambient. Precipitation or humidity was not directly manipulated at this site, so I utilized a different experiment to examine the effect of drought on trees. Genetically modified cottonwood trees were planted at two sites of differing drought intensity to test the suitability of the species as a biofuel crop in NC. The four chapters of this dissertation address different future challenges to our society, and the general question for each chapter is described below.

Table 1.1 Plant functional type (PFT) parameter values of the LPJ dynamic global vegetation model: z_1 and z_2, fraction of fine roots in the upper and lower soil layers, respectively; g_{min}, minimum canopy conductance; r_{fire}, fire resistance; a_{leaf}, leaf longevity; f_{leaf}, $f_{sapwood}$, f_{root}, leaf, sapwood, and fine root turnover times, respectively; $T_{mort,min}$, temperature base in the heat damage mortality function; S_{GDD}, growing degree-day requirement to full leaf coverage. Table from: (Sitch et al., 2003).

PFT	W/H*	z_1 (–)	z_2 (–)	g_{min} (mm s^{-1})	r_{fire} (–)	a_{leaf} (yr)	f_{leaf} (yr^{-1})	$f_{sapwood}$ (yr^{-1})	f_{root} (yr^{-1})	$T_{mort,min}$ (°C)	S_{GDD} (°C)
Tropical broad-leaved evergreen (TrBE)	W	0.85	0.15	0.5	0.12	2.0	0.5	0.05	0.5	–	–
Tropical broad-leaved raingreen (TrBR)	W	0.70	0.30	0.5	0.50	0.5	1.0	0.05	1.0	–	–
Temperate needle-leaved evergreen (TeNE)	W	0.70	0.30	0.3	0.12	2.0	0.5	0.05	0.5	–	–
Temperate broad-leaved evergreen (TeBE)	W	0.70	0.30	0.5	0.50	1.0	1.0	0.05	1.0	–	–
Temperate broad-leaved summergreen (TeBS)	W	0.80	0.20	0.5	0.12	0.5	1.0	0.05	1.0	–	200
Boreal needle-leaved evergreen (BoNE)	W	0.90	0.10	0.3	0.12	2.0	0.5	0.05	0.5	23	–
Boreal needle-leaved summergreen (BoNS)	W	0.90	0.10	0.5	0.12	0.5	1.0	0.05	1.0	23	100
Boreal broad-leaved summergreen (BoBS)	W	0.90	0.10	0.3	0.12	0.5	1.0	0.05	1.0	23	200
Temperate herbaceous (TeH)	H	0.90	0.10	0.5	1.00	1.0	1.0	–	0.5	–	100
Tropical herbaceous (TrH)	H	0.90	0.10	0.5	1.00	1.0	1.0	–	0.5	–	100

*W = Woody; H = Herbaceous.

1.6 Challenges to our Society

The human population on Earth is currently 7.028 billion and is projected to reach 9.3 billion by 2050 (US Census Bureau, 2012). Given this alarming rate of world population growth, it is going to be a major challenge to provide food, water, and energy to all people on Earth, even without considering the consequences of climate change. Estimates of energy supply versus consumption indicate the middle of this century as the critical point when energy supply will no longer keep pace with demand (Lee & Saw, 2011). If energy supplies prove inadequate for the growing world population, then population growth is expected to stagnate or even drop (Lee & Saw, 2011). A popular projection scenario, therefore, is to assume that the future world population will stabilize at around 10 billion people.

It is difficult to imagine how the future world will look and how a stable population of 10 billion people will be living. Nobel laureate Henry W. Kendall warned, "If we don't halt population growth with justice and compassion, it will be done for us by nature – brutally and without pity – and will leave a ravaged world." There are many challenges that our society will face in the coming decades. The first challenge will be to increase education and public awareness that major climate change on Earth has already begun and will continue after atmospheric greenhouse gas concentrations stabilize. Climate change is a global problem and mitigating the effects of climate change will take a global response. **The first chapter of this dissertation addresses an ideal topic for raising public awareness of climate change – the biological evidence of shifts in plant phenology (i.e. the developmental timing of organisms), which can be observed in urban settings and natural ecosystems.**

The remaining chapters of this dissertation investigate very specific questions within the much larger problems that we will face on Earth in the future, or in other words, are small pieces of a big puzzle. Conserving biodiversity and maintaining healthy ecosystems in a shifting climate should be a top priority for society. Some believe that since abrupt climate shifts have occurred in the past without causing any massive, broad-scale extinctions, species are probably more resilient than anticipated in most model assessments of the effect of modern climate change on biodiversity (Hof *et al*., 2011). Because habitat destruction and fragmentation are also serious threats to Earth's biodiversity today, however, there is considerable reason to be concerned with how current climate change is affecting ecosystems (Hof *et al*., 2011). **The second chapter of this dissertation addresses how climate change will affect physiology, growth, and reproduction of *Tipularia discolor* (crippled cranefly), a terrestrial orchid species commonly found in the understory of eastern temperate forests.**

It is important to improve predictions of climate change effects on natural ecosystems at a regional scale, which is necessary for developing the best land management practices for a given region. *In situ* warming experiments are arguably the best method for understanding plant responses to temperature increases, but they suffer from the confounding of temperature and atmospheric drought effects. As ambient air is simply warmed (with no humidity control) prior to circulation in an experimental chamber, there is an increase in vapor pressure deficit (VPD) of the air. The warmest chambers therefore also have the driest air; a temperature increase of 5.3 °C caused a VPD increase of 0.96 kPa in Duke Forest, NC. Because VPD is the driving force determining rates of transpiration, the confounding of VPD

and temperature has large implications for interpreting the results of warming experiments. **The third chapter of this dissertation aims to quantify how increased temperature (1.6–5.3 °C above ambient) and VPD (0.1–0.9 kPa above ambient) affect gas exchange and growth of four temperate forest tree species (*Acer rubrum*, red maple; *Carya tomentosa*, hickory; *Quercus alba*, white oak; *Quercus rubra*, red oak).**

Another big question that our society is facing is: How will we continue to provide water and energy to Earth's growing population in the future? Currently, fossil fuels dominate energy production, although renewable energy is projected to be the fastest growing source of primary energy over the next 25 years (EIA, 2011). Leaders in many countries view domestic bioenergy systems as more secure and sustainable than imported fossil fuels, and government policies in the US and Europe call for an expansion of cellulosic biofuel production (McBride *et al*., 2011). **The last data chapter of this dissertation investigates the suitability of *Populus trichocarpa* (black cottonwood) for biofuel production in North Carolina, as determined by water requirements per unit biomass produced.**

Finally, I close with a summary chapter to describe the main findings of my dissertation, the limitations of the experiments, and recommendations for future research.

REFERENCES

Adams HD, Guardiola-Claramonte M, Barron-Gafford GA, *et al*. (2009a) Reply to Sala: Temperature sensitivity in drought-induced tree mortality hastens the need to further resolve a physiological model of death. *Proceedings of the National Academy of Sciences of the United States of America*, **106**, E69-E69.

Adams HD, Guardiola-Claramonte M, Barron-Gafford GA, *et al*. (2009b) Temperature sensitivity of drought-induced tree mortality portends increased regional die-off under global-change-type drought. *Proceedings of the National Academy of Sciences of the United States of America*, **106**, 7063-7066.

Allen CD, Macalady AK, Chenchouni H, *et al*. (2010) A global overview of drought and heat-induced tree mortality reveals emerging climate change risks for forests. *Forest Ecology and Management*, **259**, 660-684.

Alley RB, Marotzke J, Nordhaus WD, *et al*. (2003) Abrupt climate change. *Science*, **299**, 2005-2010.

Anderegg WRL, Berry JA, Smith DD, *et al*. (2012) The roles of hydraulic and carbon stress in a widespread climate-induced forest die-off. *Proceedings of the National Academy of Sciences of the United States of America*, **109**, 233-237.

Bowen GJ, Bralower TJ, Delaney ML, *et al*. (2006) Eocene hyperthermal event offers insight into greenhouse warming. *Eos*, **87**, 165-169.

Broecker WS, Denton GH (1990) What Drives Glacial Cycles? *Scientific American*, **262**, 48-56.

Ciais P, Denning AS, Tans PP, *et al*. (1997) A three-dimensional synthesis study of $\delta^{18}O$ in atmospheric CO_2 , 1. Surface fluxes. *Journal of Geophysical Research-Atmospheres*, **102**, 5857-5872.

Ciais P, Reichstein M, Viovy N, *et al*. (2005) Europe-wide reduction in primary productivity caused by the heat and drought in 2003. *Nature*, **437**, 529-533.

Clark PU, Dyke AS, Shakun JD, *et al*. (2009) The Last Glacial Maximum. *Science*, **325**, 710-714.

Cook ER, Woodhouse CA, Eakin CM, *et al*. (2004) Long-term aridity changes in the western United States. *Science*, **306**, 1015-1018.

Crowley TJ (2000) Causes of climate change over the past 1000 years. *Science*, **289**, 270-277.

Dai A, Lamb PJ, Trenberth KE, *et al*. (2004a) The recent Sahel drought is real. *International Journal of Climatology*, **24**, 1323-1331.

Dai A, Trenberth KE, Qian TT (2004b) A global dataset of Palmer Drought Severity Index for 1870-2002: Relationship with soil moisture and effects of surface warming. *Journal of Hydrometeorology*, **5**, 1117-1130.

EIA (2011) International Energy Outlook 2011, Rep. No. DOE/EIA-0484(2011). US Energy Information Administration.

Farquhar GD, Lloyd J, Taylor JA, *et al*. (1993) Vegetation effects on the isotope composition of oxygen in atmospheric CO_2. *Nature*, **363**, 439-443.

Friedlingstein P, Cox P, Betts R, *et al*. (2006) Climate-carbon cycle feedback analysis: Results from the (CMIP)-M-4 model intercomparison. *Journal of Climate*, **19**, 3337-3353.

Fu GB, Charles SP, Yu JJ (2009) A critical overview of pan evaporation trends over the last 50 years. *Climatic Change*, **97**, 193-214.

Gautier C (2008) *Oil, Water, and Climate: An Introduction* Cambridge University Press, New York.

Hickler T, Prentice IC, Smith B, *et al*. (2006) Implementing plant hydraulic architecture within the LPJ Dynamic Global Vegetation Model. *Global Ecology and Biogeography*, **15**, 567-577.

Hof C, Levinsky I, Araujo MB, *et al*. (2011) Rethinking species' ability to cope with rapid climate change. *Global Change Biology*, **17**, 2987-2990.

Houghton RA, Goodale CL (2004) Effects of land-use change on the carbon balance of terrestrial ecosystems. In *Ecosystems and Land Use Change*, Vol. 153, pp. 85-98.

IPCC (2007) Climate Change 2007: The Physical Science Basis. Contribution of Working Group I to the Fourth Assessment Report of the Intergovernmental Panel on Climate Change.

Jackson RB, Carpenter SR, Dahm CN, *et al*. (2001) Water in a changing world. *Ecological Applications*, **11**, 1027-1045.

Jarvis PG (1976) The interpretation of the variations in leaf water potential and stomatal conductance found in canopies in the field. *Philosophical Transactions of the Royal Society of London, Series B*, **273**, 593-610.

Jentsch A, Kreyling J, Beierkuhnlein C (2007) A new generation of climate-change experiments: events, not trends. *Frontiers in Ecology and the Environment*, **5**, 365-374.

Jung M, Reichstein M, Ciais P, *et al*. (2010) Recent decline in the global land evapotranspiration trend due to limited moisture supply. *Nature*, **467**, 951-954.

Karl TR, Melillo JM, Peterson TC (2009) *Global Climate Change Impacts in the United States*. US Global Change Research Program, Cambridge University Press, New York.

Katz RW, Brown BG (1992) Extreme events in a changing climate variability is more important than averages. *Climatic Change*, **21**, 289-302.

King JS, Pregitzer KS, Kubiske ME, *et al*. (2005) Tropospheric O_3 compromises net primary production in young stands of trembling aspen, paper birch, and sugar maple in response to elevated atmospheric CO_2. *New Phytologist*, **168**, 623-636.

Knorr W (2000) Annual and interannual CO_2 exchanges of the terrestrial biosphere: process-based simulations and uncertainties. *Global Ecology and Biogeography*, **9**, 225-252.

Kump LR, Kasting JF, Crane RG (2010) *The Earth System*, 3rd edn. Prentice Hall, San Francisco.

Lambert F, Delmonte B, Petit JR, *et al*. (2008) Dust-climate couplings over the past 800,000 years from the EPICA Dome C ice core. *Nature*, **452**, 616-619.

Lee S, Saw SH (2011) Nuclear fusion energy – Mankind's giant step forward. *Journal of Fusion Energy*, **30**, 398-403.

Levis SG, Bonan GB, Vertenstein M, *et al*. (2004) The Community Land Model's Dynamic Global Vegetation Model (CLM-DGVM): Technical Description and User's Guide. National Center for Atmospheric Research, Boulder, CO.

Lisiecki LE, Raymo ME (2005) A Pliocene-Pleistocene stack of 57 globally distributed benthic delta O-18 records. *Paleoceanography*, **20**.

Liu BH, Xu M, Henderson M, *et al*. (2004) A spatial analysis of pan evaporation trends in China, 1955-2000. *Journal of Geophysical Research-Atmospheres*, **109**.

Marengo JA, Nobre CA, Tomasella J, *et al*. (2008) The drought of Amazonia in 2005. *Journal of Climate*, **21**, 495-516.

Mathez EA (2009) *Climate Change: The Science of Global Warming and Our Energy Future* Columbia University Press, New York.

McBride AC, Dale VH, Baskaran LM, *et al*. (2011) Indicators to support environmental sustainability of bioenergy systems. *Ecological Indicators*, **11**, 1277-1289.

Merico A, Tyrrell T, Wilson PA (2008) Eocene/oligocene ocean de-acidification linked to Antarctic glaciation by sea-level fall. *Nature*, **452**, 979-U6.

Nicholls N (2004) The changing nature of Australian droughts. *Climatic Change*, **63**, 323-336.

Ohmura A, Wild M (2002) Is the hydrological cycle accelerating? *Science*, **298**, 1345-1346.

Overland J, Key J, Kim BM, *et al*. (2012) Air temperature, atmospheric circulation and clouds. In *Arctic Report Card 2012*, http://www.arctic.noaa.gov/reportcard.

Patz JA, Campbell-Lendrum D, Holloway T, *et al*. (2005) Impact of regional climate change on human health. *Nature*, **438**, 310-317.

Perovich DK, Meier W, Tschudi M, *et al*. (2013) [The Arctic] Sea ice cover. In *State of the Climate in 2012*, Bulletin of the American Meteorological Society (BAMS), S126-S127.

Peterson TC, Golubev VS, Groisman PY (1995) Evaporation losing its strength. *Nature*, **377**, 687-688.

Petit JR, Jouzel J, Raynaud D, *et al*. (1999) Climate and atmospheric history of the past 420,000 years from the Vostok ice core, Antarctica. *Nature*, **399**, 429-436.

Phillips OL, Aragao L, Lewis SL, *et al*. (2009) Drought sensitivity of the Amazon rainforest. *Science*, **323**, 1344-1347.

Ray J, Pugliese A (2011) Worldwide, Blame for climate change falls on humans. Gallup, Inc.

Sitch S, Smith B, Prentice IC, *et al*. (2003) Evaluation of ecosystem dynamics, plant geography and terrestrial carbon cycling in the LPJ dynamic global vegetation model. *Global Change Biology*, **9**, 161-185.

Solomon S, Plattner GK, Knutti R, *et al*. (2009) Irreversible climate change due to carbon dioxide emissions. *Proceedings of the National Academy of Sciences of the United States of America*, **106**, 1704-1709.

van Mantgem PJ, Stephenson NL, Byrne JC, *et al*. (2009) Widespread increase of tree mortality rates in the western United States. *Science*, **323**, 521-524.

Ward JK, Kelly JK (2004) Scaling up evolutionary responses to elevated CO_2: lessons from *Arabidopsis*. *Ecology Letters*, **7**, 427-440.

Way DA, Domec JC, Jackson RB (2012) Elevated growth temperatures alter hydraulic characteristics in trembling aspen (*Populus tremuloides*) seedlings: implications for tree drought tolerance. *Plant Cell and Environment*, **36**, 103-115.

Webster PJ, Holland GJ, Curry JA, *et al*. (2005) Changes in tropical cyclone number, duration, and intensity in a warming environment. *Science*, **309**, 1844-1846.

Wentz FJ, Ricciardulli L, Hilburn K, *et al*. (2007) How much more rain will global warming bring? *Science*, **317**, 233-235.

Zachos J, Pagani M, Sloan L, *et al*. (2001) Trends, rhythms, and aberrations in global climate 65 Ma to present. *Science*, **292**, 686-693.

Zachos JC, Rohl U, Schellenberg SA, *et al*. (2005) Rapid acidification of the ocean during the Paleocene-Eocene thermal maximum. *Science*, **308**, 1611-1615.

Zeppel MJB, Adams HD, Anderegg WRL (2011) Mechanistic causes of tree drought mortality: recent results, unresolved questions and future research needs. *New Phytologist*, **192**, 800-803.

CHAPTER 2

Vegetative and reproductive phenological responses to warming differ among species in a temperate forest understory

2.1 Abstract

Increasing temperature will have a large impact on the vegetative phenology, reproductive phenology, and biodiversity of temperate forest ecosystems in the future. We measured the effect of experimental warming on the timing of budburst, leaf coloring, flowering, and fruiting in 2011 and compared phenological responses to the colder year 2013. Warming of open-top chambers in the understory of an oak-hickory forest (Duke Forest, North Carolina, USA) followed a regression design, with air temperatures ranging from 0.9–5.1 °C above ambient. Warming advanced budburst by 5–15 days in four deciduous tree and two shrub species, while leaf coloring was delayed by 14–20 days in autumn. Warming extended the growing season of the four tree species by 20–28 days. Advances in budburst of diffuse-porous trees were larger than shifts in ring-porous trees, possibly due to more conservative safety mechanisms in ring-porous species for prevention of damage by late-spring frosts. Experimental warming underpredicted advancement in mean budburst by 4-fold relative to interannual temperature variability. We found nonlinear responses of budburst phenology to

warming over 2.5 °C and budburst of all species failed to fully track warmer temperatures, however, suggesting that high rates of phenological change observed in the past are unsustainable and will decrease with warming throughout the coming century. Warming advanced flowering by 6–25 days in three species and delayed reproduction of *Tipularia discolor* by 10 days, but had no effect on three species that flower in early spring. Warming of 2 °C resulted in reproductive failure in *Chimaphila maculata* when mean May temperature exceeded 21 °C and in *T. discolor* when mean July temperature exceeded 29 °C, suggesting temperature thresholds that could severely limit the distribution of these species in the future. There were no warming-induced changes in species abundances or community diversity after three years of warming.

2.2 Introduction

Shifts in phenology provide clear evidence that climate change is already affecting Earth's biota. On average, spring phenological events are advancing at the rate of 5–6 days per °C in many regions of the world (Wolkovich *et al.*, 2012). Earlier dates of budburst and later dates of leaf senescence with climate warming have led to an extension of the vegetative growing season (Norby *et al.*, 2003; Parmesan, 2006; Vitasse *et al.*, 2009; Gunderson *et al.*, 2012). In deciduous broadleaf forests of the eastern United States, the growing season lengthened by about 5 days from 1900 to 1987 (White *et al.*, 1999). Despite these mean trends, species vary greatly in their individual responses to climate change. While most species show advancement of phenology with warming (Fitter & Fitter, 2002; Parmesan & Yohe, 2003; Root *et al.*, 2003; IPCC, 2007), other species show no response to warming (Bradley *et al.*,

1999) or even delays in phenology (Sherry *et al.*, 2007; Dorji *et al.*, 2013). Even in responsive species, phenological shifts may have limits beyond which additional warming fails to result in the same rate of change (Morin *et al*., 2010; Salk, 2011; Gunderson *et al.*, 2012). Predicting future responses of phenology to climate change in general, and warming in particular, will ultimately rely heavily upon experiments that accurately simulate future conditions (Williams & Jackson, 2007; Wolkovich *et al.*, 2012).

In theory, the optimal phenology for temperate plants is to maximize growing season length while avoiding frost damage in the spring and maximizing nutrient recovery in the fall. If plants respond in this way to warming, productivity may be expected to increase in many regions (White *et al.*, 1999; Saxe *et al.*, 2001; Picard *et al.*, 2005; Richardson *et al.*, 2010). Evolutionary constraints may limit the ability of species to respond optimally to increasing temperatures, however. Similar patterns of phenological change have been found in the flowering responses of plant families and genera (Wright & Calderon, 1995; Kang & Jang, 2004), indicating that phenology is indeed limited by shared phylogenetic constraints among closely related taxa (Kochmer & Handel, 1986). It has been suggested that plants with phenological responses cued to photoperiod may fail to respond to climate warming (Bradley *et al.*, 1999). Ring-porous tree species require longer photoperiods for budburst than many diffuse-porous species (Wang *et al.*, 1992), which is an adaptive response that limits the risk for frost-induced dysfunction in the large-diameter xylem vessels of ring-porous species. Advances in budburst and flowering with warming can thus be predicted to differ with both phylogeny (Willis *et al.*, 2008; Davis *et al.*, 2010) and plant functional type (Salk, 2011).

Warming experiments have provided valuable insights into how increased temperatures will affect species abundance and the diversity of plant communities in the future. Plant families that do not respond to warming have decreased greatly in abundance in temperate communities in the northeastern US (Willis *et al.*, 2008). Experimental warming caused declines in the biomass of forbs and increases in shrub biomass in a montane meadow in the Rocky Mountains, potentially leading to a shift in dominant vegetation in the future (Harte & Shaw, 1995). Plant species richness declined rapidly with warming in an alpine rangeland, possibly due to heat stress in aboveground plant tissue (Klein *et al.*, 2004). In a New England salt marsh, warming of <4 °C resulted in a loss of forb species diversity and replacement by a competitively dominant grass, *Spartina patens* (Gedan & Bertness, 2009). These changes in species composition have the capacity to drive large functional changes in ecosystems as climate continues to warm in the future.

Mean temperature in the southeastern US is expected to increase by 2–6 °C by 2100 (Karl *et al.*, 2009). The impact of future warming on temperate forest communities is poorly understood in part because warming experiments have focused on open-field ecosystems such as tundra (Chapin & Shaver, 1996; Arft *et al.*, 1999), alpine meadows (Harte & Shaw, 1995; Dorji *et al.*, 2013), grasslands (Sherry *et al.*, 2007), and quartz-fields (Musil *et al.*, 2005). Here we devised an experiment to understand the influence of warming on phenology of a diverse suite of 11 temperate forest species known to differ in their evolutionary history, temporal phenological niche, and xylem anatomy. Our primary goal was to understand the extent to which forest species alter spring budburst, autumn leaf coloring, and flowering time with warming. We measured changes in leaf and flower phenology inside actively heated

open-top chambers in the understory of an oak-hickory forest in Duke Forest, North Carolina, USA. Chamber heating followed a regression design, where each chamber was heated to a target of 1.5–5.5 °C above ambient temperature, with 0.5 °C increments between chambers. A recent study by Wolkovich *et al*. (2012) found that warming experiments underpredict plant responses to climate change, however. We therefore compared the effect of experimental warming on leafing and flowering date to interannual differences in phenology observations between 2011 and 2013, two years when mean spring temperature differed by about 3 °C. We tested the hypotheses that:

1. Changes in budburst timing with warming will be greater in diffuse-porous species than ring-porous species, due to evolutionary constraints that prevent advances in budburst in ring-porous species.
2. Warming will extend the length of the growing season by advancing budburst and delaying leaf coloring.
3. Species that flower in early spring are more sensitive to temperature than species that flower later in the growing season.
4. Three years of warming will decrease diversity of the temperate forest understory.

2.3 Materials and Methods

Experimental study site

This study was conducted at an ongoing, long-term warming experiment in a *c.* 80-year-old oak-hickory forest stand of Duke Forest (36° 2’ 11” N, 79° 4’ 39” W, 130 m a.s.l.), in the piedmont region near Hillsborough, North Carolina, USA (Lynch, 2006). The mean annual

temperature at Duke Forest is 15.5 °C, and the mean annual precipitation is 1140 mm. Climate data for the site are available from a nearby (8 km) weather station (Duke Forest Remote Automatic Weather Station, Orange County, NC, USA). Soil at the site is a Georgeville silt loam (Typic Kanhapludults, Ultisol), and chambers are located on a north-facing slope (6-15% slope) near a small creek. Dominant tree species include *Quercus alba*, *Quercus rubra*, *Carya tomentosa*, *Acer rubrum*, and *Oxydendrum arboreum*. There were a total of 51 vascular plant species present in the chambers.

The experimental warming site consists of 15 plots in the forest understory: nine are heated, three are unheated chamber controls, and three are control plots that lack chambers but are equal in surface area to the chambers. The octagonal, open-top chambers are 21.7 m^3 in volume: 5 m in diameter with eight walls that are 1.9 m wide by 1.2 m tall. The chambers are heated by forced air blown over hydronic radiators fed by a closed-loop mixture of hot water and propylene glycol (antifreeze). The heated air is blown into the chambers through 15-cm-diameter plastic plena which hang 45 cm above the ground and run in two concentric rings, one 0.8 m and the other 1.7 m from the chamber walls. Air enters the chambers via two rows of 2-cm-diameter holes separated by 20 cm along the bottom of the plena. Heat delivery to the chambers began in January 2010, and chambers are constantly heated year-round, both day and night. The experiment uses a regression design of chamber heating, where each chamber is heated to a target of 1.5 to 5.5 °C above ambient temperature with 0.5 °C increments between chambers. Maintaining precise target air temperatures over long time periods is difficult, and the assigned treatment levels varied by a small amount over time.

Despite this imperfection, the use of a regression design is useful for revealing potential nonlinearities and threshold effects in plant temperature responses.

Air temperature (2 temperature probes per chamber), relative humidity (HS-2000V capacitive polymer sensor; Precon, Memphis, TN, USA), soil moisture (Model CS616 TDR probes, Campbell Scientific Inc., Logan, UT, USA), and photosynthetically active radiation (PAR) (Model SQ110; Apogee Instruments Inc., Logan, UT, USA) were measured inside each experimental chamber every minute and recorded as hourly means by automated dataloggers (CR1000; Campbell Scientific Inc.). Further details of the warming experiment can be found in Pelini *et al.* (2011).

Phenological observations

The experimental site was visited weekly during the period of bud break (early March–mid-April) in 2011 and 2013 and during the period of leaf senescence (mid-October–early December) in 2011 to determine the vegetative phenological stage of four tree species (*A. rubrum*, *C. tomentosa*, *Q. alba*, *Q. rubra*) and two shrub species (*Vaccinium pallidum*, *Vaccinium stamineum*). Each species was present in multiple control and heated chambers, and one to twelve plants per species per chamber were tagged for observation. In addition, two to ten plants per species were also observed in chamberless control plots. Total sample sizes ranged from 12–129 plants per species. Most sampled plants (95%) were understory seedlings less than 50 cm tall, although plants up to 1 m tall were sampled if species abundance was low. For each plant, vegetative phenology was divided into five stages: LO, unopened buds; L1, open buds; L2, emerging leaves; L3, full leaf; L4, senescing leaves.

Budburst date (L1) was compared for the four tree species, whereas date of leaf emergence (L2) was compared for the two *Vaccinium* species due to visual difficulty determining budburst date on the tiny buds of the shrubs. At the end of the growing season, the date of full color (>50% of the leaves have changing colors, L4) in autumn was compared for all six understory species. Growing season length was calculated by subtracting the mean date of budburst from the mean date of leaf coloring for each species in each chamber.

Temperature cues for budburst are usually sensed through the cumulative heat sums above some threshold level (Rathcke & Lacey, 1985). We calculated the accumulated growing degree days (GDD) for budburst for each plant in 2011 and 2013 to compare differences in budburst between treatments and years. The GDD was calculated from either 1 February (GDD_{Feb}) or 1 March (GDD_{Mar}) to the date of budburst using the equation described by Cannell and Smith (1983):

$$T_{\mathrm{x}} = \sum_{m=1}^{n} (t_{\mathrm{m}} - x)$$

where T_{x} is the day degrees above the threshold temperature x=5 °C, n is the number of spring days with a temperature greater than x, and t_{m} is the mean daily temperature or (T_{max} + T_{min})/2. In accordance with these GDD models, we used mean February or March temperature inside each chamber to compare species responses to warming.

The experimental site was visited weekly from mid-March through October 2011 and 2013 to determine the reproductive phenology of five herbaceous species (*Chimaphila maculata*, *Hexastylis arifolia*, *Hieracium venosum*, *Thalictrum thalictroides*, *Tipularia discolor*) and two shrub species (*V. pallidum*, *V. stamineum*). Flowering individuals of each

species were present in at least two heated chambers, and 4–10 plants per species were also observed in chamberless control plots. Total sample sizes ranged from 6–29 plants per species. For each plant, reproductive phenology was divided into seven stages: FO, unopened buds; F1, open buds; F2, flowers; F3, old flowers; F4, initiated fruit; F5, expanding fruit; F6, dehisced fruit. Flowering date and fruiting date were compared for all seven understory species. The onset of flowering is correlated to mean temperature during the month of flowering for many plants (Sparks *et al.*, 2000; Menzel *et al.*, 2006a), so we used the mean temperature inside each chamber during the month of flowering to compare species responses to warming.

Community composition

We sampled naturally-occurring plants that were present at the site before the chambers were installed. Species density and cover were examined within each of the 12 chambers in June 2009, before heating began, and in August 2012, the third summer of heating. Any saplings taller than the height of the chamber (>1.2 m) were not included in the analysis. Stems for all understory vascular plant species within the 17.4 m^2 chamber were counted for species density measurements. For species with clonal growth habits, such as *V. pallidum* and *V. stamineum*, any stems separated by a distance of 2 cm were counted as distinct individuals. Percent cover for each species present in the chamber was estimated as belonging to one of the following cover classes: 0-1%, 1-2%, 2-5%, 5-10%, 10-25%, 25-50%, 50-75%, or 75-100%.

Statistical analyses

Warming effects on vegetative phenology (date of budburst, date of leaf coloring, growing season length) of individual species were analyzed using least-square regression with mean chamber response as the dependent variable, as appropriate for the experimental design. To facilitate comparisons among temperature treatments and study years, we calculated the mean phenological sensitivity to temperature (change in budburst and leaf coloring date per °C) of each chamber. Interannual differences in GDD_{Feb} and GDD_{Mar} for budburst for each species were determined by using two-way, full factorial analyses of variance (ANOVA) with year and temperature as the main effects. Reproductive phenology could only be compared between 3–5 chambers due to limited numbers of flowering individuals. Therefore, we calculated the mean phenological sensitivity to temperature (change in flowering and fruiting date per °C) of each chamber to compare responses in heated versus control chambers for each species using the Student's *t*-test statistic. Temperature had similar effects on flowering and fruiting, so only the flowering responses are depicted in tables and figures. Interannual differences in julian date of budburst and flowering for each species were determined by comparing individuals in control chambers or plots in 2011 versus 2013 using the Student's *t*-test statistic. Means were considered significantly different at $P \leq 0.05$. These analyses were performed using JMP 9.0 (SAS Institute, Cary, NC, USA).

The Mantel test using the randomization (Monte-Carlo) method was performed to compare the relationship between the species density and species cover matrices in 2009 and 2012. There was a fundamental similarity between the species composition of chambers analyzed by density and by cover in both years ($r^2 \geq 0.10$, $P \leq 0.020$), so analyses are only

described for the species cover data matrix. Changes in species richness, evenness, and diversity (Shannon-Weiner index, *H'*) among the chambers over time were analyzed using least-square regression. Changes in abundance from 2009 to 2012 of the common understory species were analyzed with two-way ANOVA including temperature and year as the main effects. Distance matrices for each sampling period were calculated using the Bray-Curtis distance measure, and then mean distance values for each chamber were calculated by averaging the 11 unique pairwise distances (e.g. chamber 1 paired with chamber 2, 3, …, 12). We compared mean chamber distances in 2009 to mean chamber distances in 2012 by standardized major axis (SMA) regression with SMATR 2.0 (Warton *et al.*, 2006), where significant deviation of chambers from the 1:1 line would represent a treatment effect. SMA was used instead of standard least-square regression, because it is not possible to functionally assign either variable as dependent. A detrended correspondence analysis (DCA) with down-weighting of rare species was used to ordinate the relationship among species composition of the 12 chambers, and successional vectors were used to show composition divergence over time. The axes were interpreted using the chi-squared distance measure. These analyses were performed using PC-ORD 5.31 (MjM Software, Gleneden Beach, Oregon, USA).

2.4 Results

Vegetative phenology

There was a large degree of variability in species budburst date within the open-top chambers in our experiment (Table 2.1). Budburst of all species varied by as much as 20–31 days within a single chamber, regardless of whether it was a control or heated chamber. Despite

this variability, warming significantly advanced the date of budburst in 2011 (r^2=0.05, P=0.050) and 2013 (r^2=0.12, P=0.005, Figure 2.1) when averaged across all six tree and shrub species. Advancement of budburst varied by species and by year. In 2011, warming of 1.2–5.1 °C advanced mean budburst by 0.8 days per °C in *V. pallidum* (t_{10}=2.43, P=0.038, Table 2.1a). In 2013, warming of 0.9–4.6 °C advanced mean budburst in *C. tomentosa* (t_{11}=4.22, P=0.002) and *Q. alba* (t_{11}=2.58, P=0.027) by 2 days per °C (Table 2.1b). There was no significant shift in budburst date of *A. rubrum* in either year when all chambers were included in the analysis, but budburst was advanced by 2.3 days per °C in 2011 (t_7=3.89, P=0.008) and 3.1 days per °C in 2013 (t_8=2.37, P=0.049) with warming of 0.9–2.0 °C (Table 2.1). Timing of budburst in 2013 was significantly correlated to temperature in the ring-porous trees *C. tomentosa* (r^2=0.70, P=0.001), *Q. alba* (r^2=0.59, P=0.004), and *Q. rubra* (r^2=0.57, P=0.012), but not in the diffuse-porous *A. rubrum* (r^2=0.01, P=0.754) or the two shrubs, *V. pallidum* (r^2=0.01, P=0.782) and *V. stamineum* (r^2=0.003, P=0.902, Figure 2.1). Mean March temperature was 3.4 °C higher in 2011 than in 2013 (10.3 vs. 6.9 °C, respectively), which resulted in significantly earlier budburst in 2011 by 1.3–4.7 days per °C across all species ($t_{12\text{-}68}\geq$2.29, $P\leq$0.043, Table 2.2a).

Since budburst date varied significantly with warming treatment and year, rather than occurring at a constant photoperiod, we compared the accumulated GDD required for budburst to determine if temperature could explain the variation. If plants are able to take full advantage of warmer temperatures and are not constrained by chilling requirements or photoperiod, the GDD for budburst would be constant across all chambers. For all species, GDD_{Mar} for budburst differed significantly among chambers ($F_{1,13–22}\geq$5.969, $P\leq$0.027), with

plants growing in warmer chambers requiring higher GDD for budburst (Figure 2.2). Irrespective of year, GDD_{Feb} sums differed among warming treatments by 170 to 300 within a single species. Using GDD_{Mar} reduced the treatment variability by 25–50%, as GDD_{Mar} differed among chambers by 90 to 220 within a species. The warmest chambers in 2013 had the same mean March temperature as the control chambers in 2011, and budburst of ring-porous tree species *C. tomentosa* (t_{20}=0.48, P=0.638), *Q. alba* (t_{21}=0.22, P=0.830), and *Q. rubra* (t_{16}=0.78, P=0.449) occurred at the same GDD_{Mar} in chambers with the same March temperature (Figure 2.2). In the diffuse-porous *A. rubrum* (t_{22}=6.08, P<0.0001) and the two shrub species *V. pallidum* (t_{16}=5.55, P<0.0001) and *V. stamineum* (t_{13}=3.33, P=0.005), budburst occurred at lower GDD_{Mar} in the control chambers in 2011 than in the heated chambers in 2013, despite the fact that the chambers had the same March temperature (Figure 2.2).

The effect of warming on leaf coloring and growing season length also differed among species. Warming significantly delayed the date of leaf coloring when averaged across all six species (r^2=0.14, P=0.003), but the timing of leaf coloring was only correlated to temperature in *A. rubrum* (r^2=0.40, P=0.021), *C. tomentosa* (r^2=0.57, P=0.008), and *Q. alba* (r^2=0.70, P=0.0004; Figure 2.3a). Leaf coloring in 2011 was delayed by 0.9–10.1 days per °C in *A. rubrum*, 0.6–2.7 days per °C in *C. tomentosa*, and 2.3–9.3 days per °C in *Q. alba*. As a result of both advanced budburst and/or delayed leaf senescence, warming of 1.2–5.1 °C extended the 2011 growing season of the four tree species by 0.2–13.5 days per °C in *A. rubrum* (r^2=0.38, P=0.025), 1.6–4.0 days per °C in *C. tomentosa* (r^2=0.63, P=0.006), 2.2–9.7 days per °C in *Q. alba* (r^2=0.67, P=0.001), and 2.3–11.5 days per °C in *Q. rubra*

(r^2=0.81, P=0.003; Fig. 2.3b). There was no significant effect of warming on growing season length of the two shrub species (VAPA: r^2=0.18, P=0.293; VAST: r^2=0.27, P=0.293; Figure 2.3b).

Reproductive phenology

There were considerable differences in the effect of warming on reproductive phenology among the seven understory species examined here (Figure 2.4). The three species that flowered earliest in the spring, *T. thalictroides* (t_{23}=0.14, P=0.887), *H. arifolia* (t_5=1.36, P=0.246), and *V. pallidum* (t_{11}=1.80, P=0.102), had no response to warming in 2011. Warming significantly advanced flowering and fruiting date in *V. stamineum* (t_{26}=3.73, P=0.001), *H. venosum* (t_{20}=3.10, P=0.006), and *C. maculata* (t_8=6.93, P=0.0002), but warming delayed reproduction of *T. discolor* (t_{15}=7.13, P<0.0001) in 2011. The shrub *V. stamineum* flowers in April, when warming advanced flowering by 7.6 days per °C (Figure 2.4) and fruiting by 9.5 days per °C. In *H. venosum*, an herb that flowers in April–May, flowering was advanced by 2.3 days per °C (Figure 2.4) and fruiting by 2.7 days per °C. The most responsive species to temperature was *C. maculata*, which flowers in May–June, where warming advanced flowering by 10 days per °C (Figure 2.4) and fruiting by 11.4 days per °C. Furthermore, temperature was significantly correlated with flowering date in *C. maculata* (r^2=0.94, P=0.006). In *T. discolor*, an orchid species that flowers in late July, warming delayed flowering by 7.3 days per °C (Figure 2.4) and fruiting by 4 days per °C.

Reproductive phenological responses differed from 2011 in the colder year 2013. Compared to flowering in 2013, flowering in 2011 was significantly advanced by 10 days in

T. thalictroides (t_{16}=2.62, P=0.019), by 18 days in *H. arifolia* (t_{6}=5.67, P=0.002), by 14 days in *V. stamineum* (t_{22}=20.51, P<0.0001), and by 8 days in *T. discolor* (t_{25}=5.53, P<0.0001; Figure 2.5). Despite the temperature difference between years, there was no interannual difference in flowering date for *V. pallidum* (t_{26}=1.53, P=0.138), *H. venosum* (t_{21}=0.39, P=0.698), and *C. maculata* (t_{14}=1.29, P=0.221; Figure 2.5). The only species significantly affected by experimental warming in 2013 was *V. stamineum* (t_{28}=3.17, P=0.004), in which flowering was advanced by 3 days per °C (Figure 2.4) and fruiting by 4.5 days per °C. There was no effect of experimental warming on reproduction in 2013 in *T. thalictroides* (t_{22}=1.14, P=0.267), *H. arifolia* (t_{9}=1.00, P=0.347), *V. pallidum* (t_{33}=0.32, P=0.754), *H. venosum* (t_{16}=0.60, P=0.558), *C. maculata* (t_{12}=1.63, P=0.132), and *T. discolor* (t_{45}=0.37, P=0.712, Figure 2.4).

We observed premature flower or fruit abortion within heated chambers for two of the seven understory species. All flowering individuals of *C. maculata* in heated chambers formed fruits, but these fruits aborted and died before seed maturation when mean May temperature was greater than 21 °C. We observed the formation of flowering stalks of the orchid *T. discolor* in multiple heated chambers, but these elongating scapes and floral buds quickly withered and died when mean July temperature was above 29 °C. Temperatures that resulted in reproductive failure for both species were as small as 2 °C above ambient temperatures.

Community composition

Species richness of the forest understory did not change significantly after three years of heating at the site (t_{11}=1.23, P=0.231), but evenness significantly declined over the study period (t_{11}=2.49, P=0.022; Table 2.3). As a result, there was a non-significant trend for decreased diversity (*H'*) in the chambers with warming (t_{11}=1.81, P=0.085; Table 2.3). Temperature was not correlated to changes in species richness (r^2=0.002, P=0.884), evenness (r^2=0.16, P=0.204), or diversity (r^2=0.01, P=0.822) among the chambers over time, however. We also examined whether any shifts in the abundance of common species occurred over the three years of experimental heating. There was a non-significant trend for decreased abundance of *A. rubrum* seedlings from 2009 to 2012 ($F_{1,23}$=3.332, P=0.082). The number of *Q. alba* tree seedlings in the chambers increased from 2009 to 2012 ($F_{1,23}$=77.348, P<0.0001), because 2010 was a mast year for acorns in Duke Forest. Change in abundance from 2009 to 2012 was not correlated with chamber temperature in *A. rubrum* (r^2=0.05, P=0.501) or *Q. alba* (r^2=0.001, P=0.919), however.

There was no evidence for a warming-induced change in community composition of the forest understory at Duke Forest, and potential composition changes were assessed via two methods. First, we compared the mean distance value of each chamber in 2009 to its distance value after resampling in 2012 (Figure 2.6). There was no divergence among chamber distance values over time, since the relationship between sampling dates was not significantly different from the 1:1 line (slope=0.873, $F_{1,11}$=0.436, P=0.524; intercept=0.047, t_{11}=0.546, P=0.597; Figure 2.6). The mean distance value of most chambers decreased from 2009 to 2012, although there were four heated chambers where the mean distance value

increased over time (Figure 2.6). We also examined community composition changes over time with a DCA ordination (Figure 2.7). Shifts in composition over time were of similar magnitude among chambers, and the direction of observed shifts did not correspond to the warming treatment (r^2=0.031). The first axis in the DCA ordination explains 27.2% of the variation in species composition among chambers, while the second axis explains an additional 4.0% of the variation (Figure 2.7). The species with the strongest influence on the placement of chambers along the first axis are *Quercus velutina* (r^2=0.59) and *Oxydendrum arboreum* (r^2=0.53), while *C. tomentosa* (r^2=0.50) and *Hexastylis virginica* (r^2=0.50) are important for determining placement of chambers along the second axis.

Table 2.1 Mean phenological sensitivity to temperature (change in budburst date per °C, ±SE) for six species in Duke Forest, NC in (a) 2011 and (b) 2013. Chamber temperature is mean March temperature in °C above ambient. Positive sensitivities mean that budburst is delayed with warming, whereas negative sensitivities mean that budburst is advanced with warming. Sample sizes ranged from 1–12 plants per chamber. Stars denote significant differences between heated and control plants: $P<0.05$, *; $P<0.01$, **; $P<0.001$, ***.

(a) 2011

Chamber *T* (°C above ambient)	*A. rubrum* (Δ Days per °C)	*C. tomentosa* (Δ Days per °C)	*Q. alba* (Δ Days per °C)	*Q. rubra* (Δ Days per °C)	*V. pallidum* (Δ Days per °C)	*V. stamineum* (Δ Days per °C)
+1.2	−2.8 ± 0.7	+4.8 ± 2.1	0 ± 0.2	−4.9	−1.3 ± 1.2	−3.0 ± 1.4
+1.5	−3.6	+4.8	+1.6 ± 0.9	+1.4	−1.5 ± 0.9	+4.7 ± 0
+1.5	−1.8 ± 0.3	+0.3 ± 2.3	−1.4 ± 0.8	−9.5		−5.8 ± 0.2
+2.0	−0.9 ± 0.4	+0.1 ± 1.7	−0.7 ± 0.7	−6.5	−1.1 ± 0.2	
+2.5	+1.5 ± 0.7	+2.2	+0.4 ± 0.2			
+3.0	−0.6 ± 0.2		+0.6 ± 0.6		−0.6 ± 0.7	−1.9 ± 0
+3.1	−1.0 ± 0.5	−0.3 ± 0.5	−0.1 ± 0.3	−1.6	+0.4 ± 0.6	0 ± 0.5
+4.1	−0.3 ± 0.1	−0.2 ± 0.6	−1.2 ± 0.3	−3.3	−1.3	
+5.1	−0.3 ± 0.1	−1.4 ± 0	−0.6 ± 0.2	−0.4	−0.3 ± 0.3	
Mean (<2.5)	−2.3 **	+2.5	−0.1	−4.9	−1.3 ***	−1.4
Mean (all)	−1.1	+1.3	−0.2	−3.5	−0.8 *	−1.2

(b) 2013

Chamber *T* (°C above ambient)	*A. rubrum* (Δ Days per °C)	*C. tomentosa* (Δ Days per °C)	*Q. alba* (Δ Days per °C)	*Q. rubra* (Δ Days per °C)	*V. pallidum* (Δ Days per °C)	*V. stamineum* (Δ Days per °C)
+0.9	−6.4 ± 2.2	−2.0 ± 0.7	−2.1 ± 2.0	+7.6	+8.7 ± 0.7	−2.5 ± 1.1
+1.3	−4.5 ± 4.1	−3.5	−0.8 ± 1.1	+1.4	+1.9 ± 1.4	+1.8 ± 0.4
+1.7	−2.1 ± 1.0	−3.0 ± 1.0	−4.9 ± 0.5	−1.0		−3.6 ± 0
+1.8	−2.9 ± 1.3	−1.4 ± 0.4	−1.8 ± 0.8	−3.2	+1.6 ± 0.5	+0.3
+2.9	+0.4 ± 0.4	−1.0 ± 0.3	−1.1 ± 0.9			
+3.3	−0.9 ± 0.7	−2.4 ± 0.6	−1.5 ± 0.7	−0.4 ± 0.8	+1.1 ± 0.3	+0.8 ± 0.3
+3.9	−0.3 ± 0.3	−1.2 ± 0.5	−2.3 ± 0.5	−2.3		
+4.0	+0.4 ± 0.2		−0.7 ± 0.5		+1.0 ± 0.8	
+4.6	−0.9 ± 0.3	−1.2 ± 0.3	−2.5 ± 0.5	−1.8 ± 1.4	−0.7 ± 0.7	
Mean (<2.5)	−3.8 *	−2.1 **	−2.9 *	+1.1	+5.2	−1.9
Mean (all)	−1.9	−2.0 ***	−2.0 *	+0.1	+2.3	−0.6

Table 2.2 Comparison of the temperature sensitivity of leafing and flowering phenology (change in days per °C) in a warming experiment to observations of interannual variability in phenology. (a) Experimental budburst is the mean sensitivity of all heated chambers in 2011, and observational budburst is the difference in control plants between 2011 and 2013, when mean March temperature was 3.4 °C higher in 2011. (b) Experimental flowering is the mean sensitivity of all plants in heated chambers in 2011, and observational flowering is the difference in control plants between 2011 and 2013. Stars denote significant differences between heated and control plants (experimental) or between years (observational): $P<0.05$, *; $P<0.01$, **; $P<0.001$, ***.

Species	Experimental (Δ Days per °C)		Observation (Δ Days per °C)	
(a) Budburst				
A. rubrum	–1.1		–4.6	***
C. tomentosa	+1.3		–3.3	***
Q. alba	–0.2		–3.0	***
Q. rubra	–3.5		–1.3	*
V. pallidum	–0.8	*	–4.0	***
V. stamineum	–1.2		–4.7	***
(b) Flowering				
T. thalictroides	+0.1		–2.8	*
H. arifolia	–3.7		–5.3	**
V. pallidum	–4.4		–0.5	
V. stamineum	–7.6	**	–4.1	***
H. venosum	–2.3	**	–1.1	
C. maculata	–10.0	***	–0.7	
T. discolor	+7.3	***	–5.8	***

Table 2.3 Species richness, evenness, and Shannon-Weiner diversity index for all chambers in Duke Forest in 2009, before heating began, and in 2012, the third year of heating. The mean growing season (March–October) temperature and treatment level of each chamber over the study period is given. Significant differences in mean chamber *R*, *E*, and *H'* between years are indicated by a star ($P<0.05$).

Temp (°C)	Richness (*R*)		Evenness (*E*)		Diversity (*H'*)	
	2009	2012	2009	2012	2009	2012
19.8 (+0)	15	12	0.95	0.91	2.58	2.27
20.0 (+0)	14	11	0.95	0.94	2.51	2.25
20.1 (+0)	19	17	0.91	0.91	2.68	2.57
21.3 (+1.2)	21	20	0.92	0.92	2.81	2.76
21.7 (+1.6)	14	12	0.91	0.87	2.41	2.16
22.0 (+1.9)	28	23	0.96	0.96	3.21	3.02
22.4 (+2.3)	14	13	0.95	0.93	2.51	2.39
23.0 (+2.9)	17	17	0.94	0.91	2.66	2.58
23.2 (+3.1)	19	17	0.90	0.89	2.65	2.52
24.2 (+4.1)	13	12	0.95	0.88	2.43	2.19
24.5 (+4.3)	17	12	0.96	0.90	2.71	2.24
25.0 (+4.9)	23	21	0.93	0.92	2.90	2.79
Mean	17.8	15.6	0.94 *	0.91 *	2.67	2.48

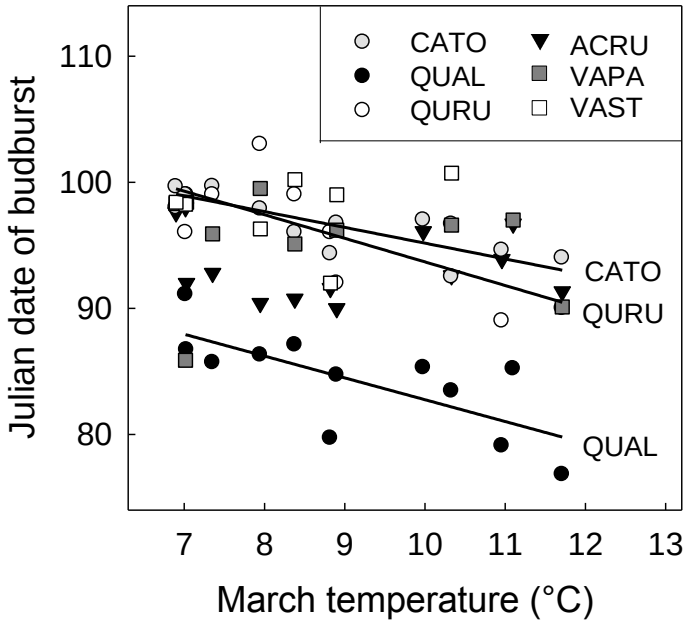

Figure 2.1 The effect of mean March chamber temperature on date of budburst in 2013. Budburst date differed significantly among species ($F_{5,430}$=80.356, P<0.0001) and with temperature (r^2=0.12, P=0.005) across all six species. Temperature was significantly correlated with budburst in CATO (r^2=0.72, P=0.001), QUAL (r^2=0.52, P=0.008), and QURU (r^2=0.51, P=0.020). Species codes: ACRU, *Acer rubrum*; CATO, *Carya tomentosa*; QUAL, *Quercus alba*; QURU, *Quercus rubra*; VAPA, *Vaccinium pallidum*; VAST, *Vaccinium stamineum*.

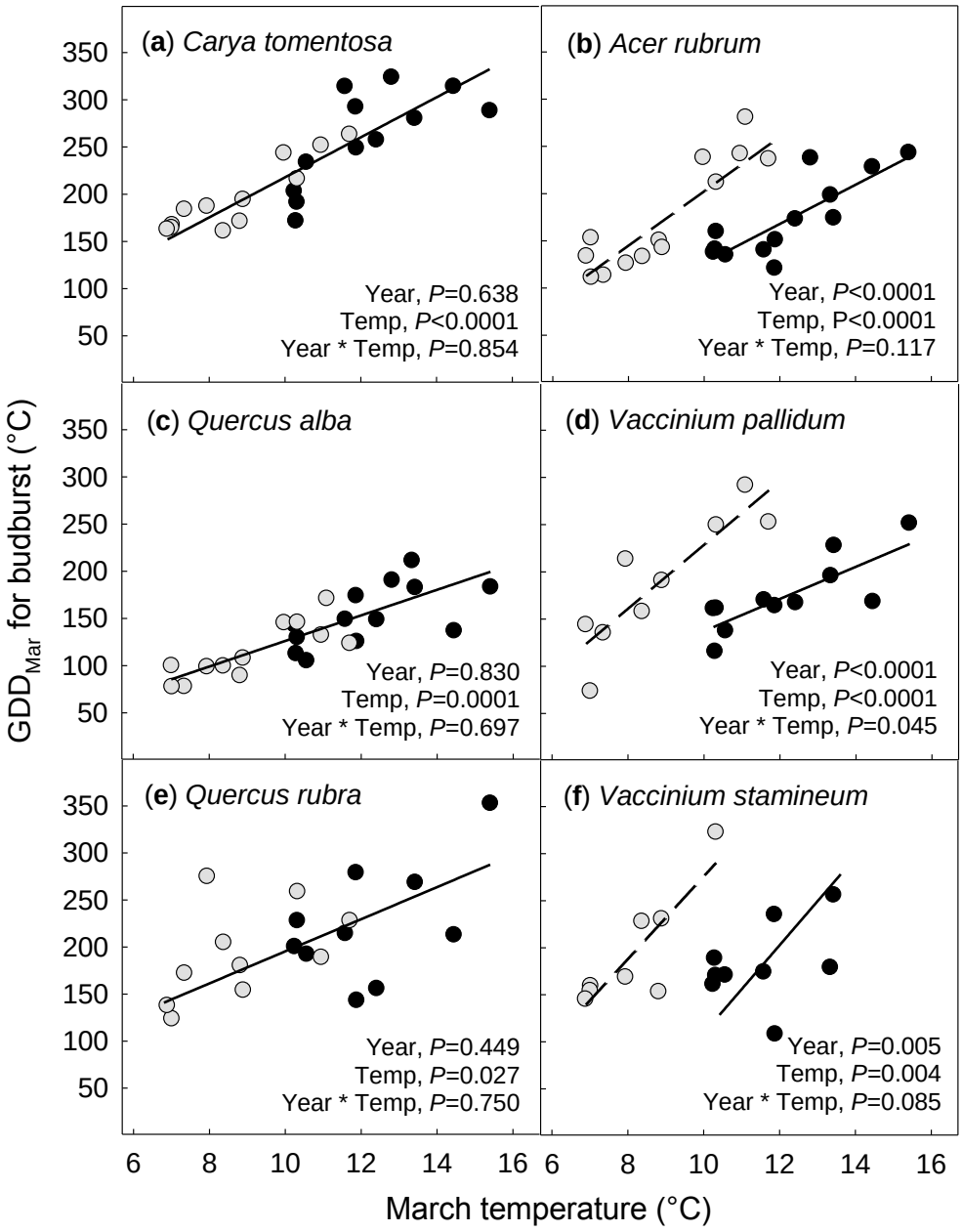

Figure 2.2 Differences among species in the effect of growth temperature on the degree-day sum for budburst in 2011 (black circles) and 2013 (gray circles). Mean March temperature was 3.4 °C higher in 2011 than in 2013. There was no difference between years in the GDD_{Mar} for budburst in (a) CATO, (c) QUAL, and (e) QURU. The GDD_{Mar} for budburst differed between study years in (b) ACRU, (d) VAPA, and (f) VAST.

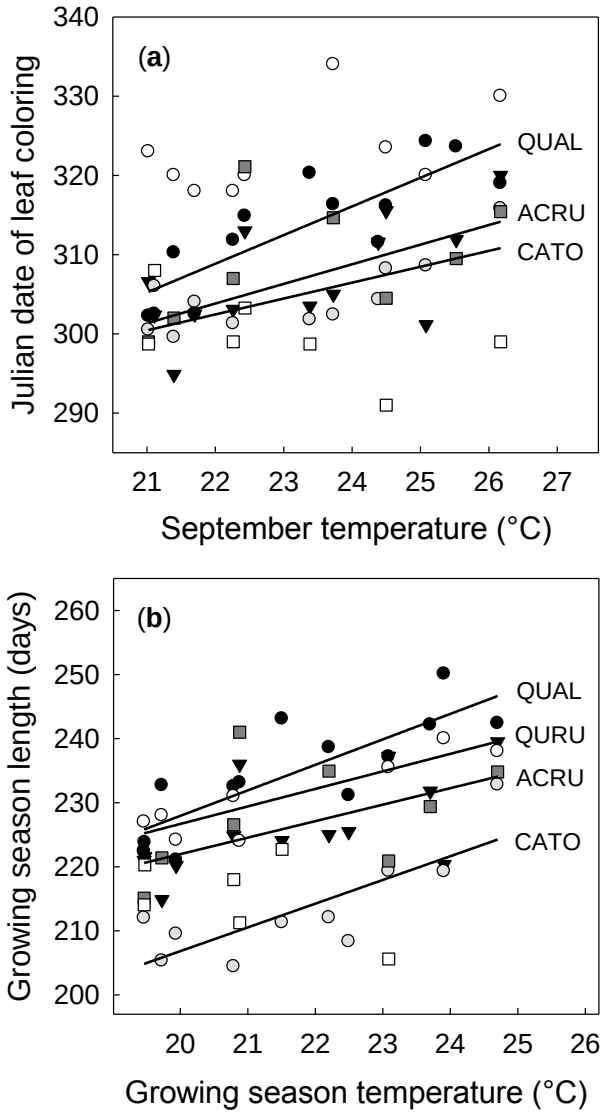

Figure 2.3 The effect of mean chamber temperature on (a) date of leaf coloring and (b) growing season length in 2011. Date of leaf coloring differed significantly among species ($F_{5,311}$=18.998, P<0.0001) and with temperature (r^2=0.14, P=0.003) across all six species. Temperature was significantly correlated with leaf coloring in ACRU (r^2=0.40, P=0.021), CATO (r^2=0.57, P=0.008), and QUAL (r^2=0.70, P=0.0004). Growing season length differed significantly among species ($F_{5,57}$=11.098, P<0.0001) and with temperature (r^2=0.22, P=0.0002) across all six species. Temperature was significantly correlated with growing season length in ACRU (r^2=0.38, P=0.025), CATO (r^2=0.63, P=0.006), QUAL (r^2=0.67, P=0.001), and QURU (r^2=0.81, P=0.003). Symbols and species codes are as in Figure 2.1.

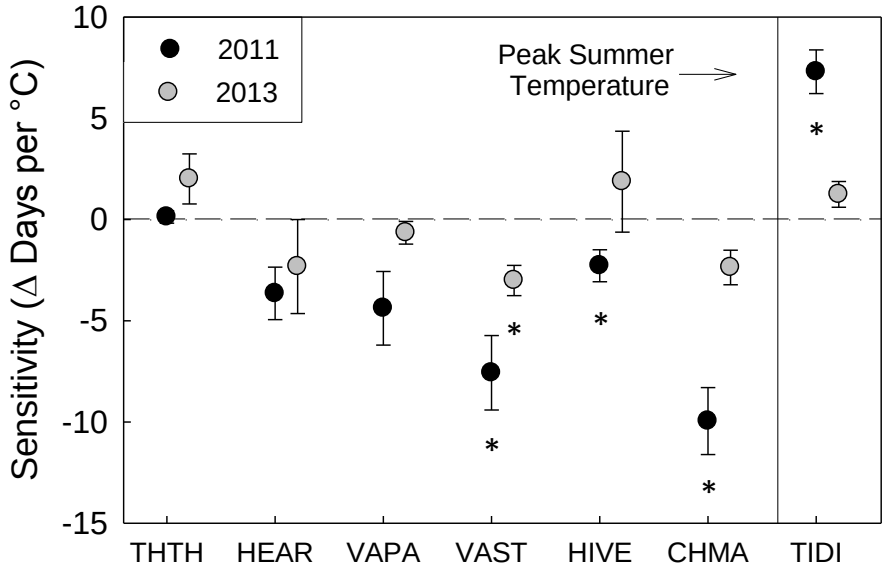

Figure 2.4 Mean phenological sensitivity to temperature (change in flowering date per °C, ±SE) for seven species in Duke Forest, NC in 2011 (black circles) and 2013 (gray circles). Mean March temperature was 3.4 °C higher in 2011 than in 2013. Species are arranged by flowering date from left to right, such that THTH flowers earliest in the spring and TIDI flowers after the peak summer temperature. Significant differences in flowering date between heated and control chambers are indicated with a star ($P \leq 0.05$). Species codes: THTH, *Thalictrum thalictroides*, HEAR, *Hexastylis arifolia*; VAPA, *Vaccinium pallidum*; VAST, *Vaccinium stamineum*; HIVE, *Hieracium venosum*; CHMA, *Chimaphila maculata*; TIDI, *Tipularia discolor*.

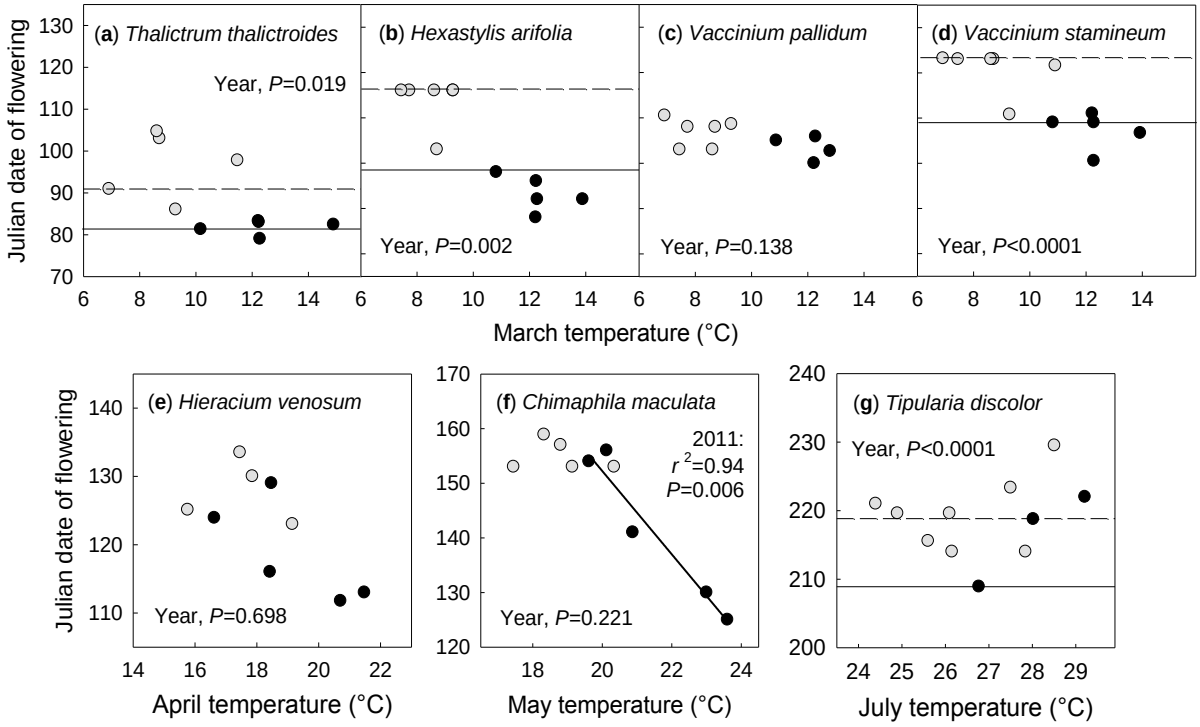

Figure 2.5 Differences among species in the effect of growth temperature on the julian date of flowering in 2011 (black circles) and 2013 (gray circles). Species are arranged by flowering date, such that the earliest flowering species in Duke Forest is (a) THTH, followed by (b) HEAR, (c) VAPA, (d) VAST, (e) HIER, (f) CHMA, and (g) TIDI. Species codes are as in Fig. 4. Horizontal lines represent significant differences in flowering date of control plants between 2011 (solid line) and the colder year 2013 (dashed line). For CHMA, temperature in 2011 was significantly correlated with flowering date.

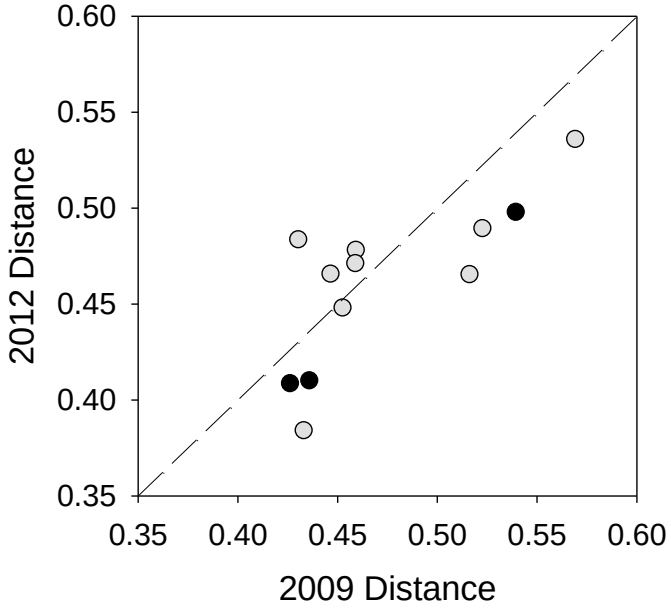

Figure 2.6 Mean Bray-Curtis distance values of each chamber in 2009 and 2012, which were calculated by averaging the 11 unique pairwise distances for each chamber. Control chambers are represented by black circles, whereas heated chambers are shown in gray. The relationship was determined using standardized major axis regression and is not significantly different from the 1:1 line, which is depicted by the dotted line. Specifically, the slope of the line is not significantly different from 1 (slope=0.873, $F_{1,11}$=0.436, P=0.524), and the intercept is not significantly different from 0 (intercept=0.047, t_{11}=0.546, P=0.597).

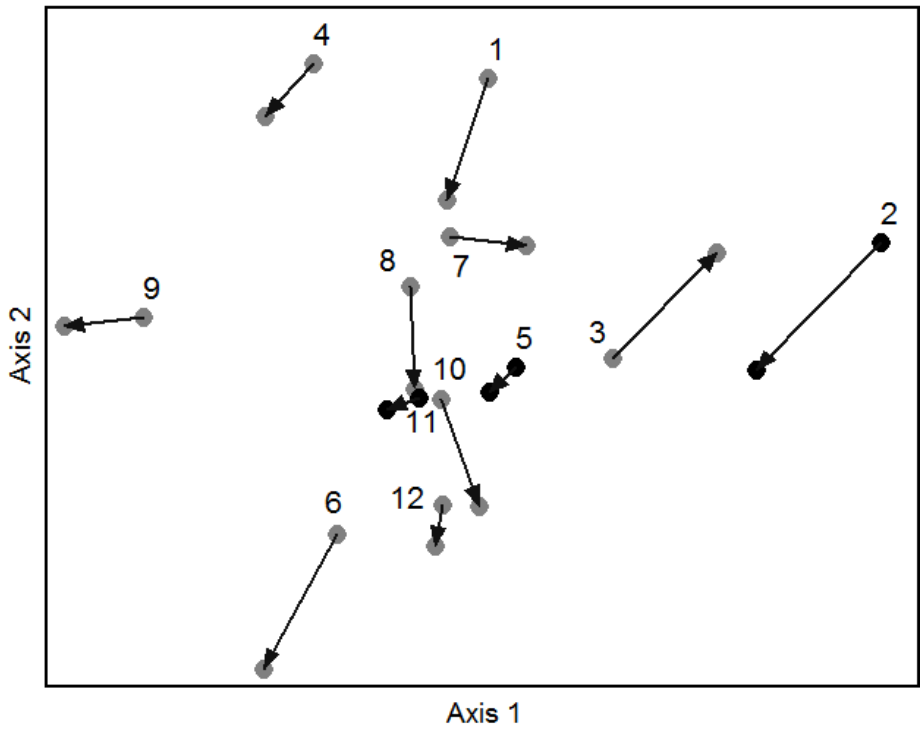

Figure 2.7 A detrended correspondence analysis (DCA) ordination of the 12 chambers in Duke Forest. Control chambers are represented by black circles, whereas heated chambers are shown in gray. Successional vectors show direction and magnitude of change from 2009, before heating began, to 2012, after three years of heating. The first axis explains 27.2% of the variation in species composition among chambers, while the second axis explains an additional 4.0% of the variation.

2.5 Discussion

Experimental warming advanced date of budburst for the six temperate species in this study, although rates of advance varied among species and ranged from 0.8–3.8 days per °C (Table 2.1, Figure 2.1). Nearly all observational and experimental studies agree that the majority of plant species advance phenology with warming (Fitter *et al.*, 1995; Fitter & Fitter, 2002; Menzel, 2003; Parmesan & Yohe, 2003; Root *et al.*, 2003; Primack *et al.*, 2004; IPCC, 2007; Wolkovich *et al.*, 2012). In other field studies, artificial warming of 1.5–5.0 °C has advanced budburst by 1–9 days per °C, with a median response of 4 days per °C (Guak *et al.*, 1998; Gunderson *et al.*, 2012; Morin *et al.*, 2010; Norby *et al.*, 2003; Repo *et al.*, 1996). Two of the tree species studied here have been previously studied, and comparable advances with warming were reported in *A. rubrum* at the rate of 2 days per °C (Norby *et al*., 2003) and *Q. rubra* at the rate of 1.5 days per °C (Gunderson *et al*., 2012). We found that chamber temperature was linearly correlated to budburst date in *C. tomentosa*, *Q. alba*, and *Q. rubra* (Figure 2.1), and linear relationships have successfully been used to describe phenological responses to temperature (Vitasse *et al*., 2010). Experimental studies with strong warming treatments (≥3 °C), which extend beyond the range of warming over the past century, have found nonlinear phenological responses in plants (Morin *et al*., 2010; Salk, 2011; Gunderson *et al.*, 2012). Our data also reveal that there are nonlinear responses of budburst phenology to strong warming, as responses were larger for warming of 0.9–2.0 °C than for 0.9–5.1 °C (Table 2.1). For *A. rubrum*, we only observed a significant advance in budburst date of 2.3–3.8 days per °C under low levels of experimental heating (<2.5 °C, Table 2.1). Such

nonlinear responses suggest that current rates of budburst advancement are unsustainable and may decrease with the strong warming predicted in the coming century.

Nonlinear phenological responses could be explained by a constraining interaction with chilling requirements or photoperiod or both (Cannell & Smith, 1983; Morin *et al*., 2009; Morin *et al*., 2010; Gunderson *et al.*, 2012). Chilling and photoperiod requirements for budburst are physiological mechanisms that minimize the risk for damage by late-spring frosts (Körner & Basler, 2010). As warming progresses, it will be increasingly possible that winter temperatures no longer drop below the threshold required to break bud dormancy (Morin *et al.*, 2009). Models predict that insufficient chilling requirements will decrease the rate of advancement of budburst in temperate species (Morin *et al*., 2009), although a diminished effect of increasing warming has been observed even under identical chilling periods (Greer *et al.*, 2006). Photoperiod has been shown to affect the phenology of some species (Myking & Heide, 1995; Linkosalo *et al.*, 2006) and is another potential environmental cue that can prevent early budburst, regardless of temperature (Körner & Basler, 2010). Under strong warming conditions, the limiting factor in phenological advancement may shift from temperature requirements to light requirements (Morin *et al*., 2010). Despite the important role of such environmental cues on plant phenology, there is still a poor understanding of how temperature and photoperiod interact to control budburst physiology.

Accumulated GDD models have led to important insights into how environmental cues affect budburst of temperate species. By optimizing the start date of a GDD model to improve predictions of budburst date, Gunderson *et al*. (2012) found that warming in mid-

winter months does not promote budburst. Similarly, we found that starting accumulation of GDD on March 1 rather than February 1 reduced treatment variability by 25–50%. The better performance of GDD_{Mar} over GDD_{Feb} suggests that an unfulfilled chilling or photoperiod requirement prevents budburst from occurring in February. Chilling and photoperiod cues promote safety of plant tissues, but represent an evolutionary constraint that may limit the potential for species to advance budburst as climate warms in the future (Salk, 2011). If plants could take full advantage of warmer temperatures, GDD for budburst would have been constant across all chambers. Budburst of all species in warmer chambers required higher GDD_{Mar} (Figure 2.2), however, indicating that the full potential of the growing season is not being used. Because phenological responses failed to fully track warmer temperatures, there will be a limited capacity for increased carbon sequestration in the future.

This experiment examined a diverse set of temperate forest species growing for multiple years under a range of warming treatments, allowing us to identify differences in the phenological response between diffuse- and ring-porous trees. The budburst of all species occurred earlier in a warm year (2011) relative to an unusually cool year (2013). Interannual budburst advances were largest in diffuse-porous species, relative to the ring-porous species (4–4.7 days per °C vs. 1.3–3.3 days per °C, respectively; Table 2.2), and occurred at lower GDD_{Mar} in the warmer year (Figure 2.2). The more conservative response to spring temperature in ring-porous trees represents an adaptive frost-avoidance strategy in trees with large-diameter xylem vessels that are prone to frost-induced dysfunction (Salk, 2011). The phenology of late-successional forest tree species such as *Quercus* is known to be sensitive to photoperiod (Körner & Basler, 2010), which may prevent large responses to global warming

in the future. Experimental warming in 2011, which was representative of warming over the coming century, resulted in advances in leafing of two of the three diffuse-porous species, but none of the three ring-porous species (Table 2.1). These findings support our hypothesis and suggest that diffuse-porous species may gain a competitive advantage over photoperiod-sensitive ring-porous species as forest communities warm in the future.

Warming effects on growing season length

Experimental warming in our study extended the growing season of four common deciduous tree species (*A. rubrum*, *C. tomentosa*, *Q. alba*, *Q. rubra*) by up to 20–29 days (Figure 2.3b), which translates to a rate of 4.0–13.5 days per °C. Warmer March temperatures of 0.9–5.1 °C advanced budburst (Figure 2.1) by as much as 5–15 days, but delays in leaf coloring due to warming were even larger than advances in budburst. Warmer September temperature delayed leaf coloring (Figure 2.3a) by up to 14–20 days or 2.7–10.1 days per °C. These results correspond closely to altitudinal studies and long-term records that have found delays in the end of the growing season by 1–6 days per °C with increasing temperature (Matsumoto *et al.*, 2003; Menzel *et al.*, 2006b; Vitasse *et al.*, 2009; Ibáñez *et al.*, 2010; Gunderson *et al.*, 2012). Field observations and model simulations indicate that an extended growing season can increase productivity in forest ecosystems (Goulden *et al.*, 1996; Rötzer *et al.*, 2004; Richardson *et al.*, 2010). Net productivity of forest ecosystems increased by 1.6% (White *et al.*, 1999) or 2% (Picard *et al.*, 2005) per day added to the growing season. Thus, productivity could potentially increase by about 30% with a 20-day extension of the growing season in the future.

Many factors may interact with phenology to limit increases in carbon sequestration of forests in the future, however. Large shifts to earlier budburst dates may increase the risk for damage by late-spring frosts, which can erase any carbon gains due to longer growing seasons (Augspurger, 2009). Earlier leaf emergence in the spring has a greater influence on seasonal carbon uptake than an equivalent delay of fall senescence, although extension of the growing season is more pronounced in autumn than in spring for many tree species (Matsumoto *et al.*, 2003; Ibáñez *et al.*, 2010; Gunderson *et al.*, 2012). Potential carbon gains in autumn can be offset by increased respiration (Piao *et al.*, 2008), which are exacerbated by lower solar radiation and late-season declines in photosynthetic capacity of old leaves (Salk, 2011; Gunderson *et al.*, 2012). Furthermore, any extension of the end of the growing season can be eliminated by early leaf abscission as a result of drought, herbivory, or disease (Taylor & Whitelaw, 2001).

Warming effects on reproduction

Reproductive phenologies of species in temperate forest communities have a bimodal distribution with peaks in spring and late summer (Kochmer & Handel, 1986). In a temperate grassland, species that flower before the peak summer temperature advanced their reproductive phenology with warming, while species that flower after the peak summer temperature delayed reproduction (Sherry *et al.*, 2007). Our results document the same phenomenon occurring in a temperate forest community. Experimental warming advanced mean flowering by 6–25 days or 2.3–10.0 days per °C in three species (*V. stamineum*, *H. venosum*, *C. maculata*) that flower before the peak summer temperature in mid-July (Figure

2.4). The orchid *T. discolor* flowers after the peak summer temperature in Duke Forest, and experimental warming delayed mean flowering in this species by 10 days or 7.3 days per °C (Figure 2.4). Long-term observations in North America and Europe have documented that flowering has advanced by a mean of 4.6 days per °C (Wolkovich *et al.*, 2012), although delays in reproductive phenology with warming have also been observed for several alpine herbs (Dorji *et al.*, 2013; Hollister *et al.*, 2005; Yu *et al.*, 2010).

The phenological divergence among species could be caused by differential responses of plant development to warming at different temperatures (Sherry *et al.*, 2007). Our results suggest that warming in the spring increased developmental rates of plant species, whereas warming in mid-summer exceeded optimal temperatures for reproduction, thus suspending reproductive development. High temperatures in this experiment inhibited reproduction in two species that flower in mid-summer, *C. maculata* and *T. discolor*. The fruit of both species are capsules that persist for months as seeds are slowly wind-dispersed. We observed early abortion and death of flowers or fruits in heated chambers before fruits could fully ripen. Premature fruit abortion occurred in *C. maculata* whenever mean May temperature exceeded 21 °C, and scapes of *T. discolor* failed to develop whenever mean July temperature exceeded 29°C (see Chapter 3). Future temperature increases of 2 °C above ambient temperature will likely result in reproductive failure for both species. Although current species distributions range as far south as Florida, both species are rare in that state (USDA, 2013). The southern limit of species ranges appears to be controlled by the inability to flower at high temperatures (Chuine, 2010), and warming in the next century will shift the southern range boundary of these species to higher latitudes.

The majority of species in our study responded to experimental warming, including *V. stamineum*, *H. venosum*, *C. maculata,* and *T. discolor* (Figure 2.4). The three non-responders, *T. thalictroides*, *H. arifolia*, and *V. pallidum*, all flower in early spring in Duke Forest (Figure 2.4), refuting our hypothesis. Most studies report that early-blooming species are more sensitive to warming (Rathcke & Lacey, 1985; Bradley *et al*., 1999; Cook *et al*., 2012; Wolkovich *et al.*, 2012, but see Menzel, 2003; Sherry *et al.*, 2007). The discrepancy among studies could be caused by complex and poorly understood interactions among environmental and evolutionary flowering cues that drive the partitioning of species into temporal niches (Pau *et al.*, 2011). Two species that did not track experimental warming, *T. thalictroides* and *H. arifolia*, advanced reproductive timing in a warmer year relative to a colder year (Figures 2.4, 2.5). This response suggests that chilling requirements restricted warming-induced shifts in flowering time in these two species (Cook *et al*., 2012). Photoperiod likely restricted shifts in flowering time of *V. pallidum*, which flowered on the same date in both years (Figure 2.5). It is surprising that different responses to warming were found between the closely related *Vaccinium* species, since genera typically have similar patterns of flowering phenology (Wright & Calderon, 1995; Kang & Jang, 2004).

The effect of warming on plant phenology differed between study years for nearly all species (Figure 2.4). In 2011, *C. maculata* had the strongest response to experimental warming, when warming of 1–3.7 °C advanced flowering by 25 days and fruiting by 24 days. Most species, including *C. maculata,* had no response to warming in the colder year 2013, however (Figure 2.4). Large shifts in flowering time may occur in a warmer future, but even responsive species have constraints that can prevent such shifts from occurring. Our results

highlight the need for multiple years of data collection for correct interpretation of phenological responses to temperature.

Implications for phenological shifts with future warming

The utility of warming experiments for forecasting future changes in plant phenology relies on the assumption that plant responses to experimental warming will match long-term responses to climate change. In a recent study, Wolkovich *et al*. (2012) tested this assumption and found that warming experiments underpredicted advances in vegetative and reproductive phenology relative to long-term historical observations. At our study site in Duke Forest, an unusually cool spring in 2013 allowed us to perform a similar comparison examining phenological responses due to experimental warming versus interannual temperature variability. The effect of experimental warming on budburst of six temperate forest species did not match observations based on interannual temperature variability in sign or magnitude, which is in agreement with previous findings across 36 species (Wolkovich *et al*. 2012). Experimental warming underpredicted advancement in mean budburst by 4-fold (Table 2.2). We found no difference in mean sensitivity of flowering to temperature between the two methods, although species differences existed between experimental and observational methods (Table 2.2). For example, experimental warming delayed flowering of *T. discolor*, but flowering was advanced in a warmer year relative to a colder year.

Large-scale warming experiments unavoidably alter other environmental factors besides temperature, but our experiment minimized many of these changes. The heating treatment did not affect soil water content but did increase atmospheric vapor pressure deficit

inside heated chambers (see Chapter 4). Chamber structure lowered irradiance and increased wind, but we found no significant difference in phenological responses between control chambers and chamberless control plots ($t_{7\text{-}37} \leq 1.89$, $P \geq 0.067$). The high variability in budburst phenology within chambers, which ranged up to 20–31 days within a single chamber, is most likely attributable to edge effects and uneven heating throughout the width of the chamber.

It is important to note that phenological responses to experimental warming in 2011 represent responses to novel warmer climatic conditions, whereas phenological responses to interannual temperature variability in this study fall within historical temperature ranges. Specifically, mean March temperature ranged from 10.3–15.4 °C inside experimental chambers in 2011, relative to the 30-year normal March temperature of 9.6 °C. The results of the two methods are therefore not directly comparable, given that the temperature range was 6.9–10.3 °C between years. In this study, we found nonlinear responses to warming and relatively muted phenological responses in some functional types (i.e. ring-porous trees, early flowering species) due to interactions among temperature and photoperiod cues. Our results suggest that the higher rates of phenological change in long-term observations (see Wolkovich *et al*., 2012) are unsustainable and will decrease with warming above about 3 °C throughout the coming century.

Warming effects on diversity of the forest community

Contrary to our hypothesis, there was no effect of three years of warming on the diversity or community composition of the forest understory (Table 2.3, Figures 2.6, 2.7). There were

also no warming-induced changes in abundance for any of the six common tree and shrub species analyzed in this study. Although rapid changes in species abundance and diversity have been observed in other ecosystems, such as alpine rangelands and salt marshes (Klein *et al.*, 2004; Gedan & Bertness, 2009), this temperate forest community was more resistant to short-term increases in temperature. We found a trend for changing community composition (Table 2.3), but this study may have been too short for significant responses to be detected. Experimental warming at the study site is still ongoing, and it would be worthwhile to continue monitoring chamber community composition to determine the long-term effects of warming. Loss of biodiversity can have large consequences for ecosystem function, potentially driving changes in nutrient dynamics and primary productivity.

REFERENCES

Arft AM, Walker MD, Gurevitch J, *et al*. (1999) Responses of tundra plants to experimental warming: Meta-analysis of the international tundra experiment. *Ecological Monographs*, **69**, 491-511.

Augspurger CK (2009) Spring 2007 warmth and frost: phenology, damage and refoliation in a temperate deciduous forest. *Functional Ecology*, **23**, 1031-1039.

Bradley NL, Leopold AC, Ross J, *et al*. (1999) Phenological changes reflect climate change in Wisconsin. *Proceedings of the National Academy of Sciences of the United States of America*, **96**, 9701-9704.

Cannell MGR, Smith RI (1983) Thermal time, chill days and prediction of budburst in *Picea sitchensis*. *Journal of Applied Ecology*, **20**, 951-963.

Chapin FS, Shaver GR (1996) Physiological and growth responses of arctic plants to a field experiment simulating climatic change. *Ecology*, **77**, 822-840.

Chuine I (2010) Why does phenology drive species distribution? *Philosophical Transactions of the Royal Society B-Biological Sciences*, **365**, 3149-3160.

Cook BI, Wolkovich EM, Parmesan C (2012) Divergent responses to spring and winter warming drive community level flowering trends. *Proceedings of the National Academy of Sciences of the United States of America*, **109**, 9000-9005.

Davis CC, Willis CG, Primack RB, *et al*. (2010) The importance of phylogeny to the study of phenological response to global climate change. *Philosophical Transactions of the Royal Society B-Biological Sciences*, **365**, 3201-3213.

Dorji T, Totland ÃR, Moe SR, *et al*. (2013) Plant functional traits mediate reproductive phenology and success in response to experimental warming and snow addition in Tibet. *Global Change Biology*, **19**, 459-472.

Fitter AH, Fitter RSR, Harris ITB, *et al*. (1995) Relationships between first flowering date and temperature in the flora of a locality in central England. *Functional Ecology*, **9**, 55-60.

Fitter AH, Fitter RSR (2002) Rapid changes in flowering time in British plants. *Science*, **296**, 1689-1691.

Gedan KB, Bertness MD (2009) Experimental warming causes rapid loss of plant diversity in New England salt marshes. *Ecology Letters*, **12**, 842-848.

Goulden ML, Munger JW, Fan SM, *et al*. (1996) Exchange of carbon dioxide by a deciduous forest: Response to interannual climate variability. *Science*, **271**, 1576-1578.

Greer DH, Wunsche JN, Norling CL, *et al*. (2006) Root-zone temperatures affect phenology of bud break, flower cluster development, shoot extension growth and gas exchange of 'Braeburn' (*Malus domestica*) apple trees. *Tree Physiology*, **26**, 105-111.

Guak S, Olsyzk DM, Fuchigami LH, *et al*. (1998) Effects of elevated CO_2 and temperature on cold hardiness and spring bud burst and growth in Douglas-fir (*Pseudotsuga menziesii*). *Tree Physiology*, **18**, 671-679.

Gunderson CA, Edwards NT, Walker AV, *et al*. (2012) Forest phenology and a warmer climate - growing season extension in relation to climatic provenance. *Global Change Biology*, **18**, 2008-2025.

Harte J, Shaw R (1995) Shifting dominance within a montane vegetation community - Results of a climate-warming experiment. *Science*, **267**, 876-880.

Hollister RD, Webber PJ, Bay C (2005) Plant response to temperature in Northern Alaska: Implications for predicting vegetation change. *Ecology*, **86**, 1562-1570.

Ibáñez I, Primack RB, Miller-Rushing AJ, *et al*. (2010) Forecasting phenology under global warming. *Philosophical Transactions of the Royal Society B-Biological Sciences*, **365**, 3247-3260.

IPCC (2007) Climate Change 2007: The Physical Science Basis. Contribution of Working Group I to the Fourth Assessment Report of the Intergovernmental Panel on Climate Change.

Kang H, Jang J (2004) Flowering patterns among angiosperm species in Korea: Diversity and constraints. *Journal of Plant Biology*, **47**, 348-355.

Karl TR, Melillo JM, Peterson TC (2009) Global Climate Change Impacts in the United States. US Global Change Research Program, Cambridge University Press, New York.

Klein JA, Harte J, Zhao XQ (2004) Experimental warming causes large and rapid species loss, dampened by simulated grazing, on the Tibetan Plateau. *Ecology Letters*, **7**, 1170-1179.

Kochmer JP, Handel SN (1986) Constraints and competition in the evolution of flowering phenology. *Ecological Monographs*, **56**, 303-325.

Körner C, Basler D (2010) Phenology under global warming. *Science*, **327**, 1461-1462.

Linkosalo T, Hakkinen R, Hanninen H (2006) Models of the spring phenology of boreal and temperate trees: is there something missing? *Tree Physiology*, **26**, 1165-1172.

Matsumoto K, Ohta T, Irasawa M, *et al*. (2003) Climate change and extension of the *Ginkgo biloba* L. growing season in Japan. *Global Change Biology*, **9**, 1634-1642.

Menzel A (2003) Plant phenological anomalies in Germany and their relation to air temperature and NAO. *Climatic Change*, **57**, 243-263.

Menzel A, Sparks TH, Estrella N, *et al*. (2006a) Altered geographic and temporal variability in phenology in response to climate change. *Global Ecology and Biogeography*, **15**, 498-504.

Menzel A, Sparks TH, Estrella N, *et al*. (2006b) European phenological response to climate change matches the warming pattern. *Global Change Biology*, **12**, 1969-1976.

Morin X, Lechowicz MJ, Augspurger CK, *et al*. (2009) Leaf phenology in 22 North American tree species during the 21st century. *Global Change Biology*, **15**, 961-975.

Morin X, Roy J, Sonie L, Chuine I (2010) Changes in leaf phenology of three European oak species in response to experimental climate change. *New Phytologist*, **186**, 900-910.

Musil CF, Schmiedel U, Midgley GF (2005) Lethal effects of experimental warming approximating a future climate scenario on southern African quartz-field succulents: a pilot study. *New Phytologist*, **165**, 539-547.

Myking T, Heide OM (1995) Dormancy release and chilling requirement of buds of latitudinal ecotypes of *Betula pendula* and *B. pubescens*. *Tree Physiology*, **15**, 697-704.

Norby RJ, Hartz-Rubin JS, Verbrugge MJ (2003) Phenological responses in maple to experimental atmospheric warming and CO_2 enrichment. *Global Change Biology*, **9**, 1792-1801.

Parmesan C, Yohe G (2003) A globally coherent fingerprint of climate change impacts across natural systems. *Nature*, **421**, 37-42.

Parmesan C (2006) Ecological and evolutionary responses to recent climate change. In *Annual Review of Ecology Evolution and Systematics*, Vol. 37, pp. 637-669.

Pau S, Wolkovich EM, Cook BI, *et al*. (2011) Predicting phenology by integrating ecology, evolution and climate science. *Global Change Biology*, **17**, 3633-3643.

Pelini SL, Bowles FP, Ellison AM, *et al*. (2011) Heating up the forest: open-top chamber warming manipulation of arthropod communities at Harvard and Duke Forests. *Methods in Ecology and Evolution*, **2**, 534-540.

Piao SL, Ciais P, Friedlingstein P, *et al*. (2008) Net carbon dioxide losses of northern ecosystems in response to autumn warming. *Nature*, **451**, 49-U3.

Picard G, Quegan S, Delbart N, *et al*. (2005) Bud-burst modelling in Siberia and its impact on quantifying the carbon budget. *Global Change Biology*, **11**, 2164-2176.

Primack D, Imbres C, Primack RB, *et al*. (2004) Herbarium specimens demonstrate earlier flowering times in response to warming in Boston. *American Journal of Botany*, **91**, 1260-1264.

Rathcke B, Lacey EP (1985) Phenological patterns of terrestrial plants. *Annual Review of Ecology and Systematics*, **16**, 179-214.

Repo T, Hanninen H, Kellomaki S (1996) The effects of long-term elevation of air temperature and CO_2 on the frost hardiness of Scots pine. *Plant Cell and Environment*, **19**, 209-216.

Richardson AD, Black TA, Ciais P, *et al*. (2010) Influence of spring and autumn phenological transitions on forest ecosystem productivity. *Philosophical Transactions of the Royal Society B-Biological Sciences*, **365**, 3227-3246.

Root TL, Price JT, Hall KR, *et al*. (2003) Fingerprints of global warming on wild animals and plants. *Nature*, **421**, 57-60.

Rötzer T, Grote R, Pretzsch H (2004) The timing of bud burst and its effect on tree growth. *International Journal of Biometeorology*, **48**, 109-118.

Salk CF (2011) *Will the timing of temperate deciduous trees' budburst and leaf senescence keep up with a warming climate?* Ph.D. Dissertation, Duke University, Durham, NC.

Saxe H, Cannell MGR, Johnsen B, *et al*. (2001) Tree and forest functioning in response to global warming. *New Phytologist*, **149**, 369-399.

Sherry RA, Zhou XH, Gu SL, *et al*. (2007) Divergence of reproductive phenology under climate warming. *Proceedings of the National Academy of Sciences of the United States of America*, **104**, 198-202.

Sparks TH, Jeffree EP, Jeffree CE (2000) An examination of the relationship between flowering times and temperature at the national scale using long-term phenological records from the UK. *International Journal of Biometeorology*, **44**, 82-87.

Taylor JE, Whitelaw CA (2001) Signals in abscission. *New Phytologist*, **151**, 323-339.

USDA (2013) The PLANTS Database. NRCS, National Plant Data Center, Baton Rouge, LA.

Vitasse Y, Porte AJ, Kremer A, *et al*. (2009) Responses of canopy duration to temperature changes in four temperate tree species: relative contributions of spring and autumn leaf phenology. *Oecologia*, **161**, 187-198.

Vitasse Y, Bresson CC, Kremer A, *et al*. (2010) Quantifying phenological plasticity to temperature in two temperate tree species. *Functional Ecology*, **24**, 1211-1218.

Wang J, Ives NE, Lechowicz MJ (1992) The relation of foliar phenology to xylem embolism in trees. *Functional Ecology*, **6**, 469-475.

Warton DI, Wright IJ, Falster DS, *et al*. (2006) Bivariate line-fitting methods for allometry. *Biological Reviews*, **81**, 259-291.

White MA, Running SW, Thornton PE (1999) The impact of growing-season length variability on carbon assimilation and evapotranspiration over 88 years in the eastern US deciduous forest. *International Journal of Biometeorology*, **42**, 139-145.

Williams JW, Jackson ST (2007) Novel climates, no-analog communities, and ecological surprises. *Frontiers in Ecology and the Environment*, **5**, 475-482.

Willis CG, Ruhfel B, Primack RB, *et al*. (2008) Phylogenetic patterns of species loss in Thoreau's woods are driven by climate change. *Proceedings of the National Academy of Sciences of the United States of America*, **105**, 17029-17033.

Wolkovich EM, Cook BI, Allen JM, *et al*. (2012) Warming experiments underpredict plant phenological responses to climate change. *Nature*, **485**, 494-497.

Wright SJ, Calderon O (1995) Phylogenetic patterns among tropical flowering phenologies. *Journal of Ecology*, **83**, 937-948.

Yu HY, Luedeling E, Xu JC (2010) Winter and spring warming result in delayed spring phenology on the Tibetan Plateau. *Proceedings of the National Academy of Sciences of the United States of America*, **107**, 22151-22156.

CHAPTER 3

Experimental warming decreases growth and reproduction in a wintergreen terrestrial orchid, *Tipularia discolor*

3.1 Abstract

Winter temperature in the eastern United States has been increasing nearly twice as fast as the annual average, but studies of warming effects on plants have focused on species that are photosynthetically active in summer. The terrestrial orchid *Tipularia discolor* is leafless in summer and acquires carbon primarily in winter. Like many plant species, the optimum temperature for photosynthesis in *T. discolor* is higher than the maximum temperature throughout most of its growing season, and therefore growth should increase with warming. Using a series of open-top chambers that heated the forest understory by 1.2–5 °C, we measured warming-induced changes in growth, reproduction, and phenology of *T. discolor*. As a consequence of heating, mean vapor pressure deficit (VPD) was higher in the chambers, ranging from 0.18–0.53 kPa above controls. Experimental warming negatively affected growth (change in leaf area from 2010 to 2012) and reproductive fitness (number of flowering stalks, flowers, fruits) in *T. discolor*. A warming of +4.4°C resulted in nearly 60% less growth than under ambient conditions, but is likely due to experimental changes to VPD and not temperature. Leaf-to-air VPD over 1.3 kPa restricted stomatal conductance of *T.*

discolor to 10–40% of maximum conductance. These results highlight the need to account for changes in VPD when estimating temperature responses of plant species under future warming scenarios. Temperature in June–July was critical for flowering, and mean July temperature greater than 29 °C (warming of 3 °C) inhibited flowering. Warming of 1.2 °C delayed the onset of flowering in *T. discolor* by an average of 10 days and fruiting by an average of 5 days. Increasing temperature in the future will be an important limiting factor to the distribution of *T. discolor*, especially along the southern edge of its range.

3.2 Introduction

Mean temperature in the United States is expected to increase by 2–6 °C by 2100 (Karl *et al.*, 2009). Plant responses to warming are highly variable, with the direction and magnitude of responses depending on species and initial environmental conditions (Arft *et al*. 1999; Rustad *et al.*, 2001; Wu *et al*., 2011). Current temperatures in the native environment of many plant species are below their growth optimum, particularly in temperate and boreal regions (Way & Oren, 2010), so future warming is expected to increase growth for many plant species. This expectation, however, is complicated by future changes to atmospheric vapor pressure deficit (VPD), which has strong effects on plant physiology that vary from species to species. Higher temperatures increase the water-holding capacity of the atmosphere, and if relative humidity remains fairly constant in the future (e.g. Trenberth *et al.*, 2005), global warming will cause VPD and the evaporative demand of the atmosphere to rise.

While species success ultimately requires net carbon gain, it also depends on successful reproduction, which may be influenced by climate. Higher temperatures often

increase plant reproduction (Dormann & Woodin, 2002; Pfeifer *et al.*, 2006; De Frenne *et al.*, 2011; Klady *et al.*, 2011), although there are exceptions (Totland & Alatalo, 2002). Warming effects on reproduction are difficult to generalize, because they are influenced by the timing of key reproductive events and interactions with pollinators. It has long been known that temperature influences the timing of flowering and fruiting in plants (Went, 1953; Rathcke & Lacey, 1985), with warming typically shifting reproductive phenology to earlier flowering dates (Fitter & Fitter, 2002; Dunne *et al.*, 2003; Parmesan & Yohe, 2003; Sherry *et al.*, 2007). Studies of the effects of warming on plant reproduction are largely based on studies in alpine and arctic ecosystems, however, and knowledge of warming effects in other ecosystems is lacking.

Studies of understory species in forests are particularly lacking. A unique feature of some understory plant species is that they are winter active and hence potentially influenced both by summer and winter temperatures. The effects of winter warming might be very different than those of summer warming. Winter temperatures in the eastern US have been increasing nearly twice as fast as the annual average (Karl *et al.*, 2009). Mean winter temperature in the eastern US has increased by 1.5–2.2 °C since 1970 (Karl *et al.*, 2009), and the recent winter of 2012 was the fourth warmest on record in the contiguous US (NOAA, 2012). Further research is needed to determine if these climate differences lead to different temperature responses for plants that are active in the winter than for plants active in summer. Ideally, one would consider the influence of climate warming on key demographic features of a winter species, such as growth, reproduction, and phenology. We do just this here.

This study examined the effects of experimental warming on the winter-active terrestrial orchid, *Tipularia discolor* Nutt., in the understory of a temperate forest (Duke Forest, North Carolina, USA). The orchid *T. discolor* has a unique wintergreen phenological pattern where leaves emerge in autumn and senesce in the spring. Due to its phenology, plants are photosynthetically active during periods of low temperature, low VPD, and relatively high light due to a leafless overstory canopy. Previous work has found that the optimal temperature for photosynthesis (T_{opt}) of *T. discolor* is 26 °C, which is over 10 °C higher than maximum temperatures throughout much of its growing season (Tissue *et al.*, 1995). Here, we test the hypothesis that experimental warming of the forest understory will increase growth and reproduction in *T. discolor*. This work was performed in an experimental warming site in the piedmont of NC, where warming was achieved by actively heating open-top chambers to 1.2–5 °C above ambient temperature. As a consequence of heating, mean VPD increased by 0.18–0.53 kPa inside the chambers. To understand how the temperature response of *T. discolor* might be confounded by simultaneous changes in VPD, we also quantified the effect of VPD on orchid physiological responses in the field and under controlled laboratory conditions. Terrestrial orchids are often the first organisms to disappear from disturbed ecosystems and thus serve as bioindicators and early warning signs of problems for ecosystem health (Swarts & Dixon, 2009). Understanding the physiological limits to plant growth and reproduction is important for developing conservation strategies for species susceptible to population declines as a result of climate change.

3.3 Materials and Methods

Study species

The crane-fly orchid, *Tipularia discolor* (Epidendroideae, Calypsoae), is a terrestrial orchid native to eastern North America. It occurs from Massachusetts west to Michigan and south to Texas and Florida (Brown, 1997). The species is summer-deciduous with leaves emerging in the fall (October–November) and senescing in the spring (late April). Individual plants typically consist of a single leaf and produce a corm at its base, which persists for several years (Snow & Whigham, 1989). Leaves are commonly found in dense clusters, and seemingly distinct plants may be genetic clones (Frye, 1993). Different genotypes have been identified within a single cluster, however, indicating genets may intermingle within dense leaf clusters (Smith *et al.*, 2002). Reproduction occurs when plants are leafless; flowers are produced in late July–August, and fruits mature in September–October (Whigham & McWethy, 1980). Only a single pollinator species, a nocturnal moth (*Pseudaletia unipuncta,* armyworm), has been identified for *T. discolor* (Whigham & McWethy, 1980).

Experimental study site

This study was conducted at an ongoing, long-term warming experiment in a *c.* 80-year-old oak-hickory forest stand of Duke Forest (36° 2’ 11” N, 79° 4’ 39” W, 130 m a.s.l.), in the piedmont region near Hillsborough, NC, USA (Lynch, 2006). The mean annual temperature at Duke Forest is 15.5 °C, and the mean annual precipitation is 1140 mm. Winter precipitation in NC has increased by approximately 0.5 mm yr^{-1} over the past 50 years (Boyles & Raman, 2003). Climate data for the site are available from a nearby (8 km)

weather station (Duke Forest Remote Automatic Weather Station, Orange County, NC, USA).

The experimental warming site consists of 15 plots in the forest understory: nine are heated, three are unheated chamber controls, and three are control plots that lack chambers but are equal in surface area to the chambers. The octagonal, open-top chambers are 21.7 m^3 in volume: 5 m in diameter with eight walls that are 1.9 m wide by 1.2 m tall. The chambers are heated by forced air blown over hydronic radiators fed by a closed-loop mixture of hot water and propylene glycol (antifreeze). The heated air is blown into the chambers through 15-cm-diameter plastic plena which hang 45 cm above the ground and run in two concentric rings, one 0.8 m and the other 1.7 m from the chamber walls. Air enters the chambers via two rows of 2-cm-diameter holes separated by 20 cm along the bottom of the plena. Heat delivery to the chambers began in January 2010, and chambers are constantly heated year-round, both day and night. The experiment uses a regression design of chamber heating, where each chamber is heated to a target of 1.5 to 5.5 °C above ambient temperature with 0.5 °C increments between chambers. Maintaining precise target air temperatures over long time periods is difficult, and the assigned treatment levels varied by a small amount over time. Despite this imperfection, the use of a regression design is useful for revealing potential nonlinearities and threshold effects in plant temperature responses. We sampled naturally-occurring plants that were present at the site before the chambers were installed. Specifically, the study species was present in nine of 15 experimental plots (0, 0, 0, 1.5, 2, 2.5, 3, 4, 4.5 °C).

Air temperature (2 temperature probes per chamber), relative humidity (HS-2000V capacitive polymer sensor; Precon, Memphis, TN, USA), soil water content (Model CS616 TDR probes, Campbell Scientific Inc., Logan, UT, USA), and photosynthetically active radiation (PAR) (Model SQ110; Apogee Instruments Inc., Logan, UT, USA) were measured inside each experimental chamber every minute and recorded as hourly means by automated dataloggers (CR1000; Campbell Scientific Inc.). To determine how environmental conditions varied among experimental chambers, mean daily air temperature, VPD, and relative extractable soil water content (REW) were calculated for each chamber. REW was calculated according to the equation:

$$REW = (\theta - \theta_{min})/(\theta_{max} - \theta_{min})$$

where θ is the hourly soil water content, θ_{min} is minimum soil water content, and θ_{max} is the mean maximum volumetric soil water content over the study period. Readings from three or four saturating rainfall events per year were averaged to determine θ_{max}. To account for soil macropore drainage and thus avoid over-estimating θ_{max}, volumetric soil water content from two hours after the peak θ of each saturating rainfall event were used. Further details of the warming experiment can be found in Pelini *et al.* (2011).

Gas exchange physiology

To determine the effect of temperature on potential photosynthetic capacity of *T. discolor* leaves, the response of net CO_2 assimilation (A_n) to varying concentrations of intercellular CO_2 (C_i) was measured from 11:00 to 15:30 h on 11 March 2011. These A_n/C_i curves were measured on five leaves in control chambers and five leaves in heated chambers.

Photosynthesis was measured using a portable infrared gas analyzer equipped with a red–blue light source (LI-6400, Li-Cor, Lincoln, NE, USA) at chamber temperature (10–15.5 °C) and VPD (0.48–1 kPa), under saturating PPFD (500 μmol m^{-2} s^{-1}). The ambient CO_2 (C_a) was decreased stepwise from 400 to 50 ppm and then increased from 400 to 1000 ppm with a total of 11 points per A_n/C_i curve. Rates of photosynthesis were recorded after two minutes at each C_a. Values of A_n were corrected for CO_2 leakage by subtracting 'apparent' photosynthesis quantified with photosynthetically inactive leaves (n=5), following Flexas *et al.* (2007).

Net CO_2 assimilation (A_n) was measured under local environmental conditions in seven experimental chambers using the LI-6400 on eight days throughout 2010–2012. For all measurements, temperature inside the cuvette was set to match the chamber treatment, the relative humidity was held ±10% of ambient conditions, and the CO_2 concentration was set to 400 ppm. Leaves (n=5 per chamber) were measured under a PAR of 100 μmol m^{-2} s^{-1} on 12 November 2010, 10 December 2010, 20 January 2011, and 7 March 2011. This level of PAR corresponds to measured light intensity in November, when the overstory is not yet leafless, and is representative of approximately 30% of daily irradiance conditions in the understory from November to March. Leaves were also measured to match the observed monthly mean daytime understory PAR (January=300, February=450, March=500 μmol m^{-2} s^{-1}) on 18 February 2011, 24 March 2011, 13 January 2012, and 6 March 2012. Photosynthetic rates in this light range are 80–100% of saturating values based on the measured relationship between PAR and A_n for *T. discolor* leaves (n=12) in the experimental chambers (data not shown). All measurements were made on clear days between 10:00 and

15:30 h. Photosynthesis measurements were recorded for a period of four minutes after conditions inside the cuvette stabilized (usually 1–2 minutes) and then averaged to determine A_n for each leaf.

The relationship between VPD and stomatal conductance (g_s) was determined under a series of leaf-to-air VPD (VPD_{leaf}, 0.4–2.6 kPa) for six orchid leaves using the LI-6400 at saturating PPFD (500 μmol m^{-2} s^{-1}) and ambient CO_2 (400 ppm). In February–March 2011, three g_s–VPD_{leaf} curves were measured in control chambers (leaf temperature=12–18 °C) and three curves were measured in heated chambers (leaf temperature=17–22 °C). The VPD inside the cuvette was varied by adjusting the flow rate and proportion of air passing through a desiccant (calcium sulfate). The VPD_{leaf} was increased stepwise from the lowest value obtainable under field conditions, 0.4–1.1 kPa, to a maximum VPD_{leaf} of 1.2–2.6 kPa, with a total of 6–8 points per g_s–VPD_{leaf} curve. Rates of stomatal conductance were recorded after 5–10 minutes at each VPD_{leaf}. The stomatal sensitivity of *T. discolor* was calculated using the approach described by Oren *et al.* (1999):

$$g_s = -m \cdot \ln(\mathrm{VPD_{leaf}}) + b$$

where m is stomatal sensitivity and is equal to the slope of the relationship between g_s and $\ln(VPD_{leaf})$ and b is a reference conductance at VPD_{leaf}=1 kPa.

Temperature curves

A laboratory experiment was conducted on 14–21 January 2013 to isolate the effect of temperature on photosynthesis under conditions of constant VPD_{leaf} (1.0–1.3 kPa). Plants (n=5) were excavated from the study site with roots undisturbed in native soil and transported

to the laboratory for gas exchange measurements, which were completed within a week of excavation. The temperature dependence of photosynthesis was analyzed under a series of leaf temperatures (10–30 °C) at ambient CO_2 (400 ppm), under both low light (PPFD=100 μmol m^{-2} s^{-1}) and saturating PPFD (500 μmol m^{-2} s^{-1}). Measurements were made using the LI-6400 equipped with an expanded temperature control kit (6400-88, Li-Cor), which consists of two metal blocks with water channels connected to a water bath to heat or cool the thermoelectric peltier coolers. The VPD inside the cuvette was held constant (1.0–1.3 kPa) during the temperature curves by adjusting the flow rate and proportion of air passing through a desiccant. Steady-state rates of photosynthesis were reached after 20–30 minutes at each temperature.

Foliar carbon isotope ratios

Carbon isotope ratios of plant leaves provide a time-integrated measure of the ratio of intercellular CO_2 concentration to atmospheric CO_2 concentration (c_i/c_a) and can be used to compare seasonal differences in stomatal regulation (Farquhar *et al*., 1989; Ehleringer, 1991). Leaves (n=5–6) of *T. discolor* were collected from the experimental chambers on 24 March 2011 and 3 April 2012 for carbon isotope analyses. Leaves were oven-dried at 70 °C and ground to a fine powder in liquid nitrogen. When necessary, two leaves were pooled to ensure adequate tissue was available for analysis. The $\delta^{13}C$ of foliar tissue was analyzed with an elemental analyzer (Carla Erba, Model 1110, Milano, Italy) coupled to a Thermo-Finnigan Delta Plus gas isotope mass spectrometer (Bremen, Germany) at the Stable Isotope Mass

Spectrometry Laboratory (Kansas State University, Manhattan, KS, USA). Values of $\delta^{13}C$ were calculated according to standard delta notation:

$$\delta = \left(R_{\text{sample}}/R_{\text{standard}} - 1\right)1000$$

where R is the ratio of the heavy isotope (^{13}C) to the lighter isotope (^{12}C). The standard was belemnite carbonate from the Pee Dee Belemnite Formation, SC, USA, and the precision of the $\delta^{13}C$ measurements was ±0.15‰.

Growth and reproduction

At the beginning of the warming experiment in 2010, there were 108 leaves of *T. discolor* distributed across 12 of the 15 study plots. To increase the sample size of leaves in the chamberless control plots (n=5), an additional 16 leaves were measured outside the experimental plots. All leaves (n=124) were numbered and mapped for relocation in subsequent years. Leaf area (A, cm^2) of these orchids was estimated annually from 2010 to 2012 by measuring leaf length (L, mm) and width (W, mm) and using the allometric equation: $A = 1.23 - 0.037L - 0.026W + 0.008LW$ (r^2=0.998, n=28).

For three years (2010, 2011, 2012) from late July through September, the experimental site was visited weekly to determine the reproductive phenological stage of all orchids. The number of flowering stalks, flower number per stalk, and fruit number per stalk were monitored for each experimental chamber. Flowering date and fruiting date were determined for each flowering stalk. Mean July temperature inside each chamber was used to compare different flowering responses, because the onset of flowering is correlated to mean

temperature during the month of flowering for many plants (Sparks *et al.*, 2000, Menzel *et al.*, 2006).

Statistical analyses

Seasonal differences in VPD among the experimental chambers were analyzed with two-way analyses of variance (ANOVA). The effects of temperature on environmental conditions in the experimental chambers (VPD, REW), growth (percent change in leaf area), foliar $\delta^{13}C$, and orchid reproductive fitness (total flowering stalks per leaf, flowers per stalk, fruits per stalk) were analyzed with least squares regression, as appropriate for the experimental design. A generalized linear model was used to test for the effect of July temperature on total flowering stalks per leaf. Because orchid reproduction was low in experimental chambers, orchid flowering and fruiting data from 2010 and 2011 were combined to increase the sample size for analyses. The relationship between A_n and C_i was fitted for heated and control plots using an exponential equation with three parameters. All temperature curves were fitted using a quadratic polynomial equation. One-way ANOVAs were used to determine if there were differences in CO_2-saturated assimilation rates and flowering phenology between heated and control plots. All analyses were performed using JMP 9.0 (SAS Institute, Cary, NC, USA).

3.4 Results

The temperate forest understory inside experimental open-top chambers in Duke Forest, NC was warmed by a mean of 1.2–5 °C, relative to control chambers, during the study period

(2010–2012). This level of warming corresponds well to expectations of temperature increases for the US over the next century, which ranges from 2–6 °C (Karl *et al.* 2009). Heating did not significantly affect the relative extractable water content (REW) of soil in the experimental chambers over the study period ($F_{1,11}$=3.19, P=0.104).

As a direct effect of temperature manipulation, VPD was also significantly higher inside the heated chambers and ranged from a mean of 0.18–0.53 kPa above controls ($F_{1,11}$=40.79, P<0.0001). This effect closely matched the increase expected due to heating of ambient air without any addition of water vapor (Figure 3.1a). The effect of warming on VPD was greater in summer (JJA) than in winter (DJF) of both years ($F_{1,11}$≥100.55, P<0.0001, Figure 3.1b), as expected from the curvilinear relationship between temperature and the saturated vapor pressure of air (e_{sat}). Mean daily summer VPD was 0.85 ± 0.03 kPa above controls in the hottest chamber, compared to an increase of 0.26 ± 0.02 kPa in mean daily winter VPD. This difference mirrors the climatic difference in the temperature–VPD relationship between summer and winter seasons in Duke Forest over the last 12 years (Figure 3.1c), where the range in mean monthly VPD is larger in the summer than the winter. Mean daytime VPD in Duke Forest, NC in winter was rarely higher than 1.5 kPa throughout the study period, whereas mean daytime VPD was frequently higher in summer, reaching values over 2.5 kPa (data not shown).

The warming treatment had a significant effect on the potential photosynthetic capacity of *T. discolor*. Mean CO_2-saturated A_n was significantly higher in the heated chambers than in the control chambers (10.80 vs. 7.39 μmol m^{-2} s^{-1}, respectively, t_9=6.39, P=0.0002, Figure 3.2). The effect of experimental warming on *in situ* rates of photosynthesis

was dependent on VPD_{leaf}. On 12 November 2010, mean VPD_{leaf} was high (1.6 kPa) and there was a negative effect of warming on A_n (r^2=0.83, P=0.004, n=7). There was a positive effect of warming on A_n (r^2=0.76, P=0.011, n=7) on 6 March 2012, however, when mean VPD_{leaf} was low (0.8 kPa). Across all sampling days, temperature had a positive effect on A_n when VPD_{leaf} was low (<1.3 kPa) under both low and high light conditions (Figure 3.3a). When VPD_{leaf} was high (>1.3 kPa), however, temperature had a negative effect on A_n (Figure 3.3a). Maximum *in situ* A_n was 4.3–5.6 μmol CO_2 m^{-2} s^{-1} under low light conditions and 8.2–11.0 μmol CO_2 m^{-2} s^{-1} under high light conditions (Figure 3.3a).

Net photosynthesis of *T. discolor* peaked at 12 °C under low light conditions and 16.9 °C under high light conditions in the field, and temperatures above or below these optimal temperatures caused declines in A_n (Figure 3.3a). While the temperature for peak A_n differed by about 5 °C with irradiance level under field conditions, the decline in A_n at high temperatures was observed at similar values of VPD_{leaf} (1.3 kPa). When VPD_{leaf} was held constant in laboratory measurements, there was a decline in A_n above the T_{opt} of 19.1 °C under low light and 19.8 °C under high light (Figure 3.3b). Irradiance did not significantly affect T_{opt} in *T. discolor* under laboratory conditions (t_9=0.73, P=0.489).

There was no difference in the g_s–VPD_{leaf} relationship among chambers (Figure 3.4a). For all *T. discolor* leaves, g_s decreased exponentially with increasing VPD_{leaf} (r^2=0.62, P<0.0001, Figure 3.4a). The critical threshold for g_s in *T. discolor* is 1.3 kPa (Figure 3.4b). At VPD_{leaf} greater than 1.3 kPa, the g_s of orchid leaves was restricted to 10–40% of maximum conductance. *In situ* g_s varied significantly with sampling date ($F_{8,256}$=37.24,

P<0.0001), ranging from a minimum of 0.001 mol m^{-2} s^{-1} in November 2010 to a maximum of 0.26 mol m^{-2} s^{-1} in March 2011.

Over the study period of 2010–2012, there was a positive correlation between mean daily VPD and the carbon isotope ratios of *T. discolor* leaves (r^2=0.40, P=0.037, n=11; Figure 3.5a). Differences in mean $\delta^{13}C$ ranged from –30.4‰ in a control chamber to –27.6‰ in a +3.9 °C heated chamber. Increases in total leaf area of *T. discolor* were observed in all chambers from 2010–2012, due to an increase in leaf number and/or leaf size (depending on the chamber). The increases in total leaf area were smaller in heated chambers than in control chambers (r^2=0.51, P=0.030, n=9; Figure 3.5b). A warming of 4.4 °C resulted in nearly 60% less leaf area than controls.

Temperature had a significant negative effect on the number of flowering stalks produced per individual ($F_{1,6}$=26.23, P=0.004), the number of flowers per stalk ($F_{1,21}$=9.34, P=0.006), and the number of fruits per stalk ($F_{1,21}$=11.76, P=0.003) in 2010–2011 (Table 3.1). Mean July temperature had a significant negative effect on the proportion of individuals producing flowering stalks (χ^2_1=6.72, P=0.010). Only individuals at +0 and +1.3 °C produced flowers that developed into fruits in 2010–2011, whereas flowering stalks aborted before any flowers or fruits were produced for orchids growing in +2.5, +3.2, and +4.4 °C chambers. In the +2.5 °C chamber, flowers were produced on one flowering stalk in 2010 and 2011, but the flowers died without producing fruits in both years.

A power failure caused chamber heating to fail from 11–24 July 2012, providing the opportunity to better understand the importance of July temperature on flowering in *T. discolor*. Loss of heating at this critical time for flowering significantly affected orchid

reproduction. In 2012, the number of flowering stalks in the chambers doubled (24 in 2012 vs. 12 in 2010 and 2011) and the mean number of flowers per stalk was significantly higher (26 in 2012 vs. 11 in 2010, 12 in 2011; $F_{1,47}$=7.92, P=0.001). While the warming treatment in July 2012 was restricted to a warming of 2.1 °C, temperature still had a negative effect on the number of flowers ($F_{1,4}$=65.39, P=0.004) produced in this orchid, although the number of fruits were unaffected ($F_{1,4}$=1.88, P=0.264).

Because only one individual flowered in the heated chambers in 2010, it was not possible to analyze the effect of temperature on flowering time in that year. In 2011, a +1.3 °C warming treatment significantly delayed the onset of flowering in *T. discolor* by an average of 10 days ($F_{1,15}$=39.97, P<0.0001) and fruiting by an average of 5 days ($F_{1,10}$=5.73, P=0.040, Table 3.2). Mean flowering date was July 28 ± 2.6 days for orchids (n=11) growing outside the chambers under ambient conditions, August 7 ± 3.1 days for orchids (n=4) at +1.3 °C, and August 10 for an orchid (n=1) at +2.6 °C. Mean fruiting date was August 17 ± 3 days for orchids (n=9) growing under ambient conditions and August 22 ± 0 days for orchids (n=2) at +1.3 °C.

Table 3.1 The number of *T. discolor* leaves, number of stalks per chamber (*n*) and per leaf, flowering stalks (%), mean flowers per stalk and per leaf, fruiting stalks (%), and mean fruits per stalk and per leaf for each experimental chamber containing reproductive individuals of *T. discolor*. A power failure prevented chamber heating from 11–24 July 2012, so mean July temperatures in 2012 are lower than in 2010 and 2011.

Year	Mean July Temp (°C)	Leaf #	*n*	Stalks per Leaf	Flower Stalks (%)	Mean Flowers per Stalk	Mean Flowers per Leaf	Fruiting Stalks (%)	Mean Fruits per Stalk	Mean Fruits per Leaf
2010	25.5 (+0)	7	3	0.43	100	25.6	3.6	100	9.7	1.4
2010	27.7 (+2.1)	13	2	0.15	50	20.0	1.5	0	0	0
2010	28.1 (+2.5)	17	2	0.12	0					
2010	28.6 (+3.2)	23	4	0.17	0					
2010	30.0 (+4.6)	28	0	0						
2011	26.2 (+0)	12	0	0						
2011	27.4 (+1.3)	26	7	0.27	57.1	15.1	0.6	28.6	0.3	0.01
2011	28.7 (+2.6)	16	2	0.13	50	11.5	0.7	0	0	0
2011	29.6 (+3.6)	12	0	0						
2011	30.4 (+4.4)	36	2	0.06	0					
2012	25.7 (+0)	12	1	0.08	100	37.0	3.1	100	12.0	1.0
2012	26.2 (+0.4)	14	3	0.21	100	36.7	2.6	33.3	0.7	0.05
2012	26.3 (+0.5)	19	7	0.37	100	30.4	1.6	57.1	4.9	0.3
2012	26.5 (+0.7)	36	7	0.19	100	30.3	0.8	100	8.9	0.2
2012	27.8 (+2.1)	44	8	0.18	62.5	14.4	0.3	12.5	0.4	0.01

Table 3.2 The number of stalks per plot (*n*), mean flowering date, and mean fruiting date for each experimental chamber containing flowering individuals of *T. discolor*. The "ambient" treatment refers to chamberless control plots. Dates followed by different letters are significantly different ($P<0.05$).

Year	Mean July Temp (°C)	*n*	Flowering Date	Fruiting Date
2010	ambient	8	July 25	August 9
2010	25.5 (+0)	3	July 30	August 15
2010	27.7 (+2.1)	1	July 21	
2011	ambient	11	July 28 a	August 17 a
2011	27.4 (+1.3)	4	August 7 b	August 22 b
2011	28.7 (+2.6)	1	August 10	

Figure 3.1 (a) Midday temperature (°C) and vapor pressure deficit (VPD, kPa) inside the experimental chambers on 15 January 2011 (control chambers, black circles; heated chambers, gray circles). The line depicts the effect of temperature on the saturated vapor pressure of air (e_{sat}), using the mean temperature in control chambers as the reference temperature. (b) Relationships between mean summer (JJA, black circles) and winter (DJF, gray circles) temperature and VPD in the 12 chambers in 2010–2011. (c) Mean monthly summer (black circles) and winter (gray circles) temperature and VPD in Duke Forest, North Carolina from 2000–2012.

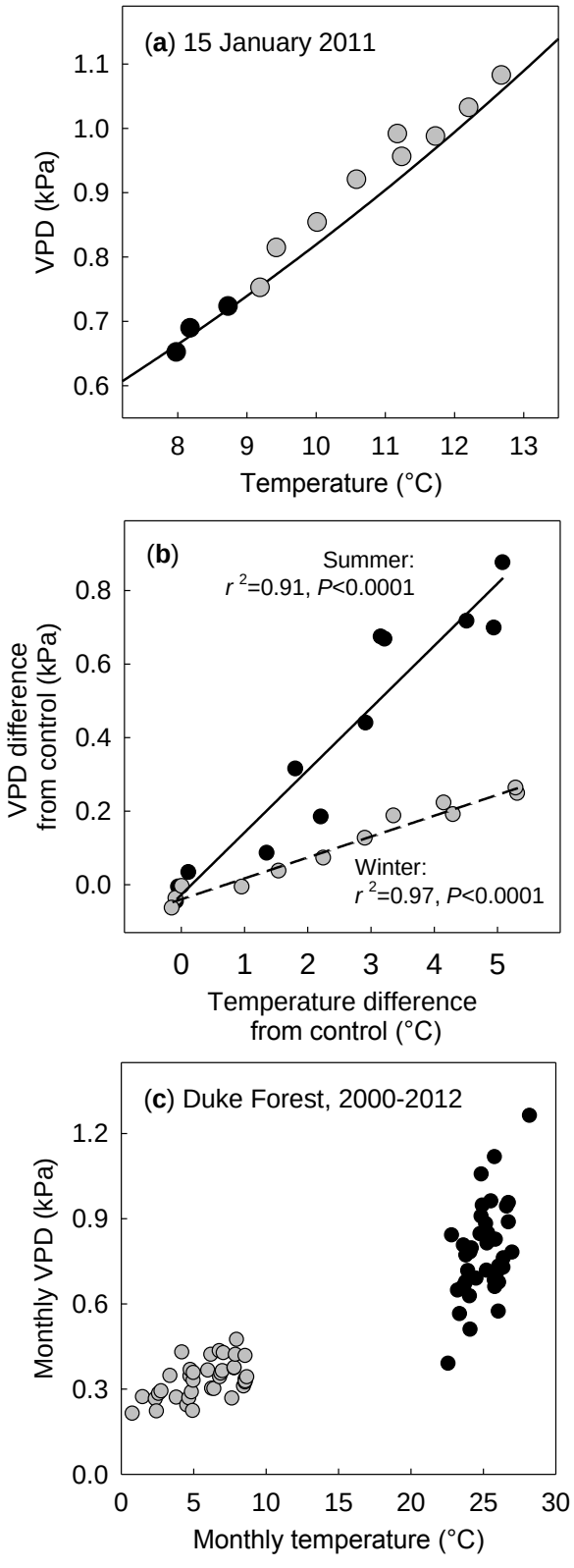
(a) 15 January 2011
VPD (kPa)
Temperature (°C)
(b)
Summer:
r 2=0.91, P<0.0001
Winter:
r 2=0.97, P<0.0001
VPD difference from control (kPa)
Temperature difference from control (°C)
(c) Duke Forest, 2000-2012
Monthly VPD (kPa)
Monthly temperature (°C)

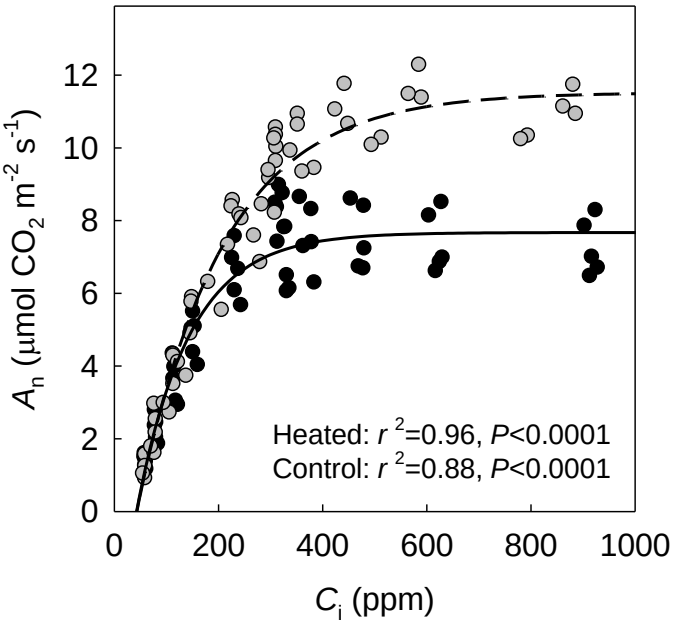

Figure 3.2 The effect of temperature on the relationship between net CO_2 assimilation (A_n) and intercellular CO_2 concentration (C_i) in *T. discolor* leaves (control chambers, black circles; heated chambers, gray circles). Curves were obtained at a temperature of 10–12 °C (control) or 14–16 °C (heated), light level of 500 μmol m^{-2} s^{-1}, and VPD of 0.5–1 kPa for 5 plants per treatment on 11 March 2011.

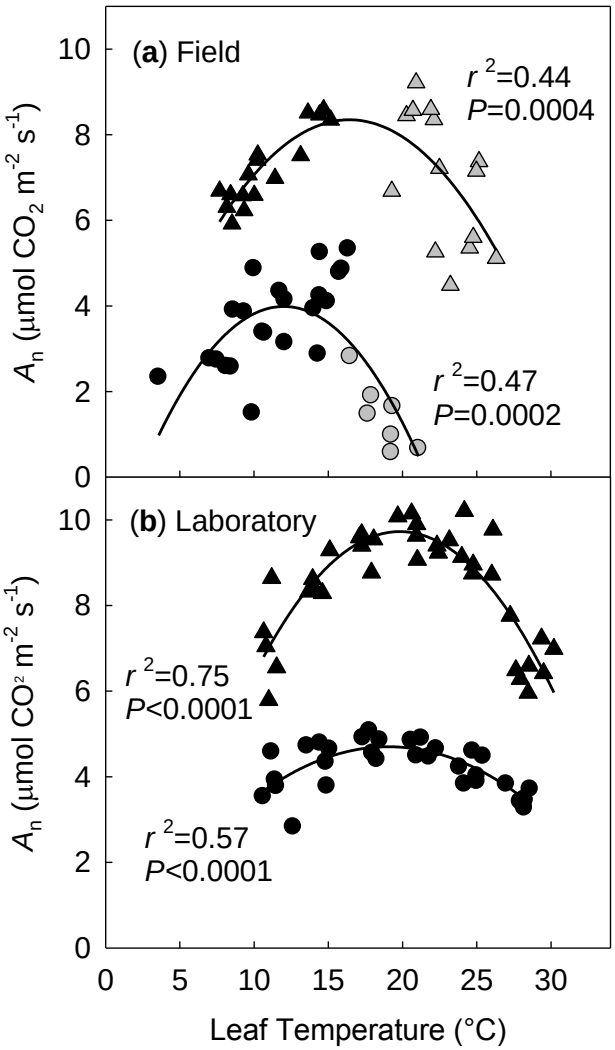

Figure 3.3 (a) Relationship between leaf temperature (°C) and mean *in situ* net CO_2 assimilation (A_n) of *T. discolor* leaves in experimental chambers (n=5) from 2010–2012. Low light conditions (PAR=100 μmol m^{-2} s^{-1}) are shown as circles, and high light conditions (PAR=300–500 μmol m^{-2} s^{-1}) are shown as triangles. Symbols are shaded gray when VPD_{leaf}>1.3 kPa. (b) Relationship between leaf temperature and A_n of orchid leaves measured in the laboratory under constant VPD_{leaf} (1.0–1.3 kPa). Low light conditions (PAR=100 μmol m^{-2} s^{-1}) are shown as circles, and high light conditions (PAR=500 μmol m^{-2} s^{-1}) are shown as triangles.

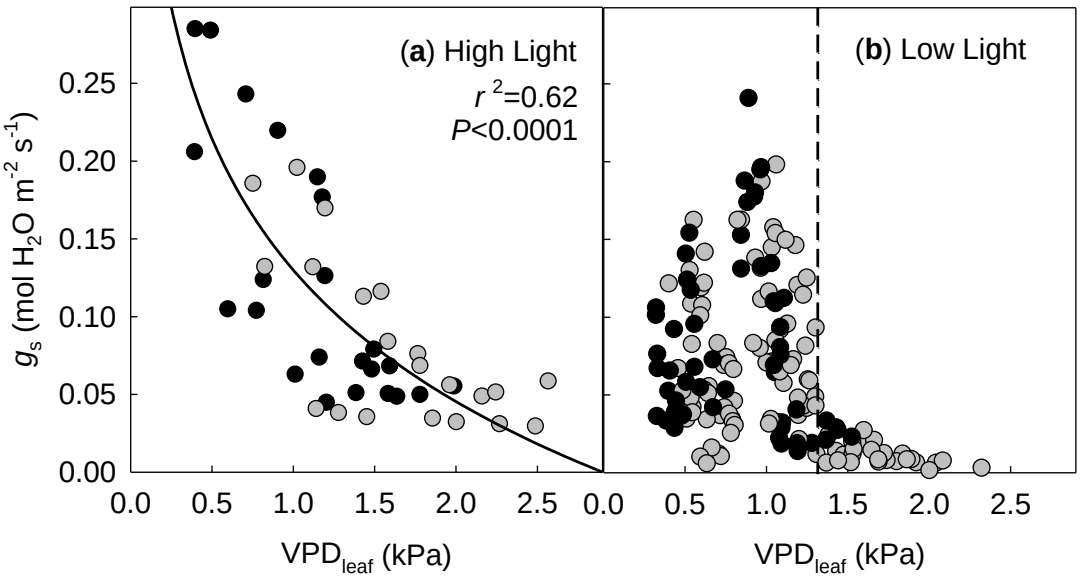

Figure 3.4 The relationship between leaf-to-air VPD (VPD_{leaf}) and stomatal conductance (g_s) of *T. discolor* leaves under (a) high light (500 μmol m^{-2} s^{-1}) and (b) low light (100 μmol m^{-2} s^{-1}) for control (black circles) and heated (gray circles) chambers. The dotted line at 1.3 kPa represents the VPD_{leaf} at which stomatal closure restricted g_s. Each panel represents data collected in Duke Forest, NC by different procedures: (a) Each g_s–VPD_{leaf} curve (n=3 per treatment) was obtained at a temperature of 12–18 °C (control) or 17–22 °C (heated) and ambient CO_2 concentration of 400 ppm in February–March 2011. The mean relationship between $\ln(VPD_{leaf})$ and g_s is plotted ($g_s = -0.122 \cdot \ln(VPD_{leaf}) + 0.131$). (b) Each value is the g_s of an individual leaf (n=161) measured under chamber conditions during winter of 2010–2011.

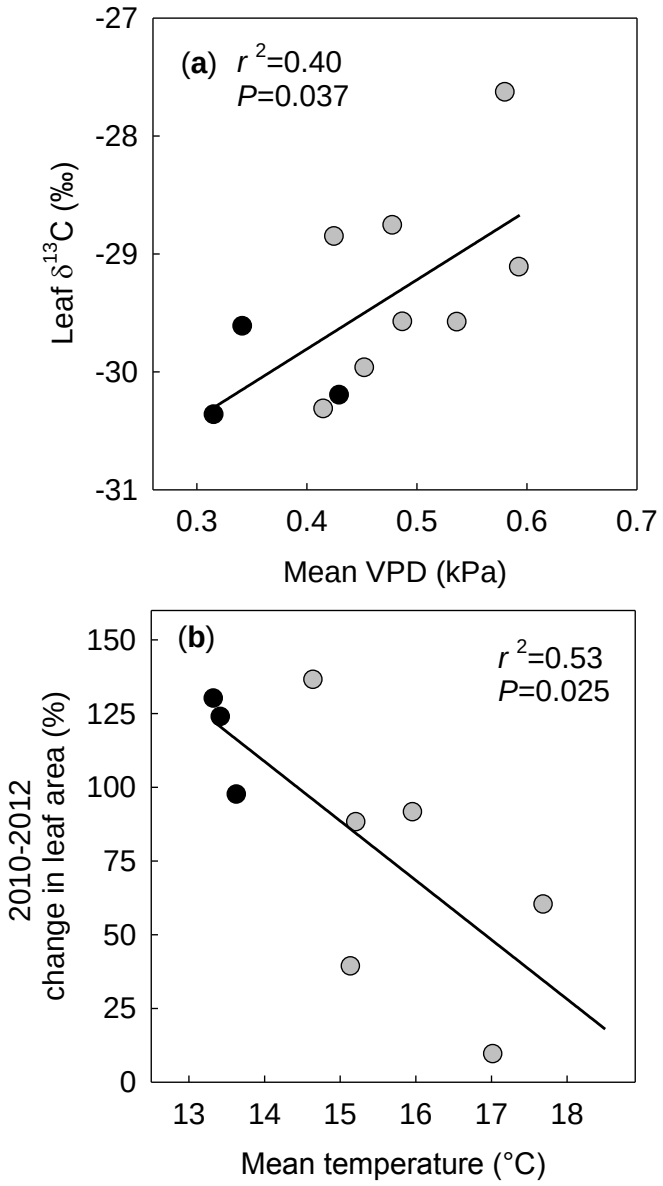

Figure 3.5 (a) Relationship between mean daily VPD and foliar carbon isotope ratios ($\delta^{13}C$) for *T. discolor* leaves. Values are means of 5–6 leaves per treatment and were collected on 24 March 2011 and 2 April 2012. (b) Relationship between mean daily temperature and change in total leaf area (%) of *T. discolor* from 2010–2012. Values are means of 2–44 leaves per chamber. Control chambers are shown in black, and heated chambers are shaded gray.

3.5 Discussion

Experimentally increased temperature had a negative effect on growth (Figure 3.5b) and reproduction (Table 3.1) of the temperate terrestrial orchid, *T. discolor*. Warming of 4.4 °C resulted in nearly 60% less leaf area in this species (Figure 3.5b). These findings are contrary to the temperature response observed in most species (Arft *et al*., 1999; Rustad *et al.*, 2001; Wu *et al*., 2011) and are particularly surprising considering that this species is photosynthetically active only in winter, when temperature is usually well below the optimum for photosynthesis. Specifically, maximum net assimilation was observed at 19–20 °C (Figure 3.3b) under conditions of fixed VPD, so the warming treatment would be expected to enhance photosynthesis on 150 of the 180 days from November to April 2010. Furthermore, orchids in heated chambers had a greater photosynthetic capacity, as indicated by higher light-saturated photosynthetic rates in heated chambers compared to controls (Figure 3.2). In another wintergreen terrestrial orchid, *Himantoglossum hircinum*, population growth was favored by warming over the past several decades in Germany (Pfeifer *et al.*, 2006).

If the decrease in growth of *T. discolor* at higher temperatures (Figure 3.5b) is inconsistent with a direct response to temperature, then why was growth of *T. discolor* negatively affected by experimental warming? Relative extractable water content was not affected by the experimental treatment, so soil water content does not explain the results. The temperature increase of 1.2–5 °C in this experiment was accompanied by a concurrent increase in VPD of 0.18–0.53 kPa, and our results reveal a dominant role of VPD on plant carbon gain. The changes in VPD in our experiment closely followed expected vapor

pressure changes due to heating, based on the relationship between temperature and e_{sat} (Figure 3.1a). Stomatal conductance decreases exponentially with increasing VPD (Figure 3.4), and under field conditions, the effect of VPD on stomatal conductance is most often noticeable as VPD_{leaf} increases to near 1 kPa (Körner, 1994). Our results indicated that stomatal conductance of *T. discolor* was severely restricted when VPD_{leaf} was above 1.3 kPa (Figure 3.4). At these high values of VPD, conductance was restricted to 10–40% of maximum conductance. Field measurements of *in situ* photosynthesis indicate that CO_2 assimilation declined when VPD_{leaf} was higher than 1.3 kPa, even though air temperature remained below the T_{opt} of *T. discolor* (Figure 3.3a). The carbon isotope ratios of *T. discolor* leaves provide a time-integrated measure of c_i/c_a, which is dependent on seasonal regulation of stomata and photosynthetic demand for CO_2 (Farquhar *et al.*, 1989; Ehleringer, 1991). The higher $\delta^{13}C$ of *T. discolor* leaves in heated chambers indicates that these orchids had lower c_i/c_a and stomatal conductance over the growing season, compared to orchids in control chambers (Figure 3.5a). Collectively, our results strongly suggest the decline in growth of *T. discolor* leaves in heated chambers is due to the response of orchid stomata to VPD.

It is possible to compare the stomatal VPD response of *T. discolor* to other mesic-adapted species, because there is a proportionality between stomatal conductance at low VPD (1 kPa) and the sensitivity of the closure response across plant functional types (Oren *et al.*, 1999). Oren *et al*. (1999) showed that the mean slope of this relationship is consistently 0.6 for mesic species. This remarkable convergence among species is in agreement with the role of stomata regulating leaf water potential near a constant value (Oren *et al.*, 1999). Here, we found that the slope for *T. discolor* is 0.122 mol m^{-2} s^{-1} $ln(kPa)^{-1}$ given a reference

conductance of 0.131 mol m^{-2} s^{-1} at a VPD of 1 kPa (Figure 3.4a), so this orchid has more sensitive stomata than most mesic species. The highly responsive stomata of *T. discolor* prevent excessive transpiration and water loss when VPD is high, but this strategy will create a reduced capacity for CO_2 assimilation if VPD increases in the future.

These results emphasize the importance of explicitly accounting for changes in VPD when estimating temperature responses of plant species under future warming scenarios. If relative humidity remains fairly constant in the future (e.g. Trenberth *et al.*, 2005), there will be widespread increases in VPD with global warming. Climate change in the future will likely have a negative impact on this species, and perhaps other winter-active species, because *T. discolor* is sensitive to increases in VPD. Increased atmospheric CO_2 concentrations may at least partially offset the VPD-induced growth reductions in *T. discolor*, as photosynthesis of *T. discolor* is not CO_2-saturated at current atmospheric CO_2 concentrations (Figure 3.2).

Warming effects on reproduction

In our study species, although photosynthesis occurs only in winter, flowering occurs in late summer when plants are leafless. Experimental warming negatively affected reproductive success (number of flowering stalks, number of flowers, number of fruits) of *T. discolor* (Table 3.1). We observed the formation of flowering stalks in multiple heated chambers, but these elongating stalks and floral buds quickly withered and died before any flowers were produced. At ambient temperatures this species produced an average of 30.8 ± 1.2 flowers and 10.7 ± 1.0 fruits per plant (n=24), similar to observations by Snow & Whigham (1989).

With a warming of 1.3–2.6 °C, reproduction was drastically reduced to a mean of 11.5–20 flowers per plant and 0–0.3 fruits per plant (Table 3.1). Warming reduced mean fruit production more than flower production in this experiment, suggesting a carbon limitation. Elsewhere it has been shown that the cost of fruit production is double the cost of producing an inflorescence in *T. discolor* (Snow & Whigham, 1989).

The timing of orchid flowering is generally not well understood, but day temperature is known to be important in controlling flowering in popular ornamental orchids such as *Phaleonopsis* (Blanchard & Runkle, 2006). Exposure to 29 °C for 8 h or longer inhibited flowering in several *Phaleonopsis* hybrids (Newton & Runkle, 2009). In this study, mean July temperatures greater than 29 °C inhibited flowering (Table 3.1). It is likely that June temperature also affects flowering in *T. discolor*, since the flowering response to warming differed between years with similar mean July temperatures (Table 3.1). Increasing summer temperature could severely limit the reproductive success of *T. discolor* in the future.

Experimental warming delayed the onset of flowering in *T. discolor* by 10 days and delayed fruiting by 5 days (Table 3.2). This phenological shift was observed with an increase in mean July temperature from 26.2 °C in the control plot to 27.4 °C in the heated chamber, corresponding to a warming of 1.3 °C. The response of *T. discolor* falls within the range of observed shifts in orchid flowering dates in Hungary (10 vs. 6–14 days, respectively) over the past 50 years (Molnar *et al.*, 2012). Most plant species respond to increasing temperatures with earlier flowering (Fitter & Fitter, 2002; Dunne *et al.*, 2003), including the majority of orchid species that have been studied (Molnar *et al.*, 2012). Delays in reproductive phenology have been observed, however, for three temperate grassland species (Sherry *et al.*,

2007) and several alpine herbs (Hollister *et al.*, 2005; Yu *et al.*, 2010; Dorji *et al.*, 2013). Sherry *et al*. (2007) reported warming-induced delays in flowering for species that flower after the peak summer temperature. Our results support their findings, since the delayed flowering of *T. discolor* occurs after the peak summer temperature in Duke Forest.

Speculations on possible disruptions of plant–pollinator interactions due to climate change are frequent in the literature (Parmesan, 2006; Hegland *et al.*, 2009). Could delayed flowering of *T. discolor* in the future cause a temporal mismatch with its pollinator, *P. unipuncta*? Pollination of *T. discolor* is important for maintaining the orchid population, as selfing is thought to be rare in this species (Whigham & McWethy, 1980; Snow & Whigham, 1989). It is not likely that *T. discolor* could easily switch from one symbiotic partner to another, because there are few pollinator species active while this orchid is flowering (Whigham & McWethy, 1980). The upper temperature limit for survival of *P. unipuncta* is 31 °C (Guppy, 1969), and high temperatures are thought to limit populations of *P. unipuncta* in the southern US (Callahan & Chapin, 1960; McLaughlin, 1962). Since the upper temperature limit for flowering in *T. discolor* is 29 °C (Table 3.1), global warming can be predicted to restrict *T. discolor* before it restricts *P. unipuncta*. No mismatch in the plant–pollinator relationship should occur as long as the phenological responses to warming in both species shift linearly and at parallel magnitudes (Hegland *et al.*, 2009). Further research is required to determine the likelihood of a future plant–pollinator mismatch between *T. discolor* and *P. unipuncta*.

Increasing temperature in the future will be an important limiting factor to reproduction in *T. discolor*, especially along the southern edge of its range. Currently, *T.*

discolor is found as far south as northern Florida, but the species is threatened in that state (Coile & Garland, 2003). The distribution of *T. discolor* will likely become smaller in the future as a result of climate change. It has been recognized that conservation of orchid species may require translocation of propagated individuals to favorable sites (Swarts & Dixon, 2009). Our findings show that suitable locations must have a mean July temperature below 29 °C for orchid seedlings to successfully reproduce.

REFERENCES

Arft AM, Walker MD, Gurevitch J, *et al*. (1999) Responses of tundra plants to experimental warming: Meta-analysis of the international tundra experiment. *Ecological Monographs*, **69**, 491-511.

Blanchard MG, Runkle ES (2006) Temperature during the day, but not during the night, controls flowering of *Phalaenopsis* orchids. *Journal of Experimental Botany*, **57**, 4043-4049.

Boyles RP, Raman S (2003) Analysis of climate trends in North Carolina (1949-1998). *Environment International*, **29**, 263-275.

Brown PM (1997) *Wild Orchids of the Northeastern United States* Cornell University Press, Ithaca, NY.

Callahan P, Chapin JB (1960) Morphology of the reproductive systems and mating in two representative members of the family Noctuidae, *Pseudaletia unipuncta* and *Peridroma margaritosa*, with comparison to *Heliothis zea*. *Ann Ent Soc Amer*, **53**, 763-782.

Coile NC, Garland MA (2003) Notes on Florida's Endangered and Threatened Plants, Botany Contribution No. 38, 4th ed. FL Dept. Agric. & Consumer Serv., Div. Plant Industry, Gainesville, FL.

De Frenne P, Brunet J, Shevtsova A, *et al*. (2011) Temperature effects on forest herbs assessed by warming and transplant experiments along a latitudinal gradient. *Global Change Biology*, **17**, 3240-3253.

Dorji T, Totland ÃR, Moe SR, *et al*. (2013) Plant functional traits mediate reproductive phenology and success in response to experimental warming and snow addition in Tibet. *Global Change Biology*, **19**, 459-472.

Dormann CF, Woodin SJ (2002) Climate change in the Arctic: using plant functional types in a meta-analysis of field experiments. *Functional Ecology*, **16**, 4-17.

Dunne JA, Harte J, Taylor KJ (2003) Subalpine meadow flowering phenology responses to climate change: Integrating experimental and gradient methods. *Ecological Monographs*, **73**, 69-86.

Ehleringer JR (1991) $^{13}C/^{12}C$ fractionation and its utility in terrestrial plant studies. In *Carbon Isotope Techniques* (eds Coleman D, Fry B) pp. 187-200. Chapman and Hall, New York.

Farquhar GD, Ehleringer JR, Hubick KT (1989) Carbon isotope discrimination and photosynthesis. *Annual Review of Plant Physiology and Plant Molecular Biology*, **40**, 503-537.

Fitter AH, Fitter RSR (2002) Rapid changes in flowering time in British plants. *Science*, **296**, 1689-1691.

Flexas J, Díaz-Espejo A, Berry JA, *et al*. (2007) Analysis of leakage in IRGA's leaf chambers of open gas exchange systems: quantification and its effects in photosynthesis parameterization. *Journal of Experimental Botany*, **58**, 1533-1543.

Frye CT (1993) *Population genetics and ecology of the clonal orchid Tipularia discolor (Pursh) Nutt. (Orchidaceae)*. Master's Thesis, Wake Forest University, Winston-Salem, North Carolina.

Guppy JC (1969) Some effects of temperature on immature stages of armyworm, *Pseudaletia unipuncta* (Lepidoptera - Noctuidae), under controlled conditions. *Canadian Entomologist*, **101**, 1320-1327.

Hegland SJ, Nielsen A, Lazaro A, *et al*. (2009) How does climate warming affect plant-pollinator interactions? *Ecology Letters*, **12**, 184-195.

Hollister RD, Webber PJ, Bay C (2005) Plant response to temperature in Northern Alaska: Implications for predicting vegetation change. *Ecology*, **86**, 1562-1570.

Karl TR, Melillo JM, Peterson TC (2009) Global Climate Change Impacts in the United States. US Global Change Research Program, Cambridge University Press, New York.

Klady RA, Henry GHR, Lemay V (2011) Changes in high arctic tundra plant reproduction in response to long-term experimental warming. *Global Change Biology*, **17**, 1611-1624.

Körner C (1994) Leaf diffusive conductances in the major vegetation types of the globe. In: *Ecophysiology of Photosynthesis* (eds Schulze ED, Caldwell MM) Ecological Studies, Vol. 100, pp. 463-484. Springer-Verlag, Berlin.

Lynch IP (2006) The Duke Forest at 75: A Resource for All Seasons. Office of the Duke Forest, Durham, North Carolina.

McLaughlin RE (1962) Effect of temperature upon larval mortality of armyworm, *Pseudaletia unipuncta* (Haworth). *Journal of Insect Pathology*, **4**, 279.

Menzel A, Sparks TH, Estrella N, *et al*. (2006) Altered geographic and temporal variability in phenology in response to climate change. *Global Ecology and Biogeography*, **15**, 498-504.

Molnar AV, Tokolyi J, Vegvari Z, *et al*. (2012) Pollination mode predicts phenological response to climate change in terrestrial orchids: a case study from central Europe. *Journal of Ecology*, **100**, 1141-1152.

Newton LA, Runkle ES (2009) High-temperature inhibition of flowering of *Phalaenopsis* and *Doritaenopsis* orchids. *Hortscience*, **44**, 1271-1276.

NOAA (2012) State of the Climate: National Overview for February 2012, Vol. 2013. NOAA National Climatic Data Center.

Oren R, Sperry JS, Katul GG, *et al*. (1999) Survey and synthesis of intra- and interspecific variation in stomatal sensitivity to vapour pressure deficit. *Plant Cell and Environment*, **22**, 1515-1526.

Parmesan C, Yohe G (2003) A globally coherent fingerprint of climate change impacts across natural systems. *Nature*, **421**, 37-42.

Parmesan C (2006) Ecological and evolutionary responses to recent climate change. *Annual Review of Ecology Evolution and Systematics*, **37**, 637-669.

Pelini SL, Bowles FP, Ellison AM, *et al*. (2011) Heating up the forest: open-top chamber warming manipulation of arthropod communities at Harvard and Duke Forests. *Methods in Ecology and Evolution*, **2**, 534-540.

Pfeifer M, Wiegand K, Heinrich W, *et al*. (2006) Long-term demographic fluctuations in an orchid species driven by weather: implications for conservation planning. *Journal of Applied Ecology*, **43**, 313-324.

Rathcke B, Lacey EP (1985) Phenological patterns of terrestrial plants. *Annual Review of Ecology and Systematics*, **16**, 179-214.

Rustad LE, Campbell JL, Marion GM, *et al*. (2001) A meta-analysis of the response of soil respiration, net nitrogen mineralization, and aboveground plant growth to experimental ecosystem warming. *Oecologia*, **126**, 543-562.

Sherry RA, Zhou XH, Gu SL, *et al*. (2007) Divergence of reproductive phenology under climate warming. *Proceedings of the National Academy of Sciences of the United States of America*, **104**, 198-202.

Smith JL, Hunter KL, Hunter RB (2002) Genetic variation in the terrestrial orchid *Tipularia discolor*. *Southeastern Naturalist*, **1**, 17-26.

Snow AA, Whigham DF (1989) Costs of flower and fruit production in *Tipularia discolor* (Orchidaceae). *Ecology*, **70**, 1286-1293.

Sparks TH, Jeffree EP, Jeffree CE (2000) An examination of the relationship between flowering times and temperature at the national scale using long-term phenological records from the UK. *International Journal of Biometeorology*, **44**, 82-87.

Swarts ND, Dixon KW (2009) Terrestrial orchid conservation in the age of extinction. *Annals of Botany*, **104**, 543-556.

Taiz L, Zeiger E (2002) *Plant Physiology*, 3rd edn. Sinauer Associates, Sunderland, MA.

Tissue DT, Skillman JB, McDonald EP, *et al*. (1995) Photosynthesis and carbon allocation in *Tipularia discolor* (Orchidaceae), a wintergreen understory herb. *American Journal of Botany*, **82**, 1249-1256.

Totland Ø, Alatalo JM (2002) Effects of temperature and date of snowmelt on growth, reproduction, and flowering phenology in the arctic/alpine herb, *Ranunculus glacialis*. *Oecologia*, **133**, 168-175.

Trenberth KE, Fasullo J, Smith L (2005) Trends and variability in column-integrated atmospheric water vapor. *Climate Dynamics*, **24**, 741-758.

Way DA, Oren R (2010) Differential responses to changes in growth temperature between trees from different functional groups and biomes: a review and synthesis of data. *Tree Physiology*, **30**, 669-688.

Went FW (1953) The effect of temperature on plant growth. *Annual Review of Plant Physiology and Plant Molecular Biology*, **4**, 347-362.

Whigham DF, McWethy M (1980) Studies on the pollination ecology of *Tipularia discolor* (Orchidaceae). *American Journal of Botany*, **67**, 550-555.

Wu ZT, Dijkstra P, Koch GW, *et al*. (2011) Responses of terrestrial ecosystems to temperature and precipitation change: a meta-analysis of experimental manipulation. *Global Change Biology*, **17**, 927-942.

Yu HY, Luedeling E, Xu JC (2010) Winter and spring warming result in delayed spring phenology on the Tibetan Plateau. *Proceedings of the National Academy of Sciences of the United States of America*, **107**, 22151-22156.

CHAPTER 4

Experimental warming increases transpiration of tree seedlings in a southeastern US temperate forest

4.1 Abstract

Climate change is expected to increase temperature and atmospheric evaporative demand in many regions in the future. We investigated the effect of experimental warming of 1.6–5.3 °C and increased vapor pressure deficit (*D*) of 0.16–0.96 kPa on the growth and physiology of small tree seedlings in the temperate forest understory (Duke Forest, North Carolina, USA). Miniature sap flow gauges were used to measure transpiration rates (*J*) of four common deciduous species (*Acer rubrum*, *Carya tomentosa*, *Quercus alba*, *Quercus rubra*) throughout the growing season, and these sap flow measurements were then used to estimate seasonal changes in stomatal conductance (g_s) of each seedling. Experimental warming for 3 years increased growth in *C. tomentosa* and *Q. alba* but not the other two tree species. Results suggest that growth of *A. rubrum* and *Q. rubra* was negatively affected by atmospheric drying and decreased annual precipitation over the study period. Plant stomata acclimated to local changes in leaf-to-air *D* (D_L) over time and across the experimental treatment, indicating that stomatal responses to D_L are dynamic within a species or even

individual plant. Acclimation of stomata to the experimental treatment resulted in warming-induced increases in g_s and stomatal sensitivity of *Q. alba*. It was unclear if future warming and elevated *D* will increase g_s in the other three species, due to the confounding of temperature and *D* in this experiment. Warming and increased *D* significantly decreased midday leaf water potential while increasing midday transpiration and daily water use, indicating that future climate change will increase the potential for temperature-induced drought stress. Differences among species indicate that the diffuse-porous *A. rubrum* had greater stomatal sensitivity and maintained higher leaf water potential, even under high *D* and drought, than the ring-porous species.

4.2 Introduction

Mean temperature in the United States is expected to increase by 2–6 °C by 2100 (Karl *et al.*, 2009), and higher temperatures increase the water-holding capacity of the atmosphere. As expected with a warmer climate, global annual evapotranspiration increased from 1982 to 1997, but has declined since 1998 (Jung *et al.*, 2010). If relative humidity does not change markedly in the future (e.g. Trenberth *et al.*, 2005), global warming will create widespread increases in atmospheric vapor pressure deficit (*D*). Regional differences in recent evapotranspiration trends exist (Jung *et al.*, 2010), which adds considerable uncertainty in the extent and magnitude of local changes in *D* in the future. It is therefore necessary to consider the roles and interactions of temperature and *D*, particularly when examining potential climate change effects on plant water relations.

Although temperature and *D* are strongly linked, they have contrasting effects on stomatal conductance (g_s) in plants. An increase in *D* nearly always causes a decline in g_s (Monteith, 1995; Oren *et al.*, 1999), whereas high temperatures usually increase g_s (Bunce, 2000; Lu *et al.*, 2000; Kudoyarova *et al.*, 2011; Sadras *et al.*, 2012; Way *et al.*, 2012). Stomata do not respond directly to air humidity or *D*, however (Mott & Parkhurst, 1991; Monteith, 1995). Most proposed mechanisms attribute stomatal responses to changes in water potential of the leaf, which are controlled by changes in transpiration (Buckley, 2005; Shope *et al.*, 2008; Pettijohn *et al.*, 2009; Peak & Mott, 2011). Stomatal closure due to increased transpiration rate can be treated as a form of negative feedback that simultaneously restricts excessive water loss and optimizes carbon gain (Friend, 1991; Buckley, 2005). Transpiration also plays an important role in plant cooling (Nobel, 1974), so larger stomatal apertures may be a physiological consequence of high temperature (Sermons *et al.*, 2012). Experimental warming studies around the globe have found that elevated temperature generally increases plant growth (Arft *et al.*, 1999; Rustad *et al.*, 2001; Wu *et al.*, 2011), although it is not clear whether higher growth is related to sustained increases in g_s or increased photosynthetic capacity of plants.

Stomatal sensitivity to *D* differs substantially across plant species (Turner *et al.*, 1984; Tardieu & Simonneau, 1998; Oren *et al.*, 1999) and can even vary over time in a single species (Kutsch *et al.*, 2001; Herbst *et al.*, 2008). It has recently been recognized that it is essential to include seasonal changes in stomatal responses to *D* to accurately model carbon uptake in temperate forests (Kosugi *et al.*, 2003; Kosugi & Matsuo, 2006). Stomatal responses to *D* were not constant throughout the growing season in a beech forest in

Germany, but stomatal behavior shifted over time and was correlated to past fluctuations of *D* (Kutsch *et al.*, 2001). This stomatal acclimation may not occur in all forests (Herbst *et al.*, 2008), and the prevalence of the response remains unknown. The sensitivity of stomata to *D* has been shown to be influenced by temperature (Sermons *et al.*, 2012), which further links stomatal processes to both temperature and *D*.

The main goal of this study was to investigate the effect of experimentally manipulated temperature and *D* on the growth and physiology of small tree seedlings in the temperate forest understory (Duke Forest, North Carolina, USA). At this experimental warming site, the forest understory was exposed to a range of climate conditions inside open-top chambers, from 1.6 °C, 0.16 kPa to 5.3 °C, 0.96 kPa above ambient temperature and *D*, respectively. We used miniature sap flow gauges to measure transpiration rates of four common deciduous species (*Acer rubrum*, *Carya tomentosa*, *Quercus alba*, *Quercus rubra*) throughout the summer, and these sap flow measurements were then used to estimate seasonal changes in g_s of each seedling. To ensure that our results accurately represent the effects of warming and increased *D* on tree physiology, we compared the observed physiological response across experimental treatments to patterns resulting from natural environmental variation throughout the summer. Specifically, we sought to establish the relationships between (1) temperature and transpiration, (2) *D* and transpiration, and (3) temperature and g_s for each tree species. This study asked five questions:

1. Does the experimental treatment increase growth of temperate trees?
2. Is the treatment effect of temperature and *D* on transpiration and g_s different from seasonal effects on tree seedlings?

3. Does warming increase g_s in temperate trees?
4. Does stomatal sensitivity to *D* shift seasonally in individual seedlings and with the experimental treatment?
5. How do physiological responses to temperature and *D* differ among tree species?

4.3 Materials and Methods

Experimental study site

This study was conducted at an ongoing, long-term warming experiment in a *c.* 80-year-old oak-hickory forest stand of Duke Forest (36° 2' 11" N, 79° 4' 39" W, 130 m a.s.l.), in the piedmont region near Hillsborough, North Carolina, USA (Lynch, 2006). Mean annual temperature in Duke Forest is 15.5 °C, and mean annual precipitation is 1140 mm. Mean annual precipitation over the study period (2010–2012) was below average for Duke Forest, NC (884 mm, 949 mm, 932 mm; respectively), and there were several moderate droughts (Palmer Drought Index= –2.0 to –2.9) during the growing season in 2010 and 2011 (NDMC, 2012). Climate data for the site are available from a nearby (8 km) weather station (Duke Forest Remote Automatic Weather Station, Orange County, NC, USA).

The experimental warming site consists of 15 plots in the forest understory: nine are heated, three are unheated chamber controls, and three are chamberless control plots that lack chambers but are equal in surface area to the chambers. The octagonal, open-top chambers are 21.7 m^3 in volume: 5 m in diameter with eight walls each 1.9 m wide and 1.2 m tall. The chambers are heated by forced air blown over hydronic radiators fed by a closed-loop mixture of hot water and antifreeze (propylene glycol). The heated air is blown into the

chambers through 15-cm-diameter plastic plena which hang 45 cm above the ground and run in two concentric rings, one 0.8 m and the other 1.7 m from the chamber walls. Air enters the chambers via two rows of 2-cm-diameter holes separated by 20 cm along the bottom of the plena. Heat delivery to the chambers began in January 2010, and chambers are constantly heated year-round, both day and night. The experiment uses a regression design of chamber heating, where each chamber is heated to a target of 1.5 to 5.5 °C above ambient temperature and there are 0.5°C increments between chambers (i.e. 1.5, 2.0, 2.5, … , 5.5 °C). Maintaining precise target air temperatures over long time periods is difficult, and the assigned treatment levels varied by a small amount over time (Figure 4.01).

Air temperature (2 temperature probes per chamber), relative humidity (HS-2000V capacitive polymer sensor; Precon, Memphis, TN, USA), soil moisture (Model CS616 TDR probes, Campbell Scientific Inc., Logan, UT, USA), and photosynthetically active radiation (PAR) (Model SQ110; Apogee Instruments Inc., Logan, UT, USA) were measured inside each experimental chamber every ten minutes and recorded by automated dataloggers (CR1000; Campbell Scientific Inc.). In addition, air temperature and relative humidity (CS215-L sensor; Campbell Scientific Inc.), soil water content (Model CS616 TDR probes, Campbell Scientific Inc.), and PAR (Model SQ110; Apogee Instruments Inc.) were measured within one meter of the *A. rubrum* seedling inside each experimental plot every ten minutes and recorded by automated dataloggers (CR1000; Campbell Scientific Inc.). Environmental data from all available sensors in an experimental chamber were averaged for data analysis, except for PAR. The data from the sensor nearest each seedling was used, unless the seedling was not located near a sensor and then the average of both PAR sensors was used. Relative

extractable soil water content (REW) was calculated for each chamber according to the equation:

$$\text{REW} = (\theta - \theta_{min})/(\theta_{max} - \theta_{min})$$

where θ is the hourly soil water content, θ_{min} is minimum soil water content, and θ_{max} is the mean maximum volumetric soil water content over the study period. Readings from three or four saturating rainfall events were averaged to determine θ_{max}. To account for soil macropore drainage and thus avoid over-estimating θ_{max}, volumetric soil water content from two hours after the peak θ of each saturating rainfall event were used. Further details of the warming experiment can be found in Pelini *et al.* (2011).

Growth of study species

The four study species (*A. rubrum*, *C. tomentosa*, *Q. alba*, *Q. rubra*) are common in Duke Forest, enabling the sampling of naturally-occurring tree seedlings (*n*=47) that were present at the site before the chambers were installed. One seedling per species per chamber was sampled, if present, and ranged from 9–84 cm in height. In addition, two seedlings per species in chamberless control plots were measured.

Initial shoot height (cm) of all study plants was measured to the nearest 0.2 cm in April 2010. To measure annual height growth, shoot height was measured again in February 2011, 2012, and 2013. Aboveground biomass from non-experimental plants (*n*=11–29) at the study site was collected and dried at 70 °C for at least 48 h to assess dry mass. Aboveground biomass (g) of each study plant was estimated annually from 2010 to 2012 using species-specific allometric linear equations relating shoot height (*H*, cm) and number of leaves (*L*) to

biomass (*A. rubrum*, Ar: $y = 0.104(L) + 0.143(H) - 2.276$, r^2=0.97, P<0.0001; *C. tomentosa*, Ct: $y = 1.490(L) + 0.129(H) - 4.325$, r^2=0.82, P<0.0001; *Q. alba*, Qa: $y = 0.182(L) + 0.185(H) - 2.510$, r^2=0.96, P<0.0001; *Q. rubra*, Qr: $y = 0.253(L) + 0.144(H) - 1.685$, r^2=0.93, P<0.0001).

Leaf water potential

Midday leaf water potentials (Ψ_L) were measured monthly on 14 June, 21 July, 29 August, and 24 September 2010, and predawn leaf water potentials (Ψ_S) were measured on 14 June and 21 July. One leaf per species per chamber was collected from non-study plants, if extra individuals were present in the chamber, and measured with a pressure chamber (Model 1000, PMS Instruments, Corvallis, OR, USA).

Foliar carbon isotope ratios

Carbon isotope ratios of plant leaves provide a time-integrated measure of the ratio of intercellular CO_2 concentration to atmospheric CO_2 concentration (c_i/c_a) and can be used to compare seasonal differences in stomatal regulation. Leaves of *A. rubrum* and *Q. alba* (n=4 seedlings) were collected from the experimental chambers on 29 August 2010 for carbon isotope analyses. Leaves of *C. tomentosa* and *Q. rubra* were not analyzed due to inadequate sample sizes in the chambers. Leaves were oven-dried at 70 °C, and 2–3 leaves from each seedling were combined and ground to a fine powder in liquid nitrogen. The $\delta^{13}C$ of foliar tissue was analyzed with an elemental analyzer (Carla Erba, Model 1110, Milano, Italy) coupled to a Thermo-Finnigan Delta Plus gas isotope mass spectrometer (Bremen, Germany)

at the Stable Isotope Mass Spectrometry Laboratory (Kansas State University, Manhattan, KS, USA). Values of $\delta^{13}C$ were calculated according to standard delta notation:

$$\delta = \left(R_{\text{sample}}/R_{\text{standard}} - 1\right)1000$$

where R is the ratio of the heavy isotope (^{13}C) to the lighter isotope (^{12}C). The standard was belemnite carbonate from the Pee Dee Belemnite Formation, SC, USA, and the precision of the $\delta^{13}C$ measurements was ±0.15‰.

Sap flow gauges

Transpiration rates (J, mmol H_2O s^{-1}) of all study seedlings were measured at 10-minute intervals from June to September 2010 using the heat ratio method (Marshall, 1958). Because the seedlings were small (1.8–6.6 mm diameter) and had low rates of sap flow, miniature sap flow gauges were made according to the design by Clearwater *et al.* (2009) with several modifications. Each gauge had a small external heater (560 Ω, film-type resistor) and two temperature sensors (fine-wire thermocouples) at equal distances (6 mm) above and below the heater (Clearwater *et al.*, 2009). These were affixed with cyanoacrylate adhesive to a cork block (32 mm long, 7 mm wide, 4.5 mm high). The gauge was placed on the surface of the main stem, firmly secured with laboratory film (Parafilm M, Alcan Packaging, Neeah, WI, USA), and insulated with foam rubber pipe insulation, bubble wrap, and foil.

The heating element was connected in series with a voltage regulator delivering 11.5 V from a 12 V battery and controlled by a datalogger (CR1000, Campbell Scientific Inc.) to deliver a 6 s heat pulse every 10 min. This procedure dissipated 0.24 W from the heating element and heated the stem by a maximum of 20 °C during application of the pulse, which

did not damage the stem. Temperature of the thermocouples was measured immediately prior to each heat pulse and at 3 s intervals thereafter to measure the change in temperature (δT). The mean heat pulse velocity (v_h) was calculated over the interval from 60 to 90 s after the heat pulse:

$$v_h = \ln\left(\frac{\delta T_1}{\delta T_2}\right)$$

where δT_1 and δT_2 are the temperature differentials (°C) measured in the top and bottom thermocouples, respectively. Despite efforts to insulate and weatherproof the gauges, sap flux measurements were highly variable during rain events, possibly due to wetting of the gauges. All measurements during rain events were discarded.

The application of an external heat pulse to the surface of a small-diameter stem violates the assumption of thermal homogeneity required for calculations of heat pulse propagation (Marshall, 1958; Clearwater *et al.*, 2009). While v_h is proportional to sap flux, empirical species-specific calibrations are required to account for the thermal properties of stems of varying diameter (Clearwater *et al.*, 2009). It was therefore necessary to determine the relationship between v_h and actual sap flux (k_s) for each species and stem diameter. Stems (n=10–12 per species) of non-experimental plants were collected from the study site, and the stem ends were recut under water in the laboratory. The stems were flushed with deionized water at 200 kPa for 20 min to remove emboli, and a sap flow gauge was installed on the stem and insulated as described above. A calibration test was conducted by supplying water at a range of pressures, beginning at a pressure of 200 kPa and reducing the applied pressure in approximately 10- to 20-kPa increments until the flow reached zero. After flows stabilized

at each pressure, v_h (i.e. the gauge signal) was recorded and the flow rate (k_s, g h^{-1}) was measured. Each calibration curve contained 10–25 points. After calibration curves were complete, stem segments were perfused with methylene blue solution to determine the cross-sectional area of active xylem (A_S). The A_S (mm^2) of each study plant was estimated using a species-specific allometric quadratic equation relating stem diameter (x, mm) to A_S, as determined from non-experimental plants (n=11–17) at the study site (Ar: $y = 0.451(x - 4.588)^2 + 4.530x - 10.459$, r^2=0.96, P<0.0001; Ct: $y = 0.759(x - 4.197)^2 + 3.028x - 7.893$, r^2=0.95, P<0.0001; Qa: $y = 0.423(x - 4.112)^2 + 3.498x - 7.437$, r^2=0.97, P<0.0001; Qr: $y = 0.442(x - 3.613)^2 + 3.238x - 6.403$, r^2=0.96, P<0.0001).

The relationship between v_h and k_s was linear at low flow rates, but high flow rates caused highly variable deviations from the linear relationship. The maximum reliable flow rates varied with A_S, ranging from approximately 2 g h^{-1} in 2.5-mm diameter stems to approximately 8 g h^{-1} in 6.5-mm diameter stems. The slope (m) of the linear relationship between measured heat pulse velocity v_h and the actual sap flux k_s was positively correlated to sapwood area A_S for each species (Ar: r^2=0.78, P=0.0003; Ct: r^2=0.75, P=0.001; Qa: r^2=0.79, P=0.0001; Qr: r^2=0.69, P=0.002). For calibration purposes, the multiplier m was estimated for each study plant based on its estimated A_S and used to convert v_h to k_s.

Significant offsets were detected in the sap flux measurements (i.e. nighttime measurements were significantly different from zero) and were caused by small errors in the positioning of the thermocouples on the gauge (Clearwater *et al.*, 2009). There was also seasonal drift in the zero offset of the gauges, possibly due to small fluctuations in stem diameter and gauge–bark contact throughout the growing season. It was therefore necessary

to re-zero sap flux measurements on a daily basis using mean v_h from the previous night (23:00 to 4:00). This procedure required the assumption of negligible nighttime transpiration rates (E_{night}), which we tested by enclosing the seedlings inside plastic bags on 22–23 October 2010 to prevent transpiration and comparing the difference between the nighttime sap flux on bagged versus unbagged nights. Maximum E_{night} per unit leaf area was less than 0.7 mol H_2O m^{-2} hr^{-1} for all plants, and species mean E_{night} were not significantly different from zero (Ar: 0.017 ± 0.041 SE; Ct: 0.140 ± 0.207; Qa: 0.014 ± 0.036; Qr: 0.012 ± 0.070 mol m^{-2} hr^{-1}). Similarly, Daley and Phillips (2006) found nighttime sap flux was less than 10% of the total daily flux in *A. rubrum* and *Q. rubra* in New England. Increased *D* has been correlated with greater E_{night} in many tree species (Caird *et al.*, 2007), however, so we also tested for an experimental treatment effect on E_{night} in each species. Experimentally increased *D* was positively correlated with E_{night} in *A. rubrum* (r^2=0.53, *P*=0.041), but the correlation was not significant in the other three species (Ct: r^2=0.01, *P*=0.884; Qa: r^2=0.06, *P*=0.505; Qr: r^2=0.26, *P*=0.136). For *A. rubrum*, the nightly zero offset was adjusted to account for increased E_{night} for seedlings heated by 2 °C or higher.

Stomatal conductance

Stomatal conductance of whole seedlings (g_s, mmol H_20 m^{-2} s^{-1}) was estimated from:

$$g_s = \left(\frac{D_L * A_L}{J * P_{atm}} - \frac{1}{g_b}\right)^{-1}$$

where D_L is vapor pressure deficit at the leaf surface (kPa), A_L is leaf area (m^2), *J* is the rate of transpiration (mmol H_2O s^{-1}), P_{atm} is atmospheric pressure (kPa), and g_b is boundary layer

conductance (mmol m^2 s^{-1}). To estimate the vapor pressure of air at the leaf surface, abaxial leaf temperature was measured on two leaves per plant with thermocouples attached to the leaf with surgical tape. The A_L of each study plant was estimated monthly by counting number of leaves and using a species-specific allometric equation relating leaf number (L), stem height (H), and stem diameter (x) to A_L, as determined from non-experimental plants (n=15–29) at the study site (Ar: $y = 6.678 \times 10^{-6}(L)^2 + 1.390 \times 10^{-3}(L)$, r^2=0.97, P<0.0001; Ct: $y = -1.387 \times 10^{-7}(L \cdot H)^2 + 4.534 \times 10^{-4}(L \cdot H)$, r^2=0.96, P<0.0001; Qa: $y = 2.531 \times 10^{-3} \ln(LH^2) - 8.179 \times 10^{-3} \ln(L \cdot H)$, r^2=0.96, P<0.0001; Qr: $y = 3.137 \times 10^{-3} \ln(Lx^2) - 3.063 \times 10^{-3} \ln(L \cdot x)$, r^2=0.91, P<0.0001).

For six to eight plants per species, g_b was estimated by measuring the rate of mass loss of water from two water-saturated filter paper leaf replicas placed among the foliage in a chamber, following the method of Roberts *et al.* (1990). Abaxial leaf surface temperature was measured on one replica with a thermocouple and recorded by a datalogger (CR1000, Campbell Scientific Inc.), while mass loss from the other leaf replica was measured at 5-min intervals. Values of g_b were calculated using the relationship:

$$g_b = (E * P_{atm})/D_L$$

where E (mmol m^2 s^{-1}) is the rate of evaporation of water from the leaf replica.

To provide independent assessment of g_s, leaf-level measurements of g_s were performed monthly using an AP4 porometer (Delta-*T*, Cambridge, UK). Stomatal conductance was measured on two leaves per plant at 2-hr intervals from sunrise to sunset on 14 June, 21 July, and 29 August and at midday on 24 September 2010. The porometer was calibrated on site before measurements and as needed throughout the day to maintain

chamber humidity at ambient values. From this comparison of sap flux-based g_s and porometric g_s, we found that eight of the 47 gauges did not function properly and exhibited extremely low g_s throughout the summer, possibly due to gauge attachment near a non-conducting stem segment or poor contact between the gauge and the stem surface. These eight seedlings were excluded from analyses, leaving the following sample sizes: *A. rubrum* (n=10), *C. tomentosa* (n=11), *Q. alba* (n=7), and *Q. rubra* (n=10). Hourly estimates of g_s based on sap flux measurements were generally lower than porometric g_s, especially for the *Quercus* species (Figure 4.2). The slope of the relationship between sap flux-based g_s and porometric g_s was not significantly different from 1, except for *Q. rubra* (Ar: m=0.985, t_{146}=0.103, P=0.749; Ct: m=0.965, t_{160}=0.460, P=0.499; Qa: m=1.067, t_{94}=0.982, P=0.324; Qr: m=1.237, t_{145}=20.027, P<0.0001). The intercept of the *Quercus* species was significantly greater than 0 (Ar: b=–0.086, t_{146}=0.448, P=0.655; Ct: b=–0.105, t_{160}=0.459, P=0.647; Qa: b=–0.944, t_{94}=2.911, P=0.005; Qr: b=–1.566, t_{145}=5.628, P<0.0001), however, so there was a tendency for the sap flow gauges to underestimate high values of g_s in these species (Figure 4.2).

Statistical analyses

Differences in growth, midday Ψ_L, foliar $\delta^{13}C$, and daily water flux due to the experimental treatment were analyzed using least-square regression for each species separately, as appropriate for the experimental design. Results were similar whether mean chamber temperature or D_L was used as the independent variable, so only one variable per response is described. Standardized major axis (SMA) regression was used to characterize the

relationship between sap flux-based and porometric g_s and between leaf water potential and g_s using SMATR 2.0 (Warton *et al.*, 2006). SMA was used because it is not possible to functionally assign either variable as dependent. Before analyses, g_s was ln-transformed to achieve normality.

The effect of midday chamber temperature on seasonal changes in midday J and midday g_s (12:00 to 14:00) was analyzed using least-square regression for each seedling. The relationship between midday J from June to September 2010 and temperature was described using the relationship:

$$J = m_{JT} \cdot T + J_{T30}$$

where m_{JT} is the sensitivity of J to temperature and J_{T30} is a reference transpiration rate at T=30 °C. The reference temperature of 30 °C was chosen because it fell within the seasonal range in temperature for all seedlings, thus enabling comparisons among conditions and species. The relationship between midday g_s from June to September 2010 and temperature was described using the relationship:

$$g_s = -m_T \cdot T + g_{sT30}$$

where $-m_T$ is the sensitivity of g_s to temperature and g_{sT30} is a reference conductance at T=30 °C.

The effect of midday D on seasonal changes in J and g_s was analyzed using least-square regression for each seedling. The relationship between midday J from June to September 2010 and $\ln D_L$ for each seedling was quantified using the relationship:

$$J = m_J \cdot \ln D_L + J_{ref}$$

where m_J is the sensitivity of J to D_L and J_{ref} is a reference transpiration rate at D_L=1 kPa. The relationship between midday g_s from June to September 2010 and lnD_L for each seedling was quantified using the relationship described by Oren *et al*. (1999):

$$g_s = -m \cdot \ln D_L + g_{sref}$$

where $-m_{gs}$ is the sensitivity of g_s to D_L and g_{sref} is a reference conductance at D_L=1 kPa.

Differences in midday J and midday g_s among experimental treatments were then analyzed for each species using least-square regression with mean chamber temperature or D_L as the independent variable and J_{T30}, g_{sT30}, J_{ref}, and g_{sref} as the dependent variable. Differences in the sensitivity of J and g_s among experimental treatments were also analyzed using least-square regression with mean chamber temperature or D_L as the independent variable and m_{JT}, m_J, $-m_T$, $-m$ as the dependent variable. This approach isolated the effect of temperature from the effect of D by comparing midday J and g_s at the reference temperature of 30 °C. Similarly, the effect of D was isolated from the effect of temperature by comparisons at the reference D_L of 1 kPa. Differences in midday J and midday g_s among experimental treatments were also analyzed for each species by day from June to September 2010 using least-square regression with mean chamber temperature and D_L as the independent variable. Results are reported when significant relationships were found for greater than 5% of the growing season.

Seasonal effects of light, lnREW, temperature, and lnD_L on midday J and g_s were analyzed for each species using two-way, full-factorial analyses of variance (ANOVAs) that included chamber as a categorical factor. When analyzing the effects of REW and light on midday J and g_s, only data between D_L=1.5–2.5 kPa were included in the analysis. When

analyzing the effects of temperature and D_L on midday J and g_s, only data with REW>25% were included in the analysis. Species and seasonal differences in Ψ_L were analyzed using a two-way, full-factorial ANOVA with species and month as the main effects. A one-way, univariate ANOVA was used to test for shifts in $-m$ and g_{sref} from June–July to August–September. Means were considered significantly different at $P \leq 0.05$. If differences among means were found, we used the Tukey HSD to test for significant differences among months. All analyses were performed using JMP 9.0 (SAS Institute, Cary, NC).

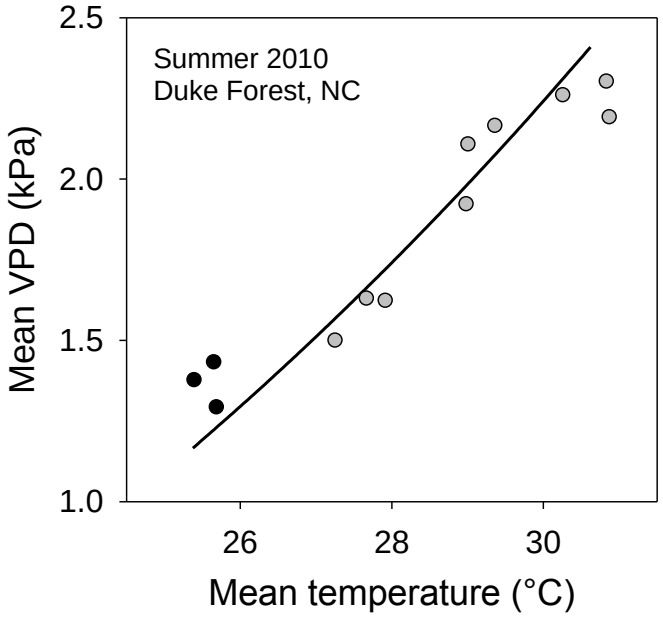

Figure 4.1 Mean daytime temperature and VPD inside the 12 experimental chambers in Duke Forest, NC in summer 2010 (control chambers, black circles; heated chambers, gray circles). The line depicts the effect of temperature on the saturated vapor pressure of air, using the mean temperature in control chambers as the reference temperature.

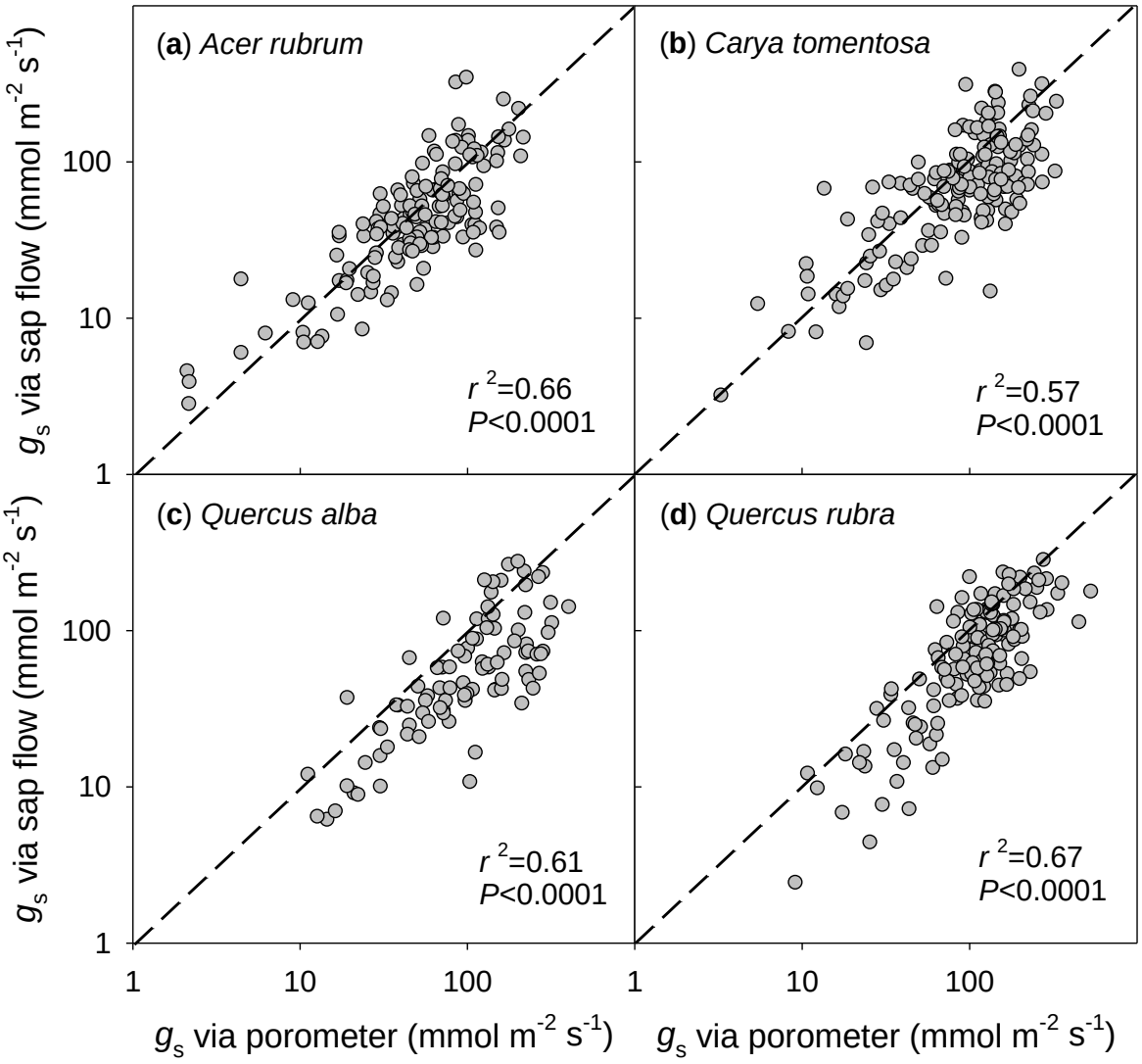

Figure 4.2 Comparison of stomatal conductance measured at the leaf-level with a porometer and estimated via whole-plant sap flux for all species. Porometer measurements (n=2 leaves per plant) were made on 14 June, 21 July, 29 August, and 24 September 2010, and sap flux measurements are hourly means of data collected every 10 minutes. The dotted line represents the 1:1 relationship. Relationships were analyzed using standardized major axis (SMA) regression, because neither variable can be functionally assigned as dependent.

4.4 Results

At the experimental warming site, mean daytime temperature inside the open-top chambers over the 2010 growing season ranged from 1.6–5.3 °C and mean daytime *D* ranged from 0.16–0.96 kPa above ambient conditions (Figure 4.1). There was no difference in mean monthly REW ($F_{1,11}$≥0.844, P≥0.380) or predawn water potential ($F_{1,43}$≥0.850, P≥0.362) among the chambers over the study period. Growth of seedlings was monitored over the first 3 years of the experiment, and warming significantly increased aboveground biomass in *C. tomentosa* (r^2=0.38, P=0.045) and *Q. alba* (r^2=0.56, P=0.021) but not in *A. rubrum* or *Q. rubra* (Ar: r^2=0.04, P=0.590; Qr: r^2=0.09, P=0.446; Figure 4.3).

Experimental treatment effects on tree physiology

The experimental treatment significantly affected midday leaf water potential (Ψ_L), midday *J*, daily water flux, and foliar $\delta^{13}C$ of multiple species. Midday Ψ_L of *A. rubrum* and *Q. alba* was significantly lower in warmer chambers in July 2010 (Ar: r^2=0.37, P=0.022; Qa: r^2=0.32, P=0.036; Figure 4.4), when volumetric soil water content was high and did not differ among chambers (REW=74 ± 1.6%). There was no significant effect on Ψ_L in *C. tomentosa* (Ct: r^2=0.02, P=0.746), and there were not sufficient seedlings in the chambers to quantify the effect in *Q. rubra*. Warming marginally increased midday J_{ref} (r^2=0.10, P=0.055) across all seedlings, and the interaction between species and temperature was significant ($F_{3,38}$=5.717, P=0.003). When analyzed by species, midday J_{ref} was only positively correlated to mean chamber temperature for *Q. alba* (Ar: r^2=0.08, P=0.395; Ct: r^2=0.28, P=0.097; Qa: r^2=0.91, P=0.001; Qr: r^2=0.06, P=0.504; Figure 4.5a). Warming

significantly increased midday *J* for 32% of the summer in *C. tomentosa* and for 94% of the summer in *Q. alba* (data not shown). There was no clear effect of experimentally elevated *D* on midday J_{T30} (r^2=0.04, *P*=0.234), except for *Q. alba* (Ar: r^2=0.17, *P*=0.210; Ct: r^2=0.18, *P*=0.198; Qa: r^2=0.82, *P*=0.005; Qr: r^2=0.12, *P*=0.337). Higher *D* significantly increased midday *J* for 11% of the summer in *Q. alba* (data not shown). Daily water flux was positively correlated to chamber temperature in *C. tomentosa* (r^2=0.57, *P*=0.007) and *Q. alba* (r^2=0.93, *P*=0.001), but not in *A. rubrum* (r^2=0.10, *P*=0.345) and *Q. rubra* (r^2=0.15, *P*=0.265, Figure 4.5b). Foliar $\delta^{13}C$ were significantly higher in warmer chambers for *A. rubrum* (r^2=0.37, *P*=0.049) but not *Q. alba* (r^2=0.10, *P*=0.305, Figure 4.6).

Elevated temperature significantly increased g_s in *Q. alba* and *C. tomentosa*, but some evidence supports warming-induced decreases in g_s for *A. rubrum* and *Q. rubra* (Figure 4.7a). Warming significantly increased g_{sref} (r^2=0.16, *P*=0.016) across all seedlings, and the interaction between species and temperature was significant ($F_{3,38}$=5.596, *P*=0.004). When analyzed by species, midday g_{sref} was also only positively correlated to warming treatment in *Q. alba* (Ar: r^2=0.01, *P*=0.733; Ct: r^2=0.25, *P*=0.120; Qa: r^2=0.88, *P*=0.002; Qr: r^2=0.01, *P*=0.795; Figure 4.7a). Warming significantly increased midday g_s for 63% of summer in *Q. alba* (data not shown). There was no clear effect of experimentally elevated *D* on midday g_{sT30} on all species (r^2=0.11, *P*=0.090; Figure 4.7b), except in *Q. alba* (Ar: r^2=0.21, *P*=0.296; Ct: r^2=0.30, *P*=0.099; Qa: r^2=0.77, *P*=0.021; Qr: r^2=0.15, *P*=0.342; Figure 4.7b). Higher *D* significantly increased midday g_s for 6% of the summer in *Q. alba*, but significantly decreased midday g_s for 18% of the summer in *A. rubrum* and for 54% of the summer in *Q. rubra* (data not shown).

Seasonal variation in tree physiology

Seasonal variation in daytime temperature and *D* in Duke Forest, NC was approximately three times larger than the applied treatment in this experiment. Mean daytime temperature spanned a range of 15 °C and *D* spanned a range of 3.5 kPa from June through September, compared to the largest experimental treatment applied here of approximately 5 °C and 1 kPa (Figure 4.1). Establishing the effect of natural seasonal variation on tree physiology of individual seedlings had the additional advantage of increased statistical power for detection of relationships. When changes in plant physiology due to the experimental treatment match the physiological response to natural seasonal variation in temperature or *D*, there is higher confidence in the prediction of the response to climate change.

There was a moderate drought in late summer in Duke Forest, NC that significantly reduced midday leaf water potential ($F_{3,143}$=69.827, P<0.0001; Figure 4.8) and midday g_s in all tree species ($F_{3,185}$=60.541, P<0.0001; data not shown). Seasonal variation in REW significantly affected midday *J* (Ar: $F_{1,437}$=568.613, P<0.0001; Ct: $F_{1,435}$=433.456, P<0.0001; Qa: $F_{1,257}$=62.783, P<0.0001; Qr: $F_{1,419}$=898.403, P<0.0001; data not shown) and midday g_s in all species (Ar: $F_{1,437}$=544.795, P<0.0001; Ct: $F_{1,435}$=329.137, P<0.0001; Qa: $F_{1,257}$=44.724, P<0.0001; Qr: $F_{1,419}$=745.655, P<0.0001; Figure 4.9). Midday *J* and midday g_s were highly restricted when REW fell below 10% (Figure 4.9).

Seasonal changes in temperature significantly affected midday *J* (Ar: $F_{1,456}$=254.806, P<0.0001; Ct: $F_{1,498}$=295.741, P<0.0001; Qa: $F_{1,320}$=33.734, P<0.0001; Qr: $F_{1,498}$=295.202, P<0.0001) and midday g_s in all species (Ar: $F_{1,456}$=33.100, P<0.0001; Ct: $F_{1,498}$=188.146, P<0.0001; Qa: $F_{1,320}$=89.086, P<0.0001; Qr: $F_{1,498}$=109.970, P<0.0001). Midday *J* increased

linearly with increasing temperature (Figure 4.10), whereas midday g_s decreased linearly with increasing temperature (Figure 4.11). The slope of the relationship between temperature and midday J (m_{JT}) differed among individual plants in *A. rubrum* ($F_{10,456}$=6.018, P<0.0001), *C. tomentosa* ($F_{10,498}$=2.913, P=0.002), and *Q. rubra* ($F_{9,498}$=6.896, P<0.0001; Table 4.1). Stomatal sensitivity to temperature (m_T) differed among individual plants in all species (Ar: $F_{10,456}$=3.591, P=0.0001; Ct: $F_{10,498}$=8.150, P<0.0001; Qa: $F_{6,320}$=7.938, P<0.0001; Qr: $F_{9,498}$=4.973, P<0.0001; Table 4.1).

Seasonal changes in D_L significantly affected midday J (Ar: $F_{1,456}$=377.542, P<0.0001; Ct: $F_{1,498}$=324.113, P<0.0001; Qa: $F_{1,320}$=75.204, P<0.0001; Qr: $F_{1,498}$=597.952, P<0.0001) and midday g_s in all species (Ar: $F_{1,999}$=582.562, P<0.0001; Ct: $F_{1,1022}$=2032.735, P<0.0001; Qa: $F_{1,624}$=1145.253, P<0.0001; Qr: $F_{1,949}$=1232.908, P<0.0001). Midday J increased with increasing D_L, but saturated at high values of D_L in all species (Figure 4.12). Midday g_s decreased exponentially with increasing D_L (Table 4.2). The slope of the relationship between D_L and midday J (m_J) differed among individual plants (Ar: $F_{10,456}$=7.889, P<0.0001; Ct: $F_{10,498}$=4.846, P<0.0001; Qa: $F_{6,320}$=6.825, P<0.0001; Qr: $F_{9,498}$=15.211, P<0.0001), and stomatal sensitivity to D_L ($-m$) also differed in all species (Ar: $F_{10,999}$=20.902, P<0.0001; Ct: $F_{10,1022}$=35.915, P<0.0001; Qa: $F_{6,624}$=108.363, P<0.0001; Qr: $F_{9,949}$=13.543, P<0.0001; Table 4.2).

Seasonal variation in light in the forest understory only significantly affected midday J in *Q. rubra* (Ar: $F_{1,447}$=0.033, P=0.856; Ct: $F_{1,442}$=0.333, P=0.564; Qa: $F_{1,257}$=0.236, P=0.627; Qr: $F_{1,430}$=4.246, P=0.040) and did not significantly affect midday g_s (Ar:

$F_{1,447}$=0.001, P=0.985; Ct: $F_{1,442}$=0.180, P=0.672; Qa: $F_{1,257}$=0.163, P=0.686; Qr: $F_{1,430}$=2.727, P=0.099; data not shown).

Stomatal sensitivity to D

The response of leaves to D_L was not constant throughout the growing season (Figure 4.12). Mean stomatal sensitivity of all tree seedlings was –52.5 mmol m^{-2} s^{-1} $ln(kPa)^{-1}$ in mid-summer, when mean REW was 44% and mean midday D was 1.5 kPa. Stomatal sensitivity increased to a mean of –76.1 mmol m^{-2} s^{-1} $ln(kPa)^{-1}$ in late summer (t_{71}=2.55, P=0.013), after mean REW declined to 15% and mean midday D increased to 1.9 kPa. When analyzed by species, differences were only significant in *Q. rubra* (Ar: t_{19}=1.61, P=0.126; Ct: t_{21}=1.15, P=0.263; Qa: t_{11}=0.65, P=0.533; Qr: t_{17}=2.87, P=0.011).

Although stomatal sensitivity to temperature differed among plants for all species (Figure 4.11), there was only a significant effect of warming on $-m_T$ for *Q. alba* (Ar: r^2=0.41, P=0.121; Ct: r^2=0.24, P=0.155; Qa: r^2=0.88, P=0.005; Qr: r^2=0.02, P=0.742). Stomatal sensitivity to D_L also differed among plants for all species (Table 4.2), but there was only a significant effect of elevated D on $-m$ for *Q. alba* (Ar: r^2=0.09, P=0.370; Ct: r^2=0.17, P=0.209; Qa: r^2=0.80, P=0.007; Qr: r^2=0.02, P=0.692). In *Q. alba*, the stomata of plants in heated chambers were more sensitive to temperature and D_L (Figure 4.14).

Species differences

The response of midday leaf water potential (Ψ_L) to drought differed among species ($F_{7,149}$=2.167, P=0.041); the three ring-porous species (*C. tomentosa*, *Q. alba*, *Q. rubra*) had

the largest declines in Ψ_L at the height of the drought (Figure 4.8a). Mean Ψ_L of diffuse-porous *A. rubrum* was significantly higher than *Q. alba* throughout the summer ($F_{3,143}$=15.544, P<0.0001; Figure 4.8a). The sensitivity of stomata to water deficit, as quantified by the slope of the relationship between ln(g_s) and Ψ_L, was highest in *A. rubrum* (Figure 4.8b). Stomata of *A. rubrum* closed more abruptly with decreasing water potential, whereas stomatal closure was more gradual in *C. tomentosa* and *Q. alba* (Figure 4.8b). Stomatal sensitivity of *A. rubrum* to D_L was lower, however, than in *C. tomentosa* and *Q. rubra* (–m=41 vs. 82 and 79, respectively; $F_{3,38}$=4.420, P=0.011; Table 4.2). There were no species differences in the stomatal sensitivity to temperature or in the sensitivity of transpiration to temperature or D_L (–m_T: $F_{3,30}$=2.190, P=0.117; m_{JT}: $F_{3,38}$=2.434, P=0.066; m_J: $F_{3,38}$=2.105, P=0.102; Tables 4.1-4.2).

Transpiration and g_s were significantly lower in *A. rubrum*, when compared to the other three species. Mean midday J_{ref} was also lower in *A. rubrum* than *C. tomentosa* ($F_{3,38}$=3.416, P=0.028), but there were no species differences in J_{T30} ($F_{3,38}$=2.858, P=0.051). Although there were no species differences in g_{sT30} ($F_{3,30}$=1.079, P=0.375) or g_{sref} ($F_{3,38}$=2.830, P=0.052; Figure 4.7), measurements of g_s with the porometer revealed that midday g_s was significantly lower in *A. rubrum* than the other three species on 21 July, 29 August, and 24 September ($F_{3,185}$=17.108, P<0.0001; data not shown).

Table 4.1 The slope (m_{JT}, mol m^{-2} hr^{-1} $°C^{-1}$) of the linear relationship between chamber temperature and midday transpiration rate as shown in Figure 4.10 and the transpiration rate at 30 °C (J_{T30}, mol m^{-2} hr^{-1}) for all seedlings. The slope (m_T, mmol m^{-2} s^{-1} $°C^{-1}$) of the linear relationship between chamber temperature and midday stomatal conductance as shown in Figure 4.11 and estimated stomatal conductance at 30 °C (g_{sT30}, mmol m^{-2} s^{-1}). Mean daytime chamber temperature throughout the growing season (T, °C) is given. Significant relationships (P<0.05) are indicated by a star, whereas marginally significant relationships (P<0.1) have no symbol and non-significant relationships (P>0.1) are indicated by ns.

Species	T (°C)	m_{JT}		J_{T30}	m_T		g_{sT30}
Ar	25.4	0.21	*	2.241	-0.28	ns	
Ar	25.4	0.15	*	1.597	-0.29	ns	
Ar	25.4 (+0)	0.55	*	6.105	-5.24		147
Ar	25.7 (+0)	0.13	*	2.401	-5.69	*	57
Ar	27.3 (+1.6)	0.25	*	4.734	-5.32	*	114
Ar	27.7 (+2.1)	0.12	*	2.569	-2.87	*	57
Ar	27.9 (+2.3)	0.30	*	4.166	-6.22		107
Ar	29.4 (+3.7)	0.16	*	1.749	0.46	ns	
Ar	30.3 (+4.8)	0.13	*	1.563	-0.86	*	43
Ar	30.9 (+5.3)	0.28	*	2.435	-3.84	*	80
Ct	25.4	0.24	*	3.971	-7.92	*	119
Ct	25.4	0.32	*	6.034	-13.26	*	180
Ct	25.4 (+0)	0.22	*	3.859	-6.38	*	105
Ct	25.7 (+0)	0.21	*	3.172	-3.57	*	79
Ct	25.7 (+0)	0.13	*	2.318	-4.98	*	70
Ct	27.7 (+2.1)	0.28	*	4.064	-3.09	*	105
Ct	27.9 (+2.3)	0.28	*	4.516	-4.05	*	123
Ct	29.0 (+3.4)	0.12	*	5.476	-7.84	*	126
Ct	29.4 (+3.7)	0.12	*	4.594	-9.91	*	118
Ct	30.9 (+5.3)	0.20	*	10.036	-18.75	*	312
Ct	30.8 (+5.2)	0.28	*	3.393	-0.37	ns	
Qa	25.4	0.12	*	1.294	-0.72	ns	
Qa	25.4	0.16	*	2.086	-2.80	*	55
Qa	25.4 (+0)	0.07		1.188	-2.84	*	29
Qa	25.7 (+0)	0.11	*	1.887	-4.41	*	51
Qa	27.3 (+1.6)	0.06	*	2.951	-9.17	*	88
Qa	29.4 (+3.7)	0.14	*	4.137	-8.56	*	123
Qa	30.8 (+5.2)	0.23		8.115	-15.29	*	280

Table 4.1 (continued)

Qr	25.4	0.39	*	4.539	1.27	ns	
Qr	25.4	0.46	*	6.294	-5.16	*	195
Qr	25.7 (+0)	0.30	*	4.714	-7.91	*	143
Qr	27.3 (+1.6)	0.17	*	4.424	-8.45	*	103
Qr	27.7 (+2.1)	0.08		2.867	-4.17	*	61
Qr	27.9 (+2.3)	0.45	*	6.568	-3.03	*	152
Qr	29.0 (+3.4)	0.20	*	5.81	-9.77	*	165
Qr	29.0 (+3.5)	0.36	*	5.577	-3.03	ns	
Qr	30.9 (+5.3)	0.22	*	3.332	-7.07	*	127
Qr	30.8 (+5.2)	0.13	*	3.213	-2.93	*	77

Table 4.2 Values used for evaluating the dependency between the two parameters in the function shown in Figure 4.12: $J = m_J \cdot \ln D_L + J_{ref}$, where J is midday transpiration rate (mol m^{-2} hr^{-1}), m_J is in mol m^{-2} hr^{-1} $ln(kPa)^{-1}$, D_L is vapor pressure deficit at the leaf surface (kPa), and J_{ref} is estimated transpiration rate at 1 kPa (mol m^{-2} hr^{-1}). Values used for evaluating the dependency between the two parameters in the function: $g_s = -m \cdot \ln D_L + g_{sref}$, where g_s is midday stomatal conductance (mmol m^{-2} s^{-1}), m is in mmol m^{-2} s^{-1} $ln(kPa)^{-1}$, and g_{sref} is estimated stomatal conductance at 1 kPa (mmol m^{-2} s^{-1}). Mean daytime chamber vapor pressure deficit throughout the growing season (D, kPa) is given. Significant relationships (P<0.05) are indicated by a star, whereas marginally significant relationships (P<0.1) have no symbol.

Species	D (kPa)	m_J		J_{ref}	m		g_{sref}
Ar	1.33	1.18	*	1.87	-17.71	*	45
Ar	1.33	0.91	*	1.34	-15.52	*	30
Ar	1.38 (+0)	2.80	*	5.40	-82.34	*	124
Ar	1.29 (+0)	0.99	*	2.16	-45.71	*	65
Ar	1.50 (+0.16)	2.30	*	4.22	-69.98	*	116
Ar	1.63 (+0.29)	0.75	*	2.36	-36.50	*	61
Ar	1.62 (+0.50)	1.90	*	3.64	-73.80	*	121
Ar	2.16 (+0.77)	1.35	*	1.42	-24.17	*	42
Ar	2.19 (+0.85)	1.99	*	2.49	-46.14	*	79
Ar	2.26 (+0.86)	1.13	*	1.62	-23.76	*	46
Ct	1.33	1.49	*	3.81	-72.84	*	118
Ct	1.33	1.89	*	5.62	-100.07	*	186
Ct	1.38 (+0)	1.10	*	3.69	-68.94	*	80
Ct	1.29 (+0)	1.27	*	2.87	-44.60	*	71
Ct	1.43 (+0)	0.75	*	2.21	-47.47	*	70
Ct	1.63 (+0.29)	2.05	*	3.76	-66.17	*	111
Ct	1.62 (+0.50)	2.11	*	4.32	-78.76	*	121
Ct	1.92 (+0.58)	0.80	*	5.36	-100.41	*	148
Ct	2.16 (+0.77)	0.63		4.61	-79.15	*	133
Ct	2.19 (+0.85)	1.92	*	9.96	-190.13	*	309
Ct	2.30 (+0.96)	1.58	*	3.35	-51.28	*	97
Qa	1.33	0.66	*	1.22	-12.20	*	30
Qa	1.33	0.94	*	1.98	-28.92	*	51
Qa	1.38 (+0)	0.28		1.12	-19.66	*	32
Qa	1.43 (+0)	0.70	*	1.81	-36.02	*	51
Qa	1.50 (+0.16)	0.37	*	2.86	-73.40	*	105

Table 4.2 (continued)

Qa	2.16 (+0.77)	1.00	*	4.14	-82.14	*	124
Qa	2.30 (+0.96)	2.74	*	7.81	-167.35	*	278
Qr	1.33	2.32	*	3.77	-34.67	*	89
Qr	1.33	3.39	*	6.02	-95.77	*	166
Qr	1.43 (+0)	2.01	*	4.56	-90.41	*	128
Qr	1.50 (+0.16)	1.26	*	3.99	-73.19	*	117
Qr	1.63 (+0.29)	0.73	*	2.62	-49.21	*	72
Qr	1.62 (+0.50)	4.02	*	5.52	-101.91	*	165
Qr	1.92 (+0.58)	1.67	*	5.73	-118.59	*	171
Qr	2.11 (+0.71)	3.01	*	5.17	-93.78	*	146
Qr	2.19 (+0.85)	1.63	*	3.75	-77.49	*	110
Qr	2.30 (+0.96)	0.78	*	3.28	-62.02	*	96

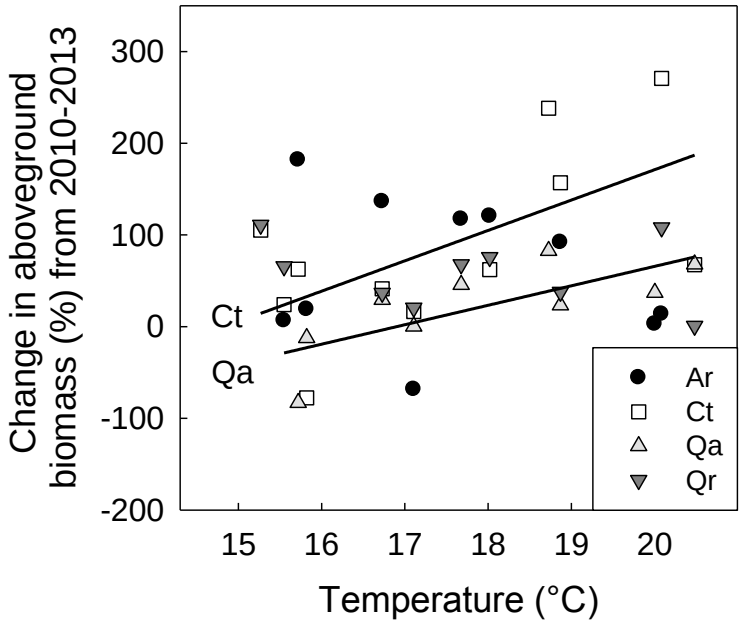

Figure 4.3 Effect of warming on change in aboveground biomass (%) after three years of experimental treatment. Warming significantly increased growth in *C. tomentosa* (r^2=0.38, P=0.045) and *Q. alba* (r^2=0.56, P=0.021) but not in *A. rubrum* or *Q. rubra* (Ar: r^2=0.04, P=0.590; Qr: r^2=0.09, P=0.446). Species codes: Ar, *Acer rubrum*; Ct, *Carya tomentosa*; Qa, *Quercus alba*; Qr, *Quercus rubra*.

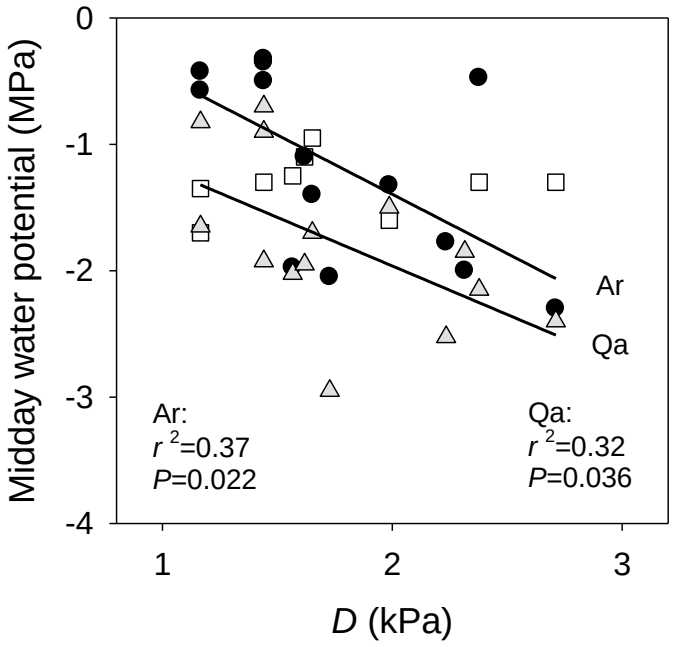

Figure 4.4 Effect of experimentally increased *D* on midday leaf water potential (n=1 leaf) on 21 July 2010 for *A. rubrum* and *Q. alba*. Midday Ψ_L was correlated to chamber *D* in Ar and Qa, but not in Ct. Mean Ψ_L was significantly higher in Ar than in Qa (t_{27}=5.304, P=0.030). Species codes are as in Figure 4.3.

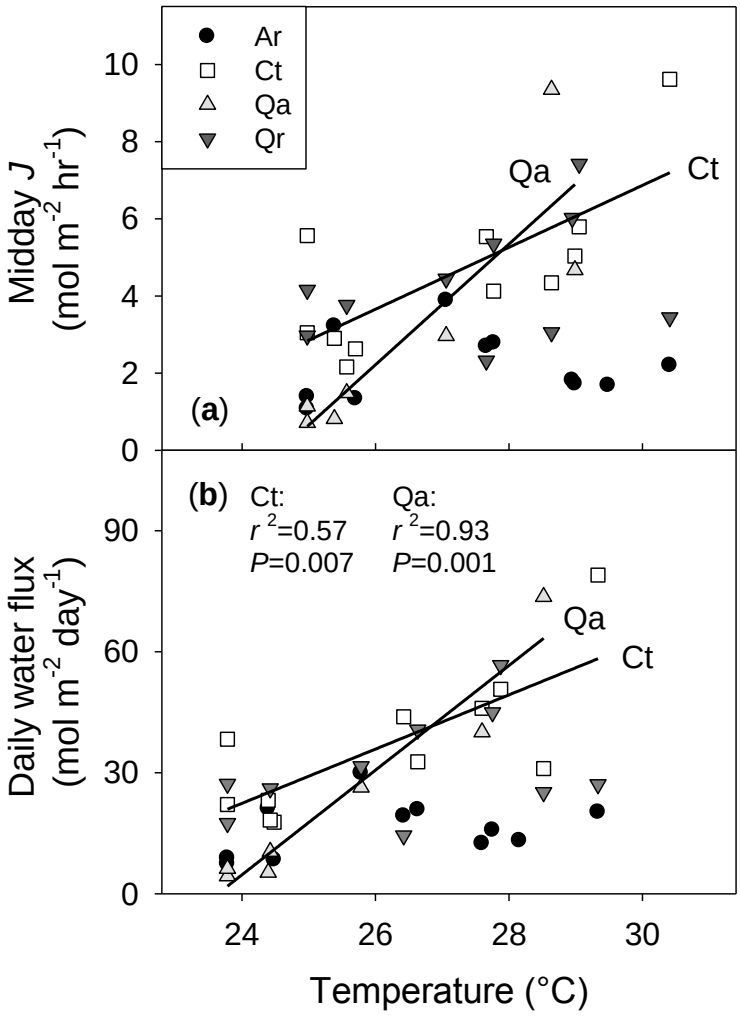

Figure 4.5 Effect of warming on (a) midday transpiration rate and (b) daily water flux on 2 August 2010 for all species. Midday *J* and daily water flux were correlated to chamber temperature in Ct and Qa, but not in Ar and Qr. Species codes are as in Figure 4.3.

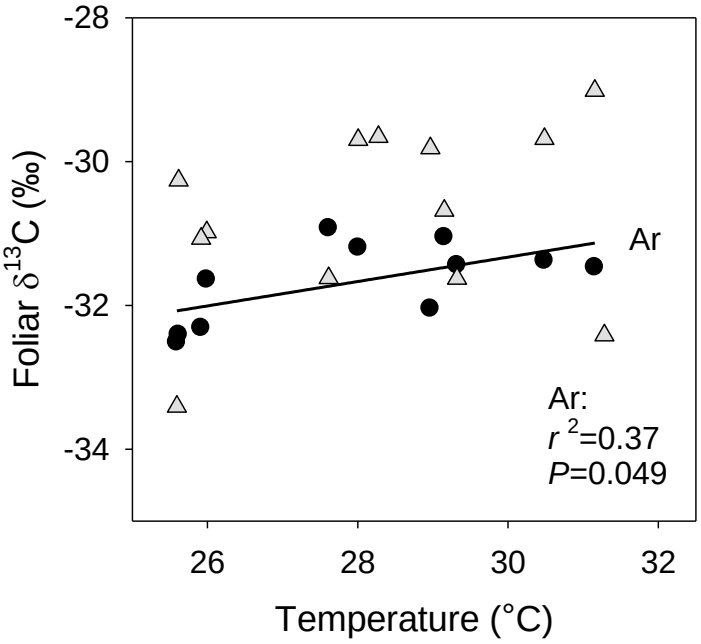

Figure 4.6 Effect of warming on foliar carbon isotope ratios of *A. rubrum* and *Q. alba*. Leaves (*n*=2–3 per seedling) were sampled on 29 August 2010, and values are means of 3–4 seedlings per chamber. Foliar $\delta^{13}C$ were correlated to chamber temperature in Ar, but not in Qa (r^2=0.10, *P*=0.305). Species codes are as in Figure 4.3.

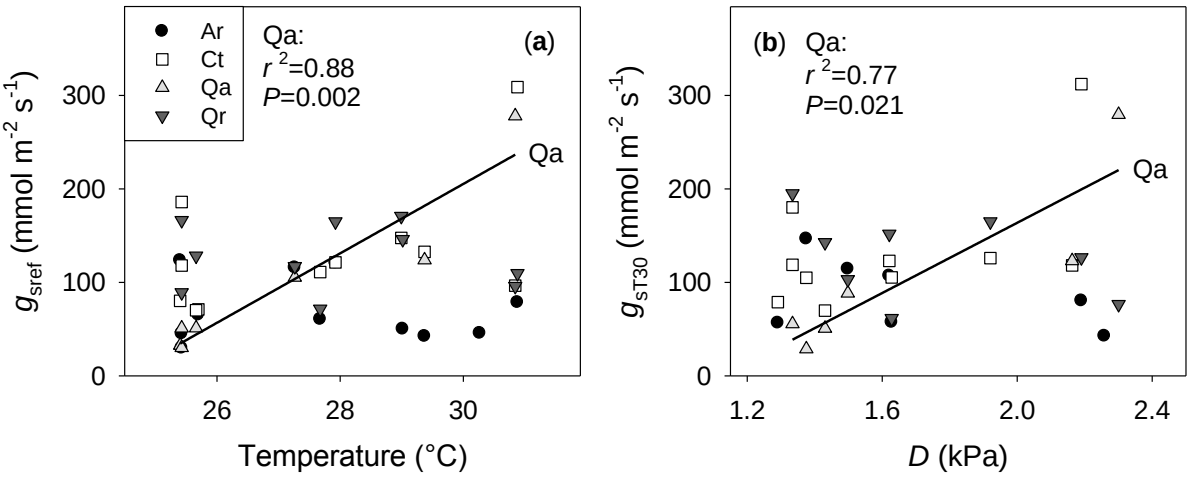

Figure 4.7 (a) Relationship between mean stomatal conductance at 1 kPa (g_{sref}) and chamber temperature for all seedlings. (b) Relationship between mean stomatal conductance at 30 °C (g_{sT30}) and mean chamber *D* among all seedlings. Both relationships were only significant for Qa when analyzed by species. Species codes are as in Figure 4.3.

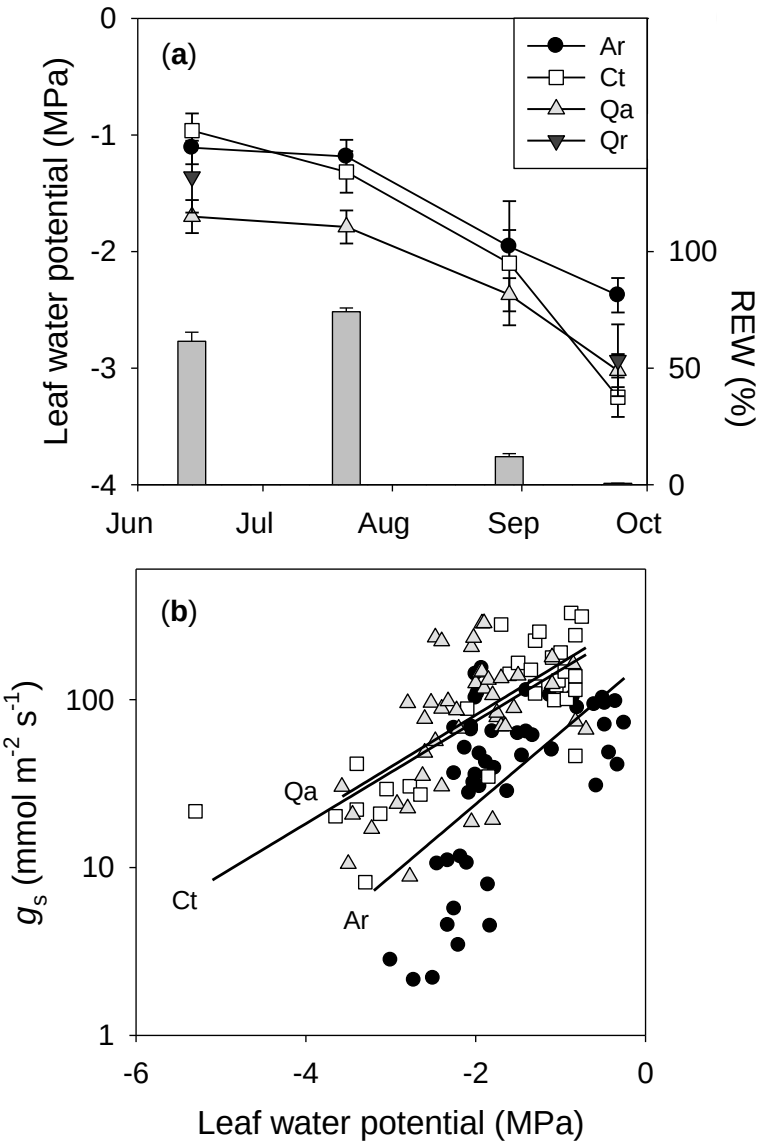

Figure 4.8 (a) Seasonal changes in midday leaf water potential and relative extractable soil water content in 2010. There were significant effects of species ($F_{2,149}$=15.544, P<0.0001) and date ($F_{3,143}$=69.827, P<0.0001) on leaf water potential, and the interaction between factors was also significant ($F_{7,149}$=2.167, P=0.041). Values are means across chambers (n=9-14 for Ar, Ct, Qa), and Qr was only measured in June and September due to low sample size (n=3). (b) Relationship between water potential and stomatal conductance measured with a porometer at midday in Ar (r^2=0.35, P<0.0001), Ct (r^2=0.65, P<0.0001), and Qa (r^2=0.30, P<0.0001). Qr could not be measured due to low sample sizes. Species codes are as in Figure 4.3.

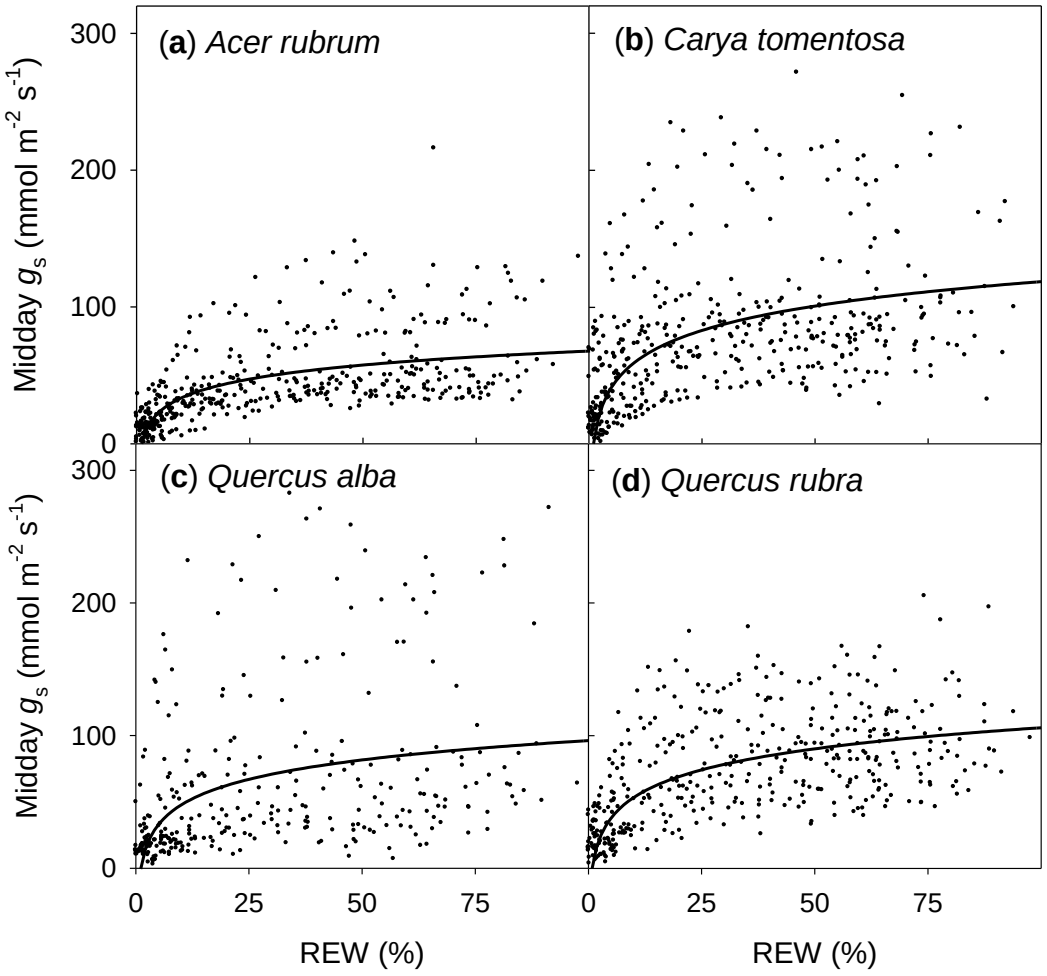

Figure 4.9 Relationship between relative extractable soil water content and midday stomatal conductance for all seedlings. Data are only shown when D_L=1.5–2.5 and lines depict the mean species relationship (Ar: r^2=0.76, P<0.0001; Ct: r^2=0.74, P<0.0001; Qa: r^2=0.57, P<0.0001; Qr: r^2=0.83, P<0.0001). Species codes are as in Figure 4.3.

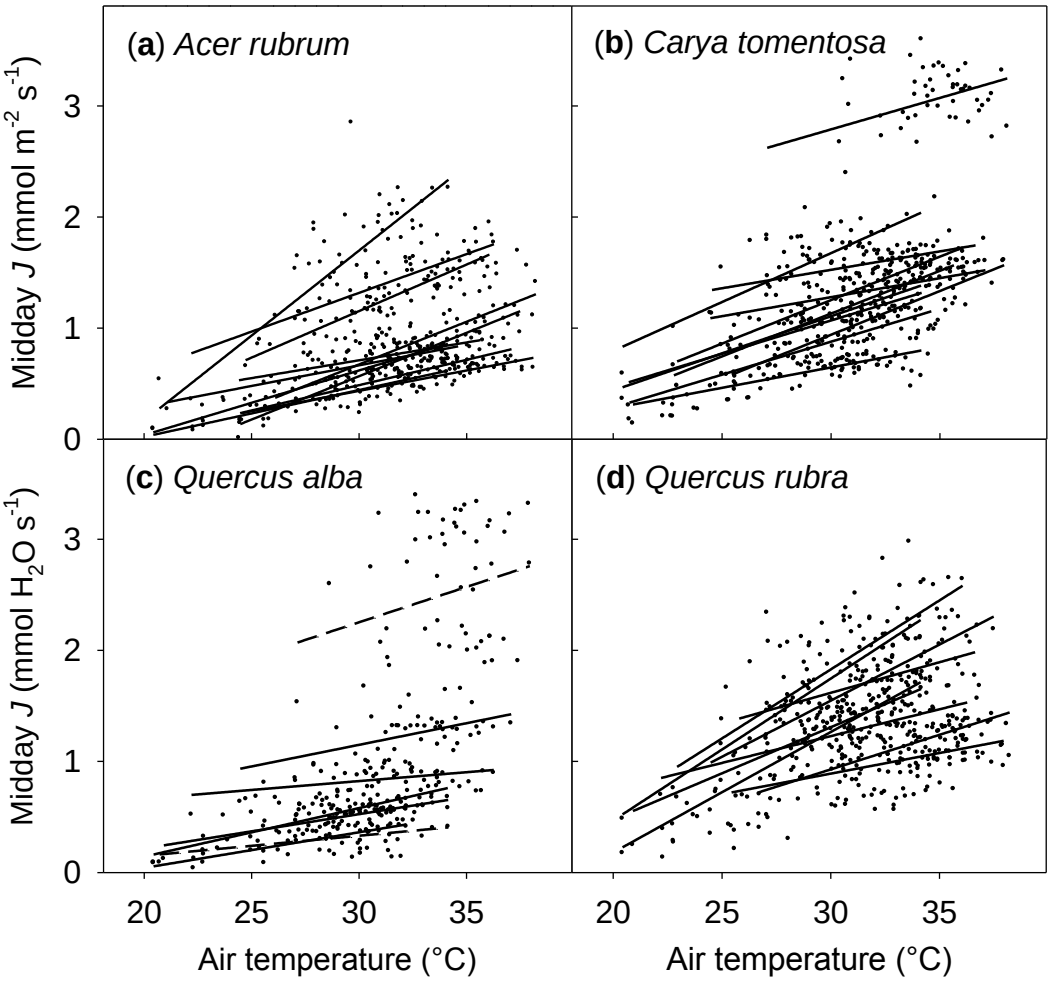

Figure 4.10 Relationship between temperature and midday transpiration rate for all seedlings. Data are only shown when REW>25%. Solid lines depict significant relationships (P<0.05) and dotted lines depict marginally significant relationships (P<0.1) for individual plants, while non-significant relationships (P>0.1) are not shown.

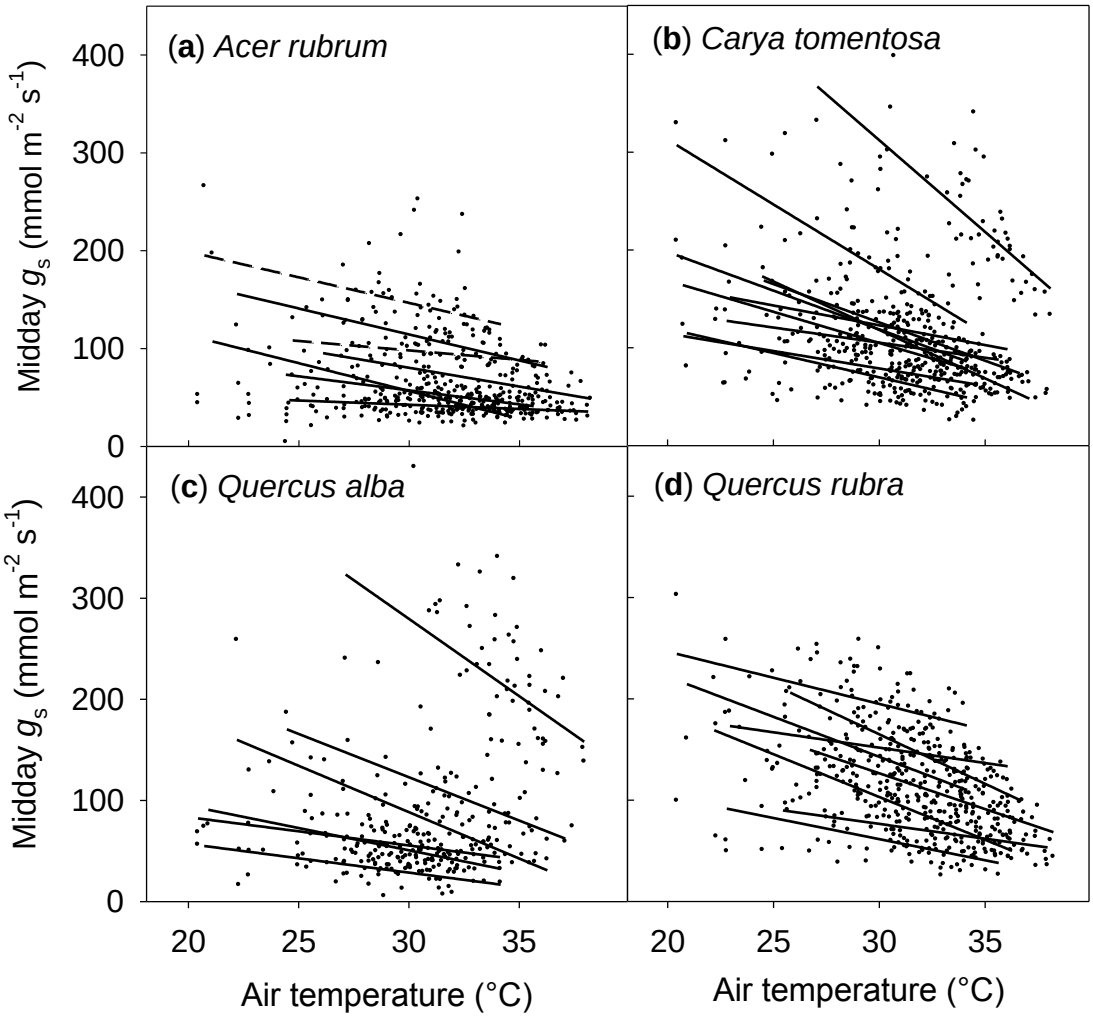

Figure 4.11 Relationship between temperature and midday stomatal conductance for all seedlings. Data are only shown when REW>25%. Solid lines depict significant relationships (P<0.05) and dotted lines depict marginally significant relationships (P<0.1) for individual plants, while non-significant relationships (P>0.1) are not shown.

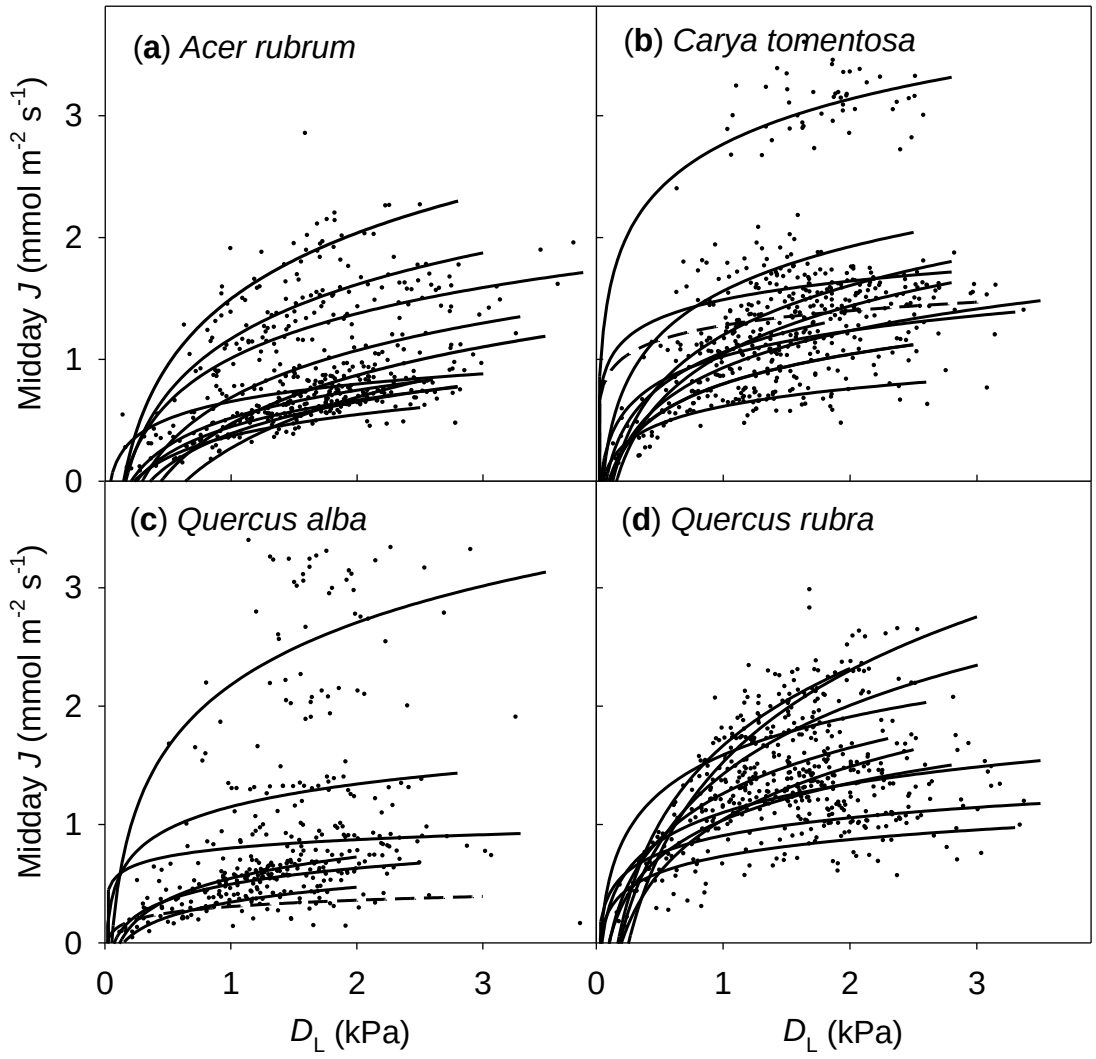

Figure 4.12 Relationship between vapor pressure deficit at the leaf surface (D_L) and midday transpiration rate for all seedlings. Data are only shown when REW>25%. Solid lines depict significant relationships (P<0.05) and dotted lines depict marginally significant relationships (P<0.1) for individual plants.

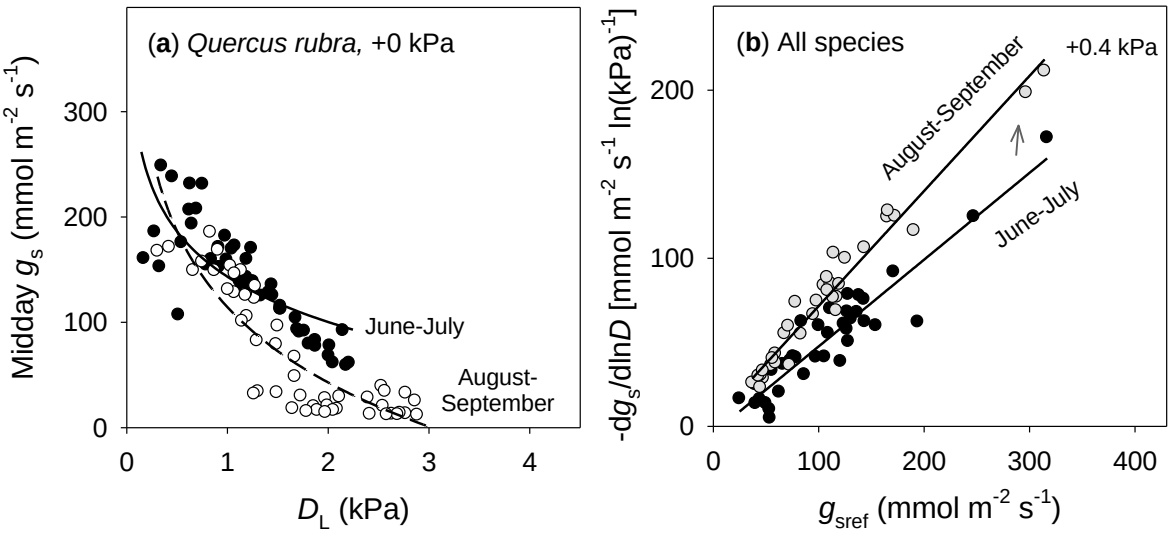

Figure 4.13 (a) Shift over time in the relationship between vapor pressure deficit at the leaf surface (D_L) and midday stomatal conductance in a *Q. rubra* seedling in a control chamber. Days in mid-summer (June–July, dark circles) are contrasted with days in late summer (August–September, gray circles). (b) The sensitivity of mean stomatal conductance to increasing vapor pressure deficit at the leaf surface ($-dg_s/d\ln D_L$) as a function of mean stomatal conductance at 1 kPa (g_{sref}) in all seedlings. The two axes represent the slope and intercept of the relationship $g_s = -m_{gs} \cdot \ln D_L + g_{sref}$ that is depicted in (a). The lines represent the least-square fit to data from one time period (mid-summer: r^2=0.87, P<0.0001; late summer: r^2=0.96, P<0.0001).

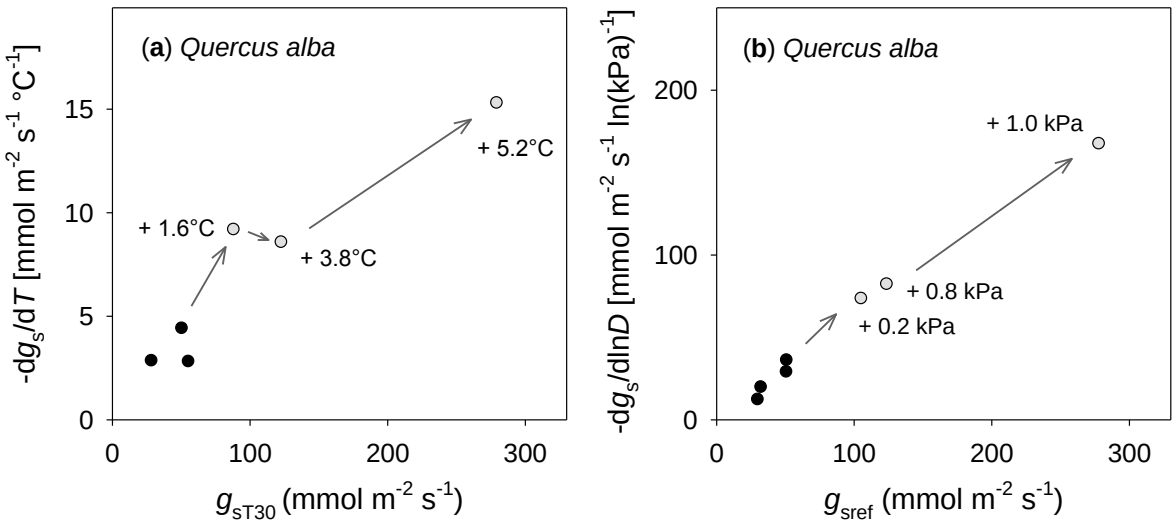

Figure 4.14 (a) The sensitivity of mean stomatal conductance to increasing temperature at the leaf surface ($-dg_s/dT$) as a function of mean stomatal conductance at 30 °C (g_{sT30}) in *Q. alba*. The two axes represent the slope and intercept of the relationship $g_s = -m_{gsT} \cdot T + g_{sT30}$. (b) The sensitivity of mean stomatal conductance to increasing vapor pressure deficit at the leaf surface ($-dg_s/d\ln D_L$) as a function of mean stomatal conductance at 1 kPa (g_{sref}) in *Q. alba*. The two axes represent the slope and intercept of the relationship $g_s = -m_{gs} \cdot \ln D_L + g_{sref}$. Control chambers are shown as black circles, and heated chambers are gray circles.

4.4 Discussion

This study assessed the effect of experimentally manipulated temperature and *D* on the growth and physiology of seedlings of four deciduous tree species in the temperate forest understory. Experimental warming significantly increased aboveground biomass of *C. tomentosa* and *Q. alba* after 3 years, but did not affect growth of *A. rubrum* and *Q. rubra* (Figure 4.3). The treatment did affect the physiology of all four species, however. Warming increased g_s in *Q. alba* (Figure 4.7), despite the concomitant rise in D_L that decreased g_s (Table 4.2). It is unclear if future warming and elevated *D* will increase g_s in the other three species, due to the confounding of temperature and *D* in this experiment. Plant stomata acclimated to changes in D_L over time (Figure 4.13) and across the experimental treatment (Figure 4.14), indicating that stomatal responses to *D* are not fixed, but are dynamic within a species or even individual plants. Acclimation of stomata tracked environmental changes to prevent excessive water loss during periods of high atmospheric evaporative demand. Warming and increased *D* caused a significant decline in midday leaf water potential (Figure 4.4) and increase in midday *J* (Figure 4.5a) and daily water use (Figure 4.5b), suggesting that future climate change will increase the potential for temperature-induced drought stress. Differences among species indicate that the diffuse-porous *A. rubrum* had greater sensitivity to declining soil moisture and elevated *D* (Figures 4.6, 4.8). Carbon gain in *A. rubrum* will be the most negatively affected by warming and increased evaporative demand in the future, if climate changes occur in the same direction as the experimental manipulation here.

Growth responses to warming

Warming of 1.6–5.3 °C for 3 years significantly increased aboveground biomass of *C. tomentosa* and *Q. alba* (Figure 4.3). A recent review found that there is a 1.7-fold increase in total biomass of deciduous tree species, relative to controls, with warming of 10 °C (Way & Oren, 2010). Results from field manipulation experiments around the globe also reveal that warming generally increases ecosystem productivity (Arft *et al.*, 1999; Rustad *et al.*, 2001; Wu *et al.*, 2011), indicating that our results for *C. tomentosa* and *Q. alba* are in agreement with previous studies. We found no growth response to warming in *A. rubrum* or *Q. rubra*, however. It is possible that the 3-year duration of the study is too short for the effect of warming on growth to be evident in these species. Two other mechanisms could have contributed to the lack of a growth response in *A. rubrum* and *Q. rubra*: (1) atmospheric drying, and (2) decreased annual precipitation over the study period.

The heating of air in this experiment led to increases in mean daytime *D* ranging from 0.16–0.96 kPa (Figure 4.1), and atmospheric drying could have limited carbon gain in warmed plants. In July 2010, midday Ψ_L was negatively correlated to chamber *D* (Figure 4.10) and led to an atmospheric drought, even under conditions of high soil water content. Reductions in Ψ_L resulted in low rates of g_s (Figure 4.8) that limited carbon gain. There was no correlation between temperature and REW among the chambers throughout the study period, so the experimental treatment was limited to atmospheric warming and atmospheric drying.

Water limitation could have contributed to the lack of a temperature response in this study, because mean annual precipitation in all three study years was below the annual mean

for Duke Forest, NC. Growth is dependent on amount of precipitation, and multi-factor precipitation and temperature experiments have shown that the positive effect of warming on aboveground biomass is lower under decreased precipitation (Wu *et al.*, 2011). Our findings confirm that drought in late summer 2010 significantly lowered Ψ_L (Figure 4.8) and decreased rates of g_s (Figure 4.9), thereby limiting plant carbon gain. Warming in the future will be associated with rises in atmospheric CO_2 concentrations, which will further stimulate plant growth or partially offset any warming-induced growth reductions in temperate trees (Norby & Luo, 2004). These responses to CO_2 are strongest under high humidity, however, and decline rapidly as *D* exceeds 1–1.5 kPa (Körner *et al.*, 2007).

Treatment effects versus seasonal effects on tree physiology

Models predict that transpiration will increase by about 50% with warming of 3 °C, although this response decreases when g_s is allowed to vary with changes in *D* (de Boeck *et al.*, 2012). We confirmed that a warmer climate increases midday *J* (Figure 4.5a) and daily water use (Figure 4.5b), although the increase was only significant in *C. tomentosa* and *Q. alba*. Seasonal variation in temperature and *D* was also positively correlated to *J* in almost all seedlings (Tables 4.1-4.2, Figures 4.10, 4.12). Thus, the effect of the experimental treatment on midday *J* and daily water flux was consistent with seasonal variation in temperature and *D*. While the relationship between temperature and *J* was linear (Figure 4.10), there was saturation of the relationship between D_L and *J* (Figure 4.12), because stomata limited water loss under high values of D_L (Table 4.2, Figure 4.13). Transpiration restriction by stomata at high *D* may be largely caused by limitations in hydraulic conductance of leaves (Brodribb &

Jordan, 2008; Sinclair *et al.*, 2008). Climate change will increase water use by temperate trees in the future, although the magnitude of this increase is dependent on regulation of g_s by trees.

The effect of warming on g_s was complicated by interactions between temperature and *D* in this study, resulting in different patterns of responses among species. It was not possible to isolate the effect of temperature from that of *D* on g_s in this experiment, due to the strong correlation between temperature and *D* among open-top chambers (Figure 4.1). Future climate changes are not expected to occur in isolation, however, and our experimental treatment represents a plausible trajectory for climate change in southeastern temperate forests in the future. Warming caused an increase in g_s in *Q. alba* (Figure 4.7), despite the concomitant rise in D_L that decreased g_s (Table 4.2). There was no strong effect of the experimental treatment on g_s of the other three species (Figure 4.7), and some evidence supported a decrease in midday g_s with the experimental treatment for *A. rubrum* and *Q. rubra*, as elevated D_L was negatively correlated to midday g_s for 18% of the summer in *A. rubrum* and 54% of the summer in *Q. rubra*. Furthermore, foliar $\delta^{13}C$ of *A. rubrum* was significantly positively correlated to chamber temperature (Figure 4.6), indicating that heated plants had greater stomatal restrictions to carbon gain over the growing season.

To clarify these contrasting responses among species, we compared these treatment responses to the effect of seasonal variation in temperature on g_s. Both temperature and elevated *D* had negative effects on g_s, but the relationship between D_L and g_s was exponential while the relationship between temperature and g_s was linear (Tables 4.1-4.2, Figure 4.11, 4.13). It seems likely that the strong relationship between D_L and g_s may have confounded

the relationship between temperature and g_s in this study. If so, the negative correlation between seasonal variation in temperature and g_s is only an artifact of the strong relationship between D_L and g_s. Thus, examining responses to seasonal climate variation led to greater confidence that there is a positive effect of warming on g_s, at least in *Q. alba*. Other studies of warming effects on g_s have confirmed that warming often has a positive effect on g_s (Bunce, 2000; Lu *et al.*, 2000; Kudoyarova *et al.*, 2011; Way *et al.*, 2012), although the effect may only be significant under conditions favoring high conductance (Sadras *et al.*, 2012). Although the direct effect of warming on g_s may be positive, we have shown here that reductions in g_s in the future are also possible if warming is associated with higher *D*.

Stomatal sensitivity to D

Stomatal sensitivity to *D* was not constant throughout the growing season (Figure 4.13) or across treatments (Figure 4.14), and shifts indicate there is acclimation of stomatal regulation of transpiration. After a moderate drought and increase in mean daytime *D* by 0.4 kPa, mean stomatal sensitivity of all seedlings increased (Figure 4.13), although this seasonal shift in stomatal sensitivity was only significant in *Q. rubra*. Under times of low soil water content and high atmospheric evaporative demand, acclimation of stomata prevented excessive water loss. Stomatal sensitivity to temperature and *D* was higher in warmer, high *D* chambers in *Q. alba* (Figure 4.14), but not in the other three species. Regardless of whether shifts were over time or across experimental treatments, prolonged exposure to high *D* resulted in increased stomatal sensitivity (Figures 4.13, 4.14). Stomatal acclimation has been reported previously in a turfgrass (Sermons *et al.*, 2012) and in deciduous trees (Kutsch *et al.*, 2001; Herbst *et al.*,

2008), and here we have shown that acclimation occurred in two *Quercus* species. Moreover, stomatal acclimation occurred in the same direction across plant functional types.

Species differences

The diffuse-porous species *A. rubrum* responded differently to the experimental treatment and to drought, when compared to the three ring-porous species (*C. tomentosa, Q. alba, Q. rubra*). Midday Ψ_L throughout the summer were consistently highest in *A. rubrum*, whether affected by seasonal variation in soil water content or experimentally increased *D* (Figures 4.4, 4.8). Transpiration (J_{ref}) and midday g_s were lowest in *A. rubrum* (Table 4.2), due to differences in stomatal sensitivity to Ψ_L. Stomata in *A. rubrum* closed more abruptly with decreasing Ψ_L, whereas stomatal closure was more gradual in *C. tomentosa* and *Q. alba* (Figure 4.8b). Other studies in eastern US forests have also found greater sensitivity of stomata to drought and increased *D* in diffuse-porous trees, when compared to ring-porous trees (Meinzer *et al.*, 2013). Carbon gain in *A. rubrum* will be the most negatively affected by warming and increased evaporative demand in the future, if climate changes occur in the same direction as the experimental manipulation here.

REFERENCES

Arft AM, Walker MD, Gurevitch J, *et al*. (1999) Responses of tundra plants to experimental warming: Meta-analysis of the international tundra experiment. *Ecological Monographs*, **69**, 491-511.

Brodribb TJ, Jordan GJ (2008) Internal coordination between hydraulics and stomatal control in leaves. *Plant Cell and Environment*, **31**, 1557-1564.

Buckley TN (2005) The control of stomata by water balance. *New Phytologist*, **168**, 275-291.

Bunce JA (2000) Responses of stomatal conductance to light, humidity and temperature in winter wheat and barley grown at three concentrations of carbon dioxide in the field. *Global Change Biology*, **6**, 371-382.

Caird MA, Richards JH, Donovan LA (2007) Nighttime stomatal conductance and transpiration in C_3 and C_4 plants. *Plant Physiology*, **143**, 4-10.

Clearwater MJ, Luo ZW, Mazzeo M, *et al*. (2009) An external heat pulse method for measurement of sap flow through fruit pedicels, leaf petioles and other small-diameter stems. *Plant Cell and Environment*, **32**, 1652-1663.

Daley MJ, Phillips NG (2006) Interspecific variation in nighttime transpiration and stomatal conductance in a mixed New England deciduous forest. *Tree Physiology*, **26**, 411-419.

de Boeck HJ, Kimball BA, Miglietta F, *et al*. (2012) Quantification of excess water loss in plant canopies warmed with infrared heating. *Global Change Biology*, **18**, 2860-2868.

Friend AD (1991) Use of a model of photosynthesis and leaf microenvironment to predict optimal stomatal conductance and leaf nitrogen partitioning. *Plant Cell and Environment*, **14**, 895-905.

Herbst M, Rosier PTW, Morecroft MD, *et al*. (2008) Comparative measurements of transpiration and canopy conductance in two mixed deciduous woodlands differing in structure and species composition. *Tree Physiology*, **28**, 959-970.

Jung M, Reichstein M, Ciais P, *et al*. (2010) Recent decline in the global land evapotranspiration trend due to limited moisture supply. *Nature*, **467**, 951-954.

Karl TR, Melillo JM, Peterson TC (2009) Global Climate Change Impacts in the United States. US Global Change Research Program, Cambridge University Press, New York.

Körner C, Morgan J, Norby R (2007) CO_2 Fertilization: When, Where, How Much? In *Terrestrial Ecosystems in a Changing World* (eds J.G. Canadell, D.E. Pataki & L.F. Pitelka), pp. 9-18. Springer, Berlin.

Kosugi Y, Matsuo N (2006) Seasonal fluctuations and temperature dependence of leaf gas exchange parameters of co-occurring evergreen and deciduous trees in a temperate broad-leaved forest. *Tree Physiology*, **26**, 1173-1184.

Kosugi Y, Shibata S, Kobashi S (2003) Parameterization of the CO_2 and H_2O gas exchange of several temperate deciduous broad-leaved trees at the leaf scale considering seasonal changes. *Plant Cell and Environment*, **26**, 285-301.

Kudoyarova G, Veselova S, Hartung W, *et al*. (2011) Involvement of root ABA and hydraulic conductivity in the control of water relations in wheat plants exposed to increased evaporative demand. *Planta*, **233**, 87-94.

Kutsch WL, Herbst M, Vanselow R, *et al*. (2001) Stomatal acclimation influences water and carbon fluxes of a beech canopy in northern Germany. *Basic and Applied Ecology*, **2**, 265-281.

Lu ZM, Quinones MA, Zeiger E (2000) Temperature dependence of guard cell respiration and stomatal conductance co-segregate in an F_2 population of Pima cotton. *Australian Journal of Plant Physiology*, **27**, 457-462.

Lynch IP (2006) The Duke Forest at 75: A Resource for All Seasons. Office of the Duke Forest, Durham, North Carolina.

Marshall DC (1958) Measurement of sap flow in conifers by heat transport. *Plant Physiology*, **33**, 385-396.

Meinzer FC, Woodruff DR, Eissenstat DM, *et al*. (2013) Above- and belowground controls on water use by trees of different wood types in an eastern US deciduous forest. *Tree Physiology*, **33**, 345-356.

Monteith JL (1995) A reinterpretation of stomatal responses to humidity. *Plant Cell and Environment*, **18**, 357-364.

Mott KA, Parkhurst DF (1991) Stomatal responses to humidity in air and helox. *Plant Cell and Environment*, **14**, 509-515.

NDMC, USDA, NOAA (2012) United States Drought Monitor, <http://droughtmonitor.unl.edu/Home.aspx>.

Nobel P (1974) *Introduction to biophysical plant physiology*. WH Freeman & Company, San Francisco, CA.

Norby RJ, Luo YQ (2004) Evaluating ecosystem responses to rising atmospheric CO_2 and global warming in a multi-factor world. *New Phytologist*, **162**, 281-293.

Oren R, Sperry JS, Katul GG, *et al*. (1999) Survey and synthesis of intra- and interspecific variation in stomatal sensitivity to vapour pressure deficit. *Plant Cell and Environment*, **22**, 1515-1526.

Peak D, Mott KA (2011) A new, vapour-phase mechanism for stomatal responses to humidity and temperature. *Plant Cell and Environment*, **34**, 162-178.

Pelini SL, Bowles FP, Ellison AM, *et al*. (2011) Heating up the forest: open-top chamber warming manipulation of arthropod communities at Harvard and Duke Forests. *Methods in Ecology and Evolution*, **2**, 534-540.

Pettijohn JC, Salvucci GD, Phillips NG, *et al*. (2009) Mechanisms of moisture stress in a mid-latitude temperate forest: Implications for feedforward and feedback controls from an irrigation experiment. *Ecological Modelling*, **220**, 968-978.

Roberts J, Cabral OMR, Deaguiar LF (1990) Stomatal and boundary-layer conductances in an Amazonian terra-firme rain forest. *Journal of Applied Ecology*, **27**, 336-353.

Rustad LE, Campbell JL, Marion GM, *et al*. (2001) A meta-analysis of the response of soil respiration, net nitrogen mineralization, and aboveground plant growth to experimental ecosystem warming. *Oecologia*, **126**, 543-562.

Sadras VO, Montoro A, Moran MA, *et al*. (2012) Elevated temperature altered the reaction norms of stomatal conductance in field-grown grapevine. *Agricultural and Forest Meteorology*, **165**, 35-42.

Sermons SM, Seversike TM, Sinclair TR, *et al*. (2012) Temperature influences the ability of tall fescue to control transpiration in response to atmospheric vapour pressure deficit. *Functional Plant Biology*, **39**, 979-986.

Shope JC, Peak D, Mott KA (2008) Stomatal responses to humidity in isolated epidermes. *Plant Cell and Environment*, **31**, 1290-1298.

Sinclair TR, Zwieniecki MA, Holbrook NM (2008) Low leaf hydraulic conductance associated with drought tolerance in soybean. *Physiologia Plantarum*, **132**, 446-451.

Tardieu F, Simonneau T (1998) Variability among species of stomatal control under fluctuating soil water status and evaporative demand: modelling isohydric and anisohydric behaviours. *Journal of Experimental Botany*, **49**, 419-432.

Trenberth KE, Fasullo J, Smith L (2005) Trends and variability in column-integrated atmospheric water vapor. *Climate Dynamics*, **24**, 741-758.

Turner NC, Schulze ED, Gollan T (1984) The responses of stomata and leaf gas exchange to vapor pressure deficits and soil water content. *Oecologia*, **63**, 338-342.

Warton DI, Wright IJ, Falster DS, *et al*. (2006) Bivariate line-fitting methods for allometry. *Biological Reviews*, **81**, 259-291.

Way DA, Domec JC, Jackson RB (2012) Elevated growth temperatures alter hydraulic characteristics in trembling aspen (*Populus tremuloides*) seedlings: implications for tree drought tolerance. *Plant Cell and Environment*, **36**, 103-115.

Way DA, Oren R (2010) Differential responses to changes in growth temperature between trees from different functional groups and biomes: a review and synthesis of data. *Tree Physiology*, **30**, 669-688.

Wu ZT, Dijkstra P, Koch GW, *et al*. (2011) Responses of terrestrial ecosystems to temperature and precipitation change: a meta-analysis of experimental manipulation. *Global Change Biology*, **17**, 927-942.

CHAPTER 5

Transgenically altered lignin biosynthesis affects water relations of field-grown *Populus trichocarpa*

5.1 Abstract

Concerns over energy security and climate forcing from fossil fuel emissions have stimulated interest in development of high-yielding, low-lignin trees for bioenergy. Black cottonwood (*Populus trichocarpa*) has been targeted as a potential bioenergy species due to its high productivity, but it is not known how transgenically altered lignin biosynthesis will affect water relations. We investigated the physiology of trees growing in short rotation woody cropping systems at two sites in southeastern USA; a mountain site more favorable for growth of *P. trichocarpa* and a hotter piedmont site that experienced frequent water stress. Maximum productivity was found at the cooler mountain site and resulted from high rates of photosynthesis (20.3 μmol CO_2 m^{-2} s^{-1}) and stomatal conductance (422.4 mmol H_2O m^{-2} s^{-1}). The two low-lignin genotypes had significantly lower mean leaf water potential, stomatal conductance, transpiration, hydraulic conductivity, and leaf-specific whole-plant hydraulic conductance than the wild-type control. The water transport capacity of vascular tissues in transgenic genotypes was severely impaired, which was particularly evident at the top of stems. Productivity was positively correlated to stem lignin content at the piedmont site, and

stunted growth of low-lignin trees was caused by (1) stomatal restriction of carbon gain due to water stress and (2) decreased biophysical and biochemical photosynthetic processes. Although there was no difference in lignin among genotypes after 3 years of growth at the mountain site, the transformation resulted in an alternative advantage for potential use in bioenergy systems – lower water consumption. Higher intrinsic water use efficiency of transgenic trees resulted in total water savings of roughly 1 kg H_2O $tree^{-1}$ day^{-1} without sacrificing productivity. Our findings indicate that effects of genetic transformation on field-grown trees are site-specific and highlight the need for a better understanding of the interaction between transgenic alteration of lignin biosynthesis and environmental conditions on whole-plant function.

5.2 Introduction

Biofuel production from cellulosic perennial crops, such as grasses and poplars, reduces greenhouse gas emissions relative to gasoline (Sims *et al*., 2006) and provides numerous advantages over non-cellulosic crops such as corn (Somma *et al*., 2010). Poplars (i.e. *Populus* species) are among the fastest growing trees in temperate regions and thus ideal candidates for short rotation woody cropping (SRWC) systems for bioethanol production in the United States. The high productivity of poplars requires a large water supply, however (Tschaplinski *et al.*, 1998), so their potential as a bioenergy cropping system may be restricted to regions with adequate water availability. *Populus* is highly susceptible to drought due to low stomatal sensitivity to water potential (Braatne *et al.*, 1992) and high vulnerability to cavitation (Fichot *et al*., 2010). Higher temperatures in the future are

expected to increase the probability of drought and temperature-induced drought stress (Karl *et al*., 2009), so selecting genotypes that minimize water use and maximize carbon sequestration and growth will be of critical importance (King *et al*., 2013). Water use efficiency (WUE) is a particularly useful trait for determining the cost of water consumption for biomass production in an individual plant and is an important determinant of the sustainability of bioenergy production systems (King *et al*., 2013).

Before commercial-scale production of cellulosic biofuels can occur, however, the cost of converting cellulose to ethanol or other biofuels must be decreased to a level competitive with gasoline and corn-starch ethanol. The reduction of lignin in cellulosic plant biomass is one promising solution that increases ethanol yield while decreasing processing inputs (Chapple *et al*., 2007). Lignins in plant secondary cell walls hinder the degradation of cell wall polysaccharides to simple sugars destined for fermentation to ethanol. Another strategy for increasing the biochemical efficiency of cellulose conversion to biofuel is to increase the ratio of syringyl (S) to guaiacyl (G) monolignol units in angiosperm lignin. Syringyl-rich lignin is substantially easier to separate from cellulose than guaiacyl-rich lignin during pulping for paper production (Li *et al*., 2000). Genetic transformations of genes that encode for enzymes along the lignin biosynthetic pathway have been developed that successfully decrease lignin quantity and increase the S:G ratio of stem tissue in *Populus* (Hu *et al*., 1999; Hancock *et al*., 2007; Horvath *et al*., 2010; Voelker *et al*., 2010). Although transgenic plants grown in controlled conditions have dramatic decreases in stem lignin content (Hu *et al*., 1999; Li *et al*., 2003), evidence is mounting that transgenic alteration of lignin biosynthesis may not remain stable when grown under natural field conditions over

long time periods (Kaur *et al*., 2012; Wang *et al*., 2012; Stout *et al.*, in review). There are 23 genes that likely encode monolignol biosynthesis enzymes during wood formation in *Populus trichocarpa* (black cottonwood), and there is likely functional redundancy in many of these enzymes (Shi *et al.*, 2010). In the 4-coumarate:coenzyme A ligase (*4CL*) gene family, three genes are expressed in wood-forming tissue of *P. trichocarpa* and have been suggested for biochemical roles in lignin synthesis (Shi *et al.*, 2010). Increases in lignin content during wood formation can be induced by environmental stressors, such as mechanical stress, drought, and pathogen attack (Vance *et al.*, 1980; Boerjan *et al.*, 2003). Lignin composition has also been observed to change in response to natural abiotic factors such as wind (Koehler and Telewski, 2006). Clearly, a better understanding of the role of lignin in plant functional responses to different environmental conditions is needed.

Lignins are functionally important in mechanical support (Vanholme *et al*., 2010; Weng and Chapple, 2010), water conductance (Tyree and Zimmermann, 2002), carbon storage, and disease resistance (Vance *et al.*, 1980). Lignified secondary cell walls provide significant compressive strength against pressures up to 40 MPa, relative to non-lignified walls (Niklas, 1992). Low-lignin *Populus* trees have been found to have decreased hydraulic conductivity and a greater susceptibility to cavitation (Coleman *et al.*, 2008; Voelker, 2009) as a result of collapsed cells and blockage of vessels by tyloses and phenolics (Kitin *et al.*, 2010). Such reductions in water transport capacity are likely to have negative effects on the productivity of transgenic trees, especially *Populus* because of its large water requirement (Tschaplinski *et al.*, 1998). It is not yet clear how universal these physiological responses are

among *Populus* genotypes and different genetic transformations, especially for plants grown under field conditions for multiple years.

The main objective of this study was to quantify physiological water relations of three genotypes of *P. trichocarpa* (wild-type and two low-lignin transgenics) under natural environmental conditions in the southeastern USA. A previous study established that lignin concentrations of *P. trichocarpa* trees increased by 1–9% after 3 years of growth in North Carolina (Stout *et al*., in review). The genetic transformation did not affect tree productivity at a relatively mesic site (mountain) but reduced productivity at a site more prone to drought stress (piedmont; Stout *et al*., in review). In this study, we first determined how drought stress affects wild-type and transgenic trees by comparing physiological responses at the two study sites. Second, we compared physiological responses of the two low-lignin transgenic lines to the wild-type control at each site. Specifically, we measured seasonal changes in growth, leaf water potential, gas exchange, leaf-specific whole-plant hydraulic conductance (G_t), and intrinsic WUE of each genotype. We also determined if wood density, foliar nitrogen concentration, and photosynthesis differed among genotypes and sites. We hypothesized that transgenic trees will have lower G_t and decreased rates of biophysical and biochemical photosynthetic processes (e.g. maximum velocity of ribulose 1·5-bisphosphate carboxylase/oxygenase, Rubisco, for carboxylation, V_{cmax}; electron transport rate, J) relative to the wild-type control.

5.3 Materials and Methods

Study species

Populus trichocarpa is the largest hardwood tree in western North America and can grow to over 60 m in height (DeBell, 1990). It grows primarily on moist sites west of the Rocky Mountains and is most productive in bottom lands of major streams and rivers. The female *P. trichocarpa* genotype "Nisqually-1" was found near the Nisqually River in central Washington, USA and is the only tree to have its complete genome sequenced (Tuskan *et al.*, 2006). Two transgenic *P. trichocarpa* (PT-1, PT-3) were produced by antisense suppression of the gene encoding 4CL in the Nisqually-1 genotype (V. Chiang, Forest Biotechnology Group, North Carolina State University, Raleigh, NC, USA). The transformations used the 4CL promoter from *P. tremuloides* and were mediated by *Agrobacterium tumefaciens*. The transgenic trees were produced from tissue culture under greenhouse conditions during fall 2008. After several months of growth, the trees were transferred to small pots and placed in a covered greenhouse in January 2009 for cold acclimation before planting in April 2009. Under greenhouse conditions, the two low-lignin lines had lignin concentrations of 13.9% and 17.4%, while the wild-type control contained 22% lignin (Stout *et al*., in review; Table 5.1). The S:G ratios of the low-lignin lines were approximately 40% greater than the control at the time of planting (Table 5.1).

Experimental study sites

Trees were planted in the mountain and piedmont regions of North Carolina, USA. The mountain site was located in Fletcher, Henderson County, NC (35° 25.700' N, 82° 33.467'

W, 647 m a.s.l.), and the piedmont site was located in Oxford, Granville County, NC (36° 18.167' N, 78° 36.733' W, 146 m a.s.l.). At the cooler and wetter mountain site, mean annual temperature is 12.9 °C and mean annual precipitation is 1312 mm. Mean annual temperature at the warmer and drier piedmont site is 14.4 °C and mean annual precipitation is 1158 mm. Mean growing season temperature (May–September) during the study year (2012) was lower at the mountain site than the piedmont site (21.2 vs. 23.5 °C, respectively; Figure 5.1). Growing season precipitation (May–September) was lower at the mountain site than the piedmont site in 2012 (456 vs. 808 mm, respectively), which is contrary to the average precipitation patterns for these regions (mountain: 584 mm, piedmont: 526 mm). Despite having lower rainfall, measurements of predawn leaf water potential indicated that plant-available soil water was greater at the mountain site than the piedmont site during the 2012 growing season (–0.09 vs. –0.64, respectively; t_{29}=2.47, P=0.020), likely due to soil differences between sites. Soil at the mountain site is a well-drained loam (Hayesville loam), while soil at the piedmont site is a moderately well-drained sandy-loam (Helena sandy loam) with a compacted plow pan soil layer that restricts root growth and water movement. Soil nitrogen concentrations were higher at the mountain than the piedmont site (0.22% vs. 0.05%, respectively; Stout, 2011).

Trees were planted in the field at a spacing of 0.6 m within rows and 1.2 m between rows to achieve a final planting density of approximately 13,500 trees ha^{-1}. Each row consisted of a single transgenic line, with two rows of the wild-type control at each end of the plot. At the mountain site, 78 trees were planted over an area of approximately 45 m^2, whereas at the piedmont site, 149 trees were planted over an area of approximately 100 m^2.

Due to the small size of the plots, we considered within-plot variability of environmental conditions to be negligible.

Throughout the first growing season (2009), both sites were drip irrigated to aid establishment. The drip tape was removed after the establishment year to test how the trees grew without water inputs under the environmental conditions of each region. Throughout the experiment, the site was hand weeded and mowed with a push mower to decrease weed competition. Defoliating pests were controlled with Conserve SC (Spinosad, Dow Agrosciences, Indianapolis, IN, USA), when necessary. All trees were coppiced in January 2011 at 5 cm above the base of the tree and in January 2012 at 10 cm above the base of the tree.

A previous study found that after 3 years of growth in natural field conditions, mean lignin concentrations of *P. trichocarpa* genotypes had increased by 1–9% and S:G ratios decreased by 0.5–2, with the largest changes occurring in the transgenic lines (Stout *et al*., in review; Table 5.1). Stout *et al*. (in review) established that the effect of the genetic transformation on lignin quantity and composition differed between sites. At the mountain site, there were no significant differences in stem lignin concentration between the two transgenic lines and the wild-type control after 3 years of growth (Table 5.1). At the piedmont site, however, the wild-type control had significantly higher stem lignin content than the two transgenic lines (26.4% vs. 21.6% and 23.0%, respectively) in January 2012 (Table 5.1). There were no differences in the S:G ratio of stem tissue among the three genotypes at either site after 3 years of growth (Table 5.1).

Leaf area

Seasonal changes in leaf area were estimated for each plant in May, July, and September 2012. Height (m) was measured for all stems, while leaf number and leaf area were measured for a subset of stems of varying height for each plant. Total leaf area (A_L, m^2) per plant was estimated as: $A_L = \sum(n \cdot n_{L,H} \cdot a_{L,H})$ where n is the number of stems of a given height, $n_{L,H}$ is the mean leaf number for that stem height, and $a_{L,H}$ is the mean leaf area for that stem height. Allometric equations relating stem height to leaf number and leaf area were used to determine $n_{L,H}$ and $a_{L,H}$, respectively, within each genotype at each sampling date. Leaf area was measured using a portable laser leaf area meter (CI-202, CID Bio-Science Inc., Camas, WA, USA).

Gas exchange and photosynthetic processes

Gas exchange measurements were made under local environmental conditions using a portable infrared gas analyzer equipped with a red–blue light source (LI-6400, Li-Cor, Lincoln, NE, USA) on sunny days in May, July, and September 2012 from 11:00 to 15:30 h. All measurements were made under saturating light (1500 μmol m^{-2} s^{-1}) and ambient CO_2 concentration (400 ppm). Each sampling day, the block temperature was held constant at ambient temperature and the relative humidity was held within 10% of ambient conditions. Fully-developed leaves (n=15-31 per genotype per month) were measured at a range of stem heights (top, middle, base) on each plant to examine how gas exchange varied along the stem. Photosynthesis measurements were recorded for a period of 2–3 minutes after conditions inside the cuvette stabilized (usually 1–2 minutes) and then averaged to determine

net CO_2 assimilation (A_n), stomatal conductance (g_s), transpiration (E), and intrinsic WUE (A_n:g_s) for each leaf.

To determine if the genetic transformation affected biophysical and biochemical photosynthetic processes of *P. trichocarpa* leaves, the response of A_n to varying concentrations of intercellular CO_2 (C_i) was measured between 11:00 and 15:30 h in July 2012. These A_n/C_i curves were measured on four leaves per genotype at each site. Photosynthesis was measured using the LI-6400 at ambient temperature and relative humidity, under saturating PPFD (1500 μmol m^{-2} s^{-1}). The external CO_2 (C_a) was lowered stepwise from 400 to 50 ppm and then increased from 400 to 1000 ppm with a total of 11 points per A_n/C_i curve. Rates of photosynthesis were recorded after two minutes at each C_a. Values of A_n were corrected for CO_2 leakage by subtracting 'apparent' photosynthesis quantified with six photosynthetically inactive leaves from the wild-type control, following Flexas *et al.* (2007). For comparisons among genotypes, the parameters V_{cmax} (maximum velocity of ribulose 1·5-bisphosphate carboxylase/oxygenase, Rubisco, for carboxylation), J (photosynthetic electron transport rate), *TPU* (triose phosphate use), R_d (daytime respiration), and g_m (mesophyll conductance) were estimated at 25 °C for each curve using the procedure described by Sharkey *et al*. (2007).

Leaf-specific whole plant hydraulic conductance

Based on an Ohm's-law analogy of water transport, we estimated leaf-specific whole-plant hydraulic conductance (G_t, mmol m^{-2} s^{-1} MPa^{-1}, n=5 plants per genotype) at both sites on

three dates throughout summer 2012 (May, July, September) using the method described by Schafer *et al*. (in review):

$$G_{\mathrm{t}} = \frac{(D_{\mathrm{L}}/P_{\mathrm{atm}}) * g}{(\Psi_{\mathrm{soil}} - \Psi_{\mathrm{leaf}})}$$

where D_{L} (kPa) is vapor pressure deficit at the leaf surface, P_{atm} (kPa) is atmospheric pressure for each study site, g (mmol m^{-2} s^{-1}) is leaf conductance, Ψ_{soil} (MPa) is soil water potential, and Ψ_{leaf} (MPa) is midday leaf water potential. This expression assumes a steady state in which transpiration is equal to the rate of water flow through the plant. Measurements of air temperature and relative humidity (CS215-L sensor; Campbell Scientific Inc., Logan, UT, USA) were measured every 2 minutes during the midday sampling periods (11:30–14:30), recorded by automated dataloggers (CR1000; Campbell Scientific Inc.), and combined with leaf temperature measurements to calculate D_{L} for each plant. For Ψ_{soil}, one or two fully-developed leaves per plant per sampling date were collected from the top of the stem between 5:00 and 6:30. For Ψ_{leaf}, two to three fully-developed leaves per plant were collected from the top of the stem between 11:30 and 14:30. Predawn and midday leaf water potentials were measured with a pressure chamber (Model 1000, PMS Instruments, Corvallis, OR, USA) and averaged to determine Ψ_{soil} and Ψ_{leaf} of each plant.

Total leaf conductance (g) incorporated both stomatal (g_{s}) and boundary layer (g_{b}) conductance as follows:

$$g = \left(\frac{1}{g_s} + \frac{1}{g_b}\right)^{-1}$$

Midday g_s was measured as described above on the same two leaves sampled for Ψ_{leaf}, immediately before excision. To estimate g_b, we used the relationship described by Nobel (1999):

$$g_b = \frac{D_w}{\delta_b}\left(\frac{P_{atm}}{R \cdot T}\right)$$

where D_w (m^2 s^{-1}) is the diffusion coefficient of water vapor in air, δ_b (mm) is boundary layer thickness, R (8.314 J mol^{-1} K^{-1}) is the ideal gas constant, and T (K) is air temperature. To estimate δ_b, we used the relationship: $\delta_b = 4.0 \cdot (w/v)^{1/2}$, where w is the mean leaf width (m) and v is the ambient wind speed (m s^{-1}). We measured wind speed with a cup anemometer (Inspeed, Sudbury, MA, USA) every 5 seconds and recorded mean wind speed over 2 minute periods on a datalogger (CR1000, Campbell Scientific, Inc.). We determined the average leaf width for each plant using a portable laser leaf area meter (CI-202, CID Bio-Science Inc.).

Hydraulic conductivity and wood density

Xylem-specific hydraulic conductivity (k_s, g m^{-1} min^{-1} kPa^{-1}) of stems (n=5 per genotype per site) was measured in September 2012 at both sites. Unbranched stems less than 1 year in age and at least 1 m in length were excised from the plant and immediately recut under water. The stems were transported to the laboratory with the cut end submerged in water and the uncut end covered in an opaque plastic bag. In the laboratory, branches were again cut underwater to remove at least 25 cm from each end, leaving stem segments of 15–25 cm in length with xylem diameter of 3–6 mm. The branch was connected to a hydraulic apparatus

filled with deionized water at an applied pressure of 13 kPa. Hydraulic conductivity was measured over three or four time intervals and averaged for each stem. All measurements were completed within 1 day of stem collection. Xylem-specific hydraulic conductivity (k_s, g m^{-1} s^{-1} kPa^{-1}) was calculated according to Darcy's law:

$$k_s = \frac{Q \cdot l}{A \cdot P}$$

where Q (g s^{-1}) is the volume flow rate, l (m) is the length of the segment, A (m^2) is the cross-sectional area of the stem segment, and P (kPa) is the pressure applied to the segment. Both ends of the stem segment were perfused with methylene blue solution before determining A. Small discolored patches of non-conducting xylem were observed within stems of both transgenic lines and were included in the estimate of A. Patches of non-conducting xylem were not observed in the wild-type control.

To measure wood density (g cm^{-3}), the stems collected for hydraulic conductivity were cut to about 6.0 cm length and stripped of bark. Each segment was split and the pith was removed before determining fresh volume using the water displacement method. The sample was then dried to a constant mass at 70 °C and weighed.

Foliar carbon isotope ratios and nitrogen content

Carbon isotope ratios of plant leaves provide a time-integrated measure of the ratio of intercellular CO_2 concentration to atmospheric CO_2 concentration (c_i/c_a) and can be used to indirectly estimate intrinsic WUE of each plant. Fully-developed sun leaves were collected from the top of the stem on the south side of each plant (n=5-7 plants per genotype) in

October 2011 at both sites. Leaves were oven-dried at 70 °C, and three leaves from each plant were combined and ground to a fine powder in liquid nitrogen. The $\delta^{13}C$ of foliar tissue was analyzed with an elemental analyzer (Carlo Erba, Model 1110, Milan, Italy) coupled to a Thermo-Finnigan Delta Plus gas isotope mass spectrometer (Bremen, Germany) at the Stable Isotope Mass Spectrometry Laboratory (Kansas State University, Manhattan, KS, USA). Values of $\delta^{13}C$ were calculated according to standard delta notation:

$$\delta = \left(R_{\text{sample}}/R_{\text{standard}} - 1\right)1000$$

where R is the ratio of the heavy isotope (^{13}C) to the lighter isotope (^{12}C). The standard was belemnite carbonate from the Pee Dee Belemnite Formation, SC, USA, and the precision of the $\delta^{13}C$ measurements was ±0.15‰. These same ground leaf tissue samples (1.8–2.2 mg) were also analyzed for carbon and nitrogen concentration (%) with an elemental analyzer (Carlo Erba, Model 1110, Milan, Italy) at the SIMS Laboratory (Kansas State University).

Statistical analyses

Differences in mean lignin content and composition, A_L, shoot height, foliar $\delta^{13}C$ and C:N, wood density, k_s, V_{cmax}, J, TPU, R_d, g_m, A_n, g_s, E, WUE, Ψ_{leaf}, and G_t between the two field sites were analyzed using multivariate, full-factorial analyses of variance (ANOVAs) with site and genotype as the main effects. Due to large differences among genotypes, we also compared site differences in growth, morphology, and physiology of wild-type *P. trichocarpa* using the Student's *t*-test statistic ($P \leq 0.05$). Data from the three sampling dates (when available) were combined for analyses to ensure observed differences were consistent over time. All data were tested for normality with the Shapiro and Wilk's test and A_L, shoot

height, G_t, k_s, and g_m were ln-transformed to achieve normality. Means were considered significantly different at $P \leq 0.05$.

To determine if physiological differences existed among genotypes, statistical comparisons were analyzed within the same site due to the pronounced differences in climate, soil characteristics, and plant responses between the two sites. We performed one-way, univariate ANOVAs with genotype as the main effect and total lignin, S:G ratio, A_L, foliar N and C content, foliar $\delta^{13}C$, wood density, k_s, V_{cmax}, J, TPU, R_d, g_m, A_n, g_s, E, WUE, Ψ_{leaf}, and G_t as dependent variables. If differences among means were found ($P \leq 0.05$), we used the Tukey HSD to test for significant differences among genotype means. Seasonal differences in A_L, shoot height, A_n, g_s, E, WUE, Ψ_{leaf}, and G_t were then analyzed for each site using a repeated measures analysis with month as the within-subjects factor and genotype as the between-subjects factor using SPSS version 21 (IBM Corporation, Armonk, NY, USA). To test for differences among months, we used pairwise significance tests adjusted for multiple comparisons with the Bonferroni correction. Least squares regression was used to examine relationships between stem lignin concentration and A_L, wood density, k_s, J, TPU, g_m, A_n, g_s, E, Ψ_{leaf}, and G_t at the piedmont site. All analyses were performed using JMP 9.0 (SAS Institute, Cary, NC, USA).

Table 5.1 Lignin concentrations (%) and the ratio of syringyl to guaiacyl (S:G) monolignol units in the two transgenic lines and the wild-type control of *P. trichocarpa* at the time of planting (April 2009) and after 3 years of growth in the field (January 2012). Means not connected by the same letter within each site are significantly different (Tukey HSD, $P<0.05$). Data reproduced from: (Stout *et al.*, in review).

Site	Genetic Line	2009 Lignin Conc (%)	2012 Lignin Conc (%)	2009-2012 Change in Lignin (%)	2009 S:G	2012 S:G	2009-2012 Change in S:G
Mountain	WT	22	23.4 a	+1.4	2.5	2.0 a	–0.5
Mountain	PT-3	17.4	23.4 a	+6.0	3.6	2.1 a	–1.5
Mountain	PT-1	13.9	23.1 a	+9.2	3.4	2.1 a	–1.3
Piedmont	WT	22	26.4 a	+4.4	2.5	1.7 a	–0.8
Piedmont	PT-3	17.4	21.6 b	+4.2	3.6	1.5 a	–2.1
Piedmont	PT-1	13.9	23.0 b	+9.1	3.4	1.8 a	–1.6

Table 5.2 Results of full-factorial ANOVAs including genotype and environment as main effects and measures of growth, morphology, and physiology of *P. trichocarpa* as dependent variables. Data from the three sampling dates (when available) were combined to ensure observed differences were consistent over time, and A_L, shoot height, G_t, k_s, and g_m were ln-transformed to achieve normality. Degrees of freedom (df), *F*-statistic, and *P*-value are given. Bold denotes significance at $P \leq 0.05$.

Response	Effect	df	*F*	*P*
Leaf area (m^2)	Genotype	2,89	30.30	**<0.0001**
	Environment	1,89	682.37	**<0.0001**
	G x E	2,89	24.77	**<0.0001**
Total shoot height (m) (all stems + branches)	Genotype	2,89	32.10	**<0.0001**
	Environment	1,89	654.12	**<0.0001**
	G x E	2,89	19.97	**<0.0001**
Foliar C:N	Genotype	2,35	8.83	**0.001**
	Environment	1,35	2.77	0.106
	G x E	2,35	4.45	**0.020**
Foliar $\delta^{13}C$ (‰)	Genotype	2,35	0.848	0.438
	Environment	1,35	1.293	0.265
	G x E	2,35	1.993	0.154
Wood density ($g\ cm^{-3}$) ($g\ cm^{-3}$)	Genotype	2,29	1.33	0.284
	Environment	1,29	0.27	0.610
	G x E	2,29	2.19	0.134
Predawn ψ_{leaf} (MPa) (MPa)	Genotype	2,89	0.50	0.610
	Environment	1,89	17.30	**<0.0001**
	G x E	2,89	0.65	0.524
Midday ψ_{leaf} (MPa) (MPa)	Genotype	2,89	3.07	0.052
	Environment	1,89	25.72	**<0.0001**
	G x E	2,89	1.44	0.242
g_s ($mmol\ H_2O\ m^{-2}\ s^{-1}$)	Genotype	2,409	7.79	**0.001**
	Environment	1,409	481.13	**<0.0001**
	G x E	2,409	0.285	0.752
E ($mol\ H_2O\ m^{-2}\ hr^{-1}$)	Genotype	2,409	12.75	**<0.0001**
	Environment	1,409	62.03	**<0.0001**
	G x E	2,409	4.46	**0.012**
G_t ($mmol\ m^{-2}\ s^{-1}\ MPa^{-1}$)	Genotype	2,84	5.06	**0.009**
	Environment	1,84	1.13	0.290
	G x E	2,84	1.11	0.335

Table 5.2 (continued)

k_s		Genotype	2,29	23.13	**<0.0001**
	(g m^{-1} min^{-1} kPa^{-1})	Environment	1,29	0	0.996
		G x E	2,29	1.18	0.325
V_{cmax}		Genotype	2,29	1.73	0.199
	(μmol m^{-2} s^{-1})	Environment	1,29	4.10	0.054
		G x E	2,29	2.86	0.077
J		Genotype	2,29	2.02	0.155
	(μmol m^{-2} s^{-1})	Environment	1,29	3.99	0.057
		G x E	2,29	6.65	**0.005**
TPU		Genotype	2,29	3.01	0.068
	(μmol m^{-2} s^{-1})	Environment	1,29	0.13	0.721
		G x E	2,29	8.12	**0.002**
R_d		Genotype	2,29	1.40	0.265
	(μmol m^{-2} s^{-1})	Environment	1,29	73.43	**<0.0001**
		G x E	2,29	0.41	0.669
g_m		Genotype	2,29	3.83	**0.036**
	(μmol m^{-2} s^{-1} Pa^{-1})	Environment	1,29	30.27	**<0.0001**
		G x E	2,29	1.53	0.238
A_n		Genotype	2,409	8.11	**0.0004**
	(μmol CO_2 m^{-2} s^{-1})	Environment	1,409	183.98	**<0.0001**
		G x E	2,409	4.50	**0.012**
WUE		Genotype	2,409	0.30	0.744
	(μmol CO_2 $mmol^{-1}$ H_2O)	Environment	1,409	129.35	**<0.0001**
		G x E	2,409	0.56	0.569

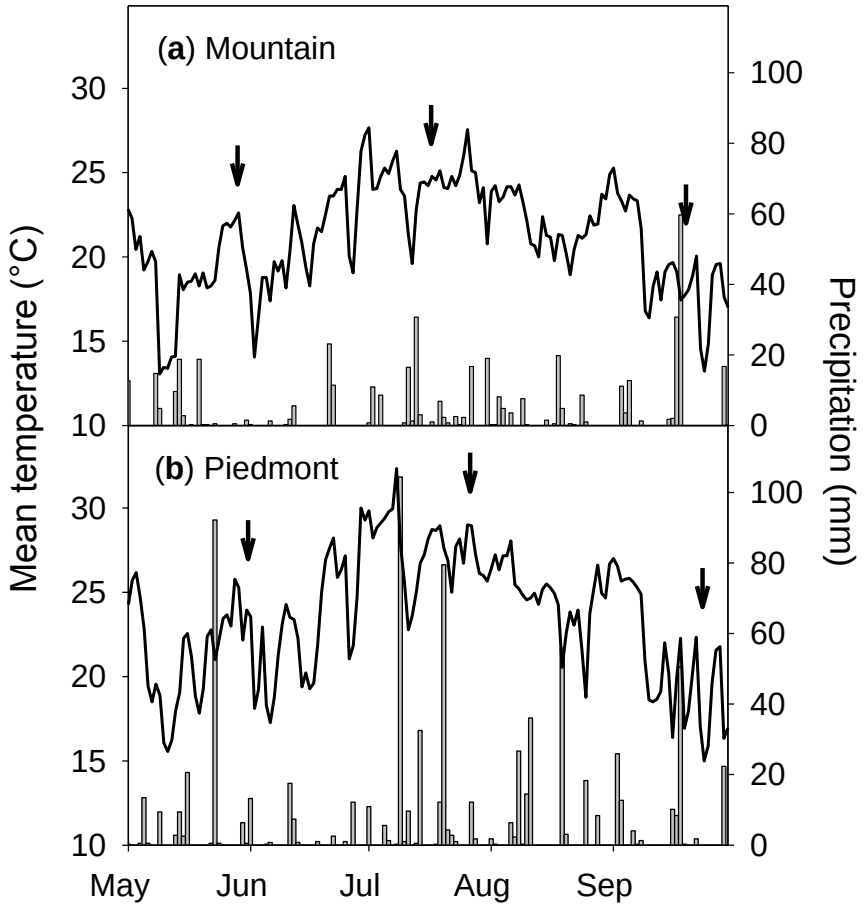

Figure 5.1 Mean daily temperature and total precipitation from May to September 2012 at the (a) mountain field site and (b) piedmont field site. The arrows represent sampling dates at each site.

5.4 Results

The lignin content of wild-type *P. trichocarpa* was significantly higher (t_8=6.00, P=0.001) at the piedmont site than at the mountain site in 2012 (26.4 vs. 23.4%, respectively; Table 5.1). Mean lignin composition of all genotypes differed significantly between sites ($F_{1,23}$=38.480, P<0.0001), due to a greater reduction of S:G ratios over time at the piedmont site than the mountain site (1.6 vs. 2.1, respectively; Table 5.1).

Growth and physiology differences between sites

Trees had greater leaf area and were significantly taller at the mountain site than at the piedmont site (Table 5.2, Figure 5.2). Specifically, mean A_L was 8 times higher and mean shoot height was 6 times higher at the mountain site. Leaf area of *P. trichocarpa* significantly increased from May to September at the mountain site ($F_{2,11}$=28.751, P<0.0001), whereas A_L decreased over the same time period at the piedmont site ($F_{2,11}$=7.596, P=0.003; Figure 5.2). Although there were no site differences in foliar C:N ratios across all genotypes (Table 5.2), wild-type trees at the mountain site had significantly lower foliar C:N than at the piedmont site (t_{11}=5.85, P=0.0002).

Differences in water relations and photosynthesis of *P. trichocarpa* trees were observed across genotypes between the two field sites. Mean Ψ_{soil} and Ψ_{leaf} were higher at the mountain site than the piedmont site (Table 5.2, Figure 5.3c,d). Large differences in g_s also existed between sites, as mean g_s was 2.5 times higher at the mountain site than the piedmont site (Table 5.2, Figures 5.3-5.4). Trees at the mountain site transpired approximately 3.5 mol H_2O m^{-2} hr^{-1} more at midday than trees at the piedmont site (Table 5.2, Figure 5.5c,d). At the

mountain site, A_n of tree leaves was significantly higher than at the piedmont site (Figure 5.5a,b) due to higher g_s, lower R_d, and higher g_m (Table 5.4). There were additional site differences in photosynthetic parameters when only wild-type *P. trichocarpa* was analyzed; tree leaves at the mountain site had lower V_{cmax} (t_9=3.65, P=0.007), J (t_9=2.31, P=0.050), and *TPU* (t_9=3.49, P=0.008) than at the piedmont site. Differences in gas exchange between sites resulted in a lower intrinsic WUE at the mountain site (Table 5.2, Figure 5.5e,f). No consistent differences in foliar $\delta^{13}C$, wood density, k_s, or G_t were found between sites (Table 5.2).

Seasonal differences in plant water relations also existed between sites. At the piedmont site, mean Ψ_{leaf} ($F_{2,10}$=37.211, P<0.0001) and g_s ($F_{2,11}$=19.475, P<0.0001) reached minimum values in July and partially recovered in September (Figure 2b,d). This pattern was not observed at the mountain site, where mean Ψ_{leaf} ($F_{2,11}$=7.960, P=0.002) and g_s ($F_{2,11}$=10.514, P=0.003) and g_s decreased throughout the growing season (Figure 2a,c). Seasonal declines in photosynthesis at the mountain and piedmont sites were of similar magnitude (6.2 vs. 6.3 μmol m^{-2} s^{-1}, respectively), but the seasonal decline in transpiration was larger at the mountain site than the piedmont site (7.8 vs. 2.3 mol H_2O m^{-2} hr^{-1}, respectively; Figure 5.5a-d). There was a large increase in intrinsic WUE from July to September at the piedmont site ($F_{2,41}$=42.431, P<0.0001), whereas only a small increase in intrinsic WUE occurred from May to July at the mountain site ($F_{2,39}$=3.693, P=0.046; Figure 5.5e,f).

Differences among genotypes

There were some similarities in the effect of the genetic transformation on the physiology of *P. trichocarpa* genotypes, despite the large difference in wood chemistry between sites. The two low-lignin genotypes had significantly lower mean Ψ_{leaf}, g_s, E, k_s, and G_t, compared to the wild-type control at both sites (Table 5.3, Figures 5.3-5.5). The g_s of leaves at the top of stems decreased in comparison with leaves lower on the stem in the low-lignin line PT-1, while no decreases in g_s were found along the stem in the wild-type control (Figure 5.4).

There were additional differences in growth, morphology, and physiology among the genotypes that were only present at one field site. At the warmer piedmont site, total shoot height and A_L were significantly higher in the wild-type control than the two transgenic lines (Figure 5.2b,d). Leaves of the wild-type control had significantly higher nitrogen content than the transgenic lines at the mountain site (Table 5.3), but we found no differences in biophysical or biochemical photosynthetic parameters or A_n among genotypes at this site (Table 5.4, Figure 5.5a). At the piedmont site, however, the low-lignin line PT-1 had significantly lower J, TPU, and g_m when compared to the wild-type control (Table 5.4). Furthermore, A_n was significantly higher in the wild-type control at the piedmont site (Figure 5.5b). Decreased g_s of leaves at the top of stems were observed in the transgenic line PT-3 at the piedmont site, but not at the mountain site (Figure 5.4). Mean intrinsic WUE of PT-1 was significantly higher than the wild-type control at the mountain site in 2012 (0.052 vs. 0.047 μmol CO_2 $mmol^{-1}$ H_2O, respectively; $F_{2,223}$=3.408, P=0.035). No significant differences in wood density, foliar carbon content, or $\delta^{13}C$ were observed between the transgenic and wild-type trees at either site (Table 5.3).

Lignin quantity differed among the genotypes at the piedmont site, and there was a significant positive correlation between lignin concentration and A_L (r^2=0.58, P=0.004), total shoot height (r^2=0.64, P=0.002), k_s (r^2=0.51, P=0.009), and J (r^2=0.34, P=0.047; Figure 5.6). Lignin concentration was positively correlated to G_t (r^2=0.45, P=0.016) in May and to A_n (r^2=0.45, P=0.016), g_s (r^2=0.49, P=0.011), and E (r^2=0.38, P=0.033) in July (Figure 5.6). There was no correlation between lignin quantity and wood density (r^2=0.12, P=0.267), *TPU* (r^2=0.21, P=0.134), g_m (r^2=0.26, P=0.093), and Ψ_{leaf} (r^2=0.04, P=0.549) at this site (Figure 5.6).

Table 5.3 Mean values (±SE) of foliar nitrogen and carbon content, foliar carbon isotope ratios, wood density, and hydraulic conductivity of *P. trichocarpa* genotypes. The leaves (*n*=5-7 leaves per genotype) for N, C, and $\delta^{13}C$ were collected in October 2011, and stems (*n*=5 stems per genotype) for wood density and hydraulic conductivity were collected in September 2012. Means not connected by the same letter within each site are significantly different (Tukey HSD, $P<0.05$).

Site	Line	Nitrogen (%)	Carbon (%)	$\delta^{13}C$ (‰)	Wood density ($g\ cm^{-3}$)	Hydraulic Conductivity ($g\ m^{-1}\ min^{-1}\ kPa^{-1}$)
Mountain	WT	2.5 (0.05) a	47.2 (0.60) a	–26.07 (0.16) a	0.44 (0.02) a	4.50 (0.44) a
Mountain	PT-3	2.0 (0.09) b	46.5 (1.33) a	–27.43 (1.32) a	0.46 (0.02) a	0.42 (0.27) b
Mountain	PT-1	2.0 (0.04) b	47.4 (0.36) a	–26.37 (0.53) a	0.47 (0.03) a	0.81 (0.28) b
Piedmont	WT	2.1 (0.03) a	47.1 (0.19) a	–27.01 (0.91) a	0.47 (0.01) ab	3.45 (0.31) a
Piedmont	PT-3	1.9 (0.04) a	46.9 (0.23) a	–25.74 (0.43) a	0.49 (0.02) a	0.73 (0.34) b
Piedmont	PT-1	2.2 (0.12) a	47.4 (0.19) a	–25.18 (0.19) a	0.43 (0.01) b	0.43 (0.12) b

Table 5.4 Mean values (±SE) of the photosynthetic parameters V_{cmax} (maximum velocity of Rubisco for carboxylation), *J* (rate of photosynthetic electron transport), *TPU* (triose phosphate use), R_d (daytime respiration), and g_m (mesophyll conductance) of *P. trichocarpa* genotypes (*n*=5 leaves per genotype). Data were collected at two field sites in North Carolina in July 2012. Means not connected by the same letter within each site are significantly different (Tukey HSD, $P<0.05$).

Site	Line	V_{cmax} (μmol m^{-2} s^{-1})	*J* (μmol m^{-2} s^{-1})	*TPU* (μmol m^{-2} s^{-1})	R_d (μmol m^{-2} s^{-1})	g_m (μmol m^{-2} s^{-1} Pa^{-1})
Mountain	WT	153 (15.0) a	146 (7.3) a	9.7 (0.3) a	0.81 (0.13) a	2.57 (0.83) a
Mountain	PT-3	202 (26.7) a	165 (14.7) a	10.6 (0.9) a	1.39 (0.28) a	1.46 (0.21) a
Mountain	PT-1	179 (16.6) a	162 (6.5) a	10.8 (0.3) a	1.17 (0.29) a	1.93 (0.46) a
Piedmont	WT	234 (16.2) a	166 (4.3) a	12.1 (0.6) a	3.50 (0.27) a	1.15 (0.16) a
Piedmont	PT-3	220 (19.5) a	146 (5.7) a	11.2 (0.5) a	4.00 (0.56) a	0.81 (0.07) ab
Piedmont	PT-1	174 (14.8) a	119 (9.4) b	8.4 (0.8) b	3.27 (0.43) a	0.59 (0.09) b

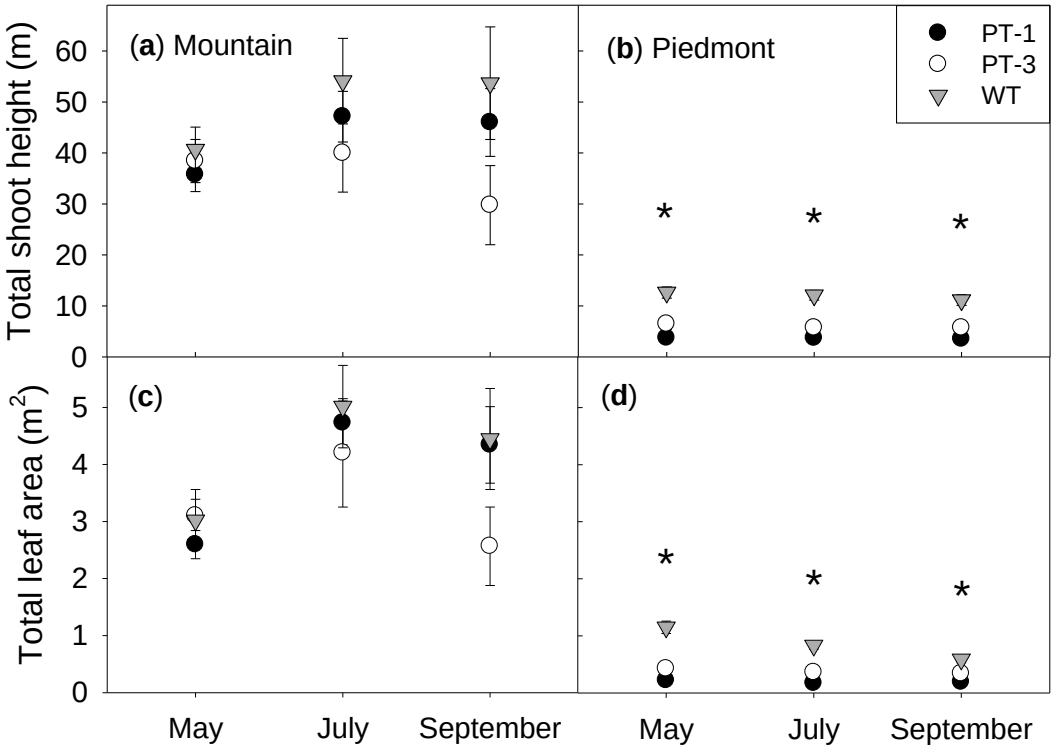

Figure 5.2 Seasonal changes in (a-b) total shoot height, including all stems and branches, and (c-d) total leaf area at two field sites in North Carolina in 2012. The wild-type control is indicated by a gray triangle, while the two transgenic lines are indicated by circles. Months with significant differences among the genotypes are indicated by a star (*). Values are means of 5 trees, and error bars indicate SE.

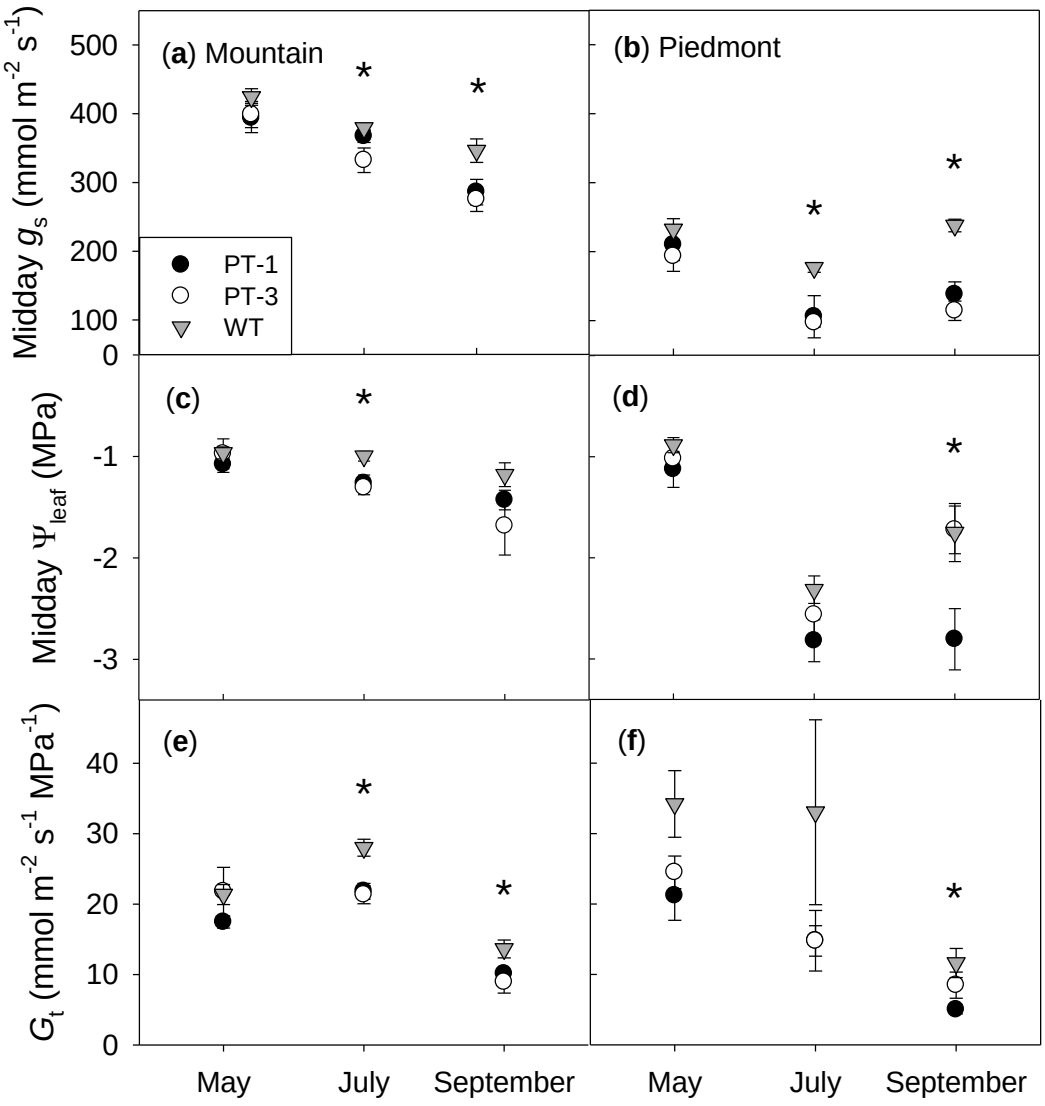

Figure 5.3 Seasonal changes in (a-b) midday stomatal conductance (g_s), (c-d) midday leaf water potential (Ψ_{leaf}), and (d-e) leaf-specific whole-plant hydraulic conductance (G_t) at two field sites in North Carolina in 2012. Midday g_s and Ψ_{leaf} were measured on the same leaves from the top of stems (n=10 stems per genotype) and used to calculate G_t. The wild-type control is indicated by a gray triangle, while the two transgenic lines are indicated by circles. Months with significant differences among the genotypes are indicated by a star (*). Values are means of 5 trees, and error bars indicate SE.

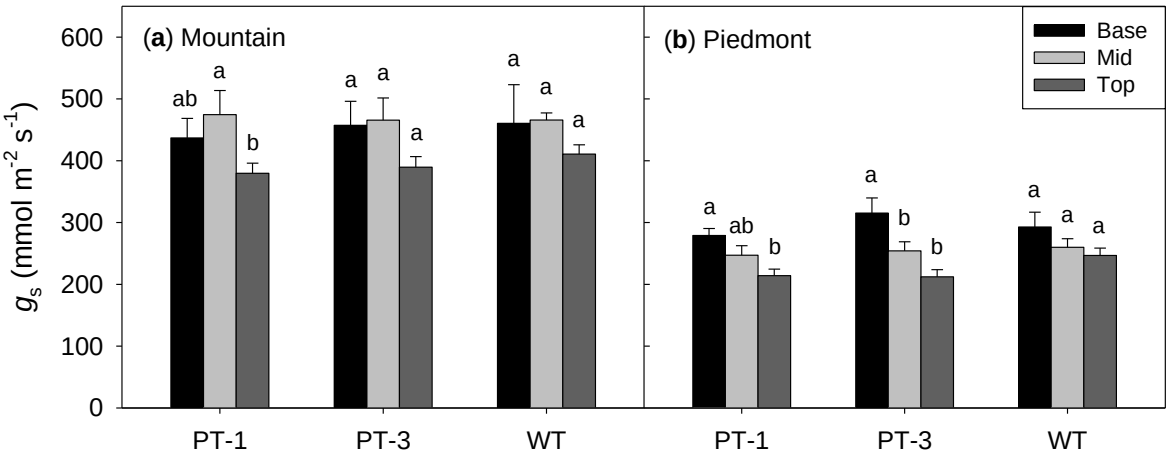

Figure 5.4 Variation in stomatal conductance (g_s) along the height of the main stem at the (a) mountain site and (b) piedmont site in North Carolina in May 2012. Leaves (n=5-34 per height) were sampled at the base of the stem, mid-stem, and the top of the stem. Means not connected by the same letter within each set of bars are significantly different (Tukey HSD, P<0.05). Error bars indicate SE.

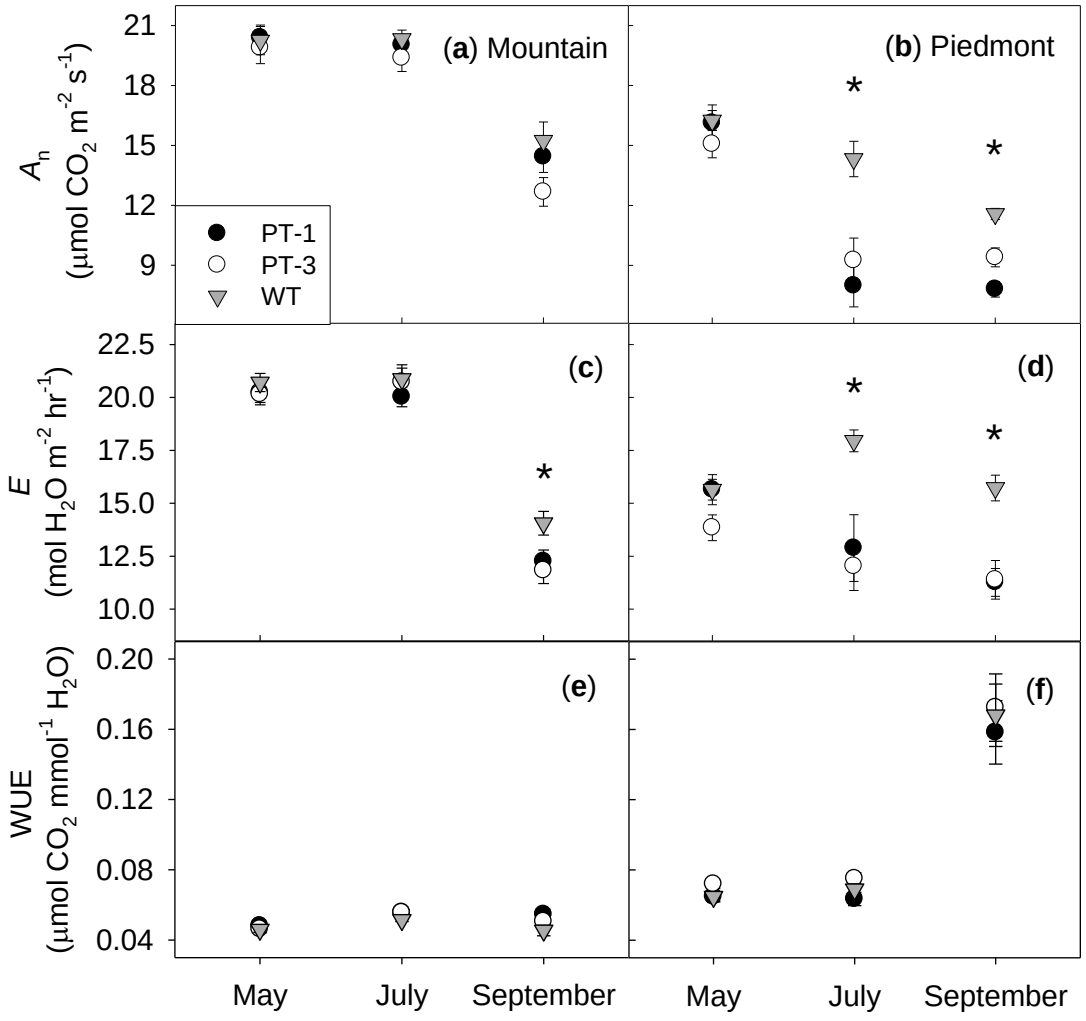

Figure 5.5 Seasonal changes in gas exchange parameters of fully-developed leaves (*n*=15-31 per genotype per month), including (a-b) net assimilation rate (A_n), (c-d) transpiration rate (E), and (e-f) intrinsic water use efficiency (WUE) at two field sites in North Carolina in 2012. The wild-type control is indicated by a gray triangle, while the two transgenic lines are indicated by circles. Months with significant differences among the genotypes are indicated by a star (*). Values are means of 5 trees, and error bars indicate SE.

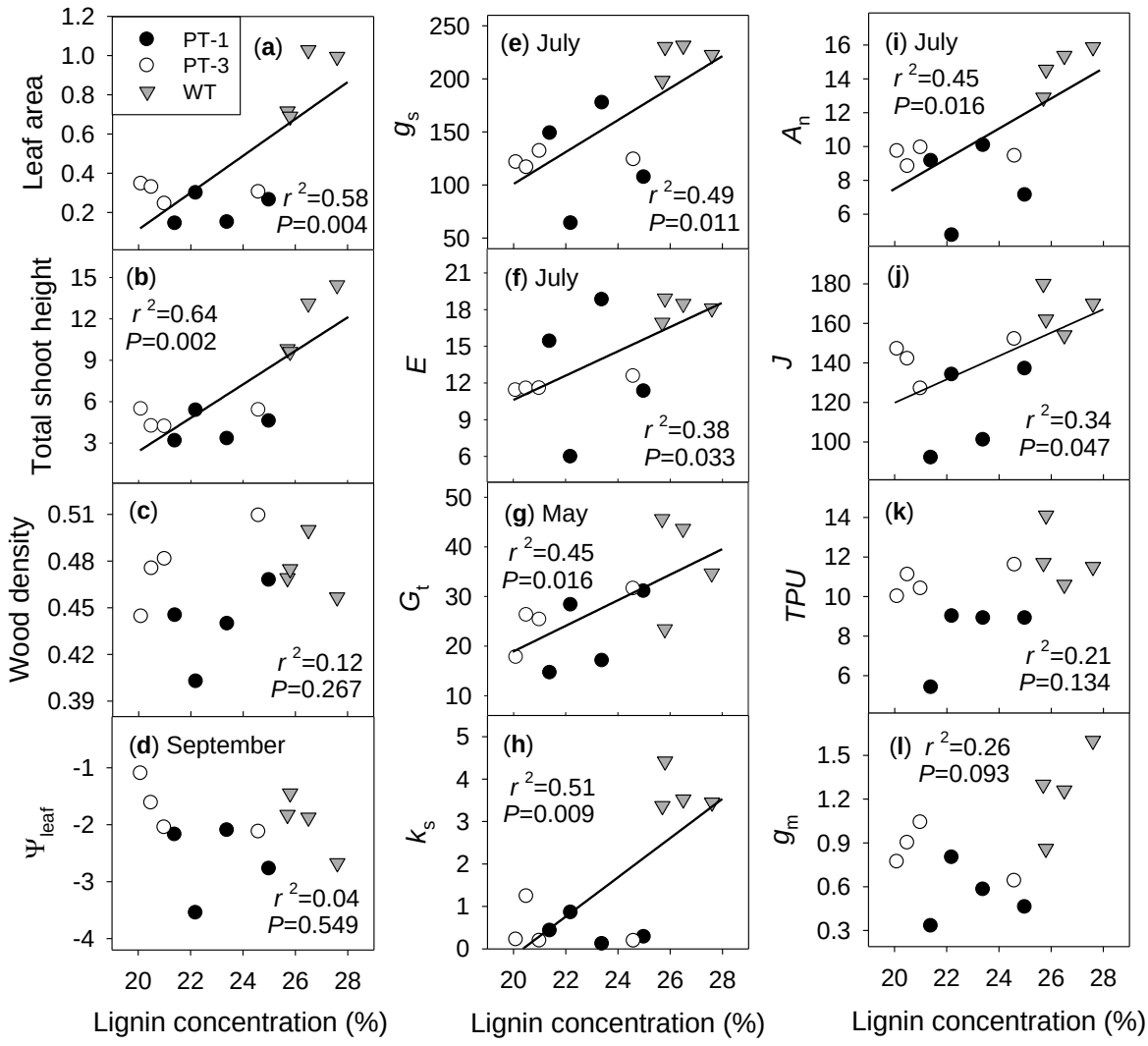

Figure 5.2 Relationship between stem lignin concentration and (a) leaf area (m^2), (b) total shoot height (m), including all stems and branches, (c) wood density (g cm^{-3}), (d) midday leaf water potential (MPa), (e) stomatal conductance (mmol H_2O m^{-2} s^{-1}), (f) transpiration (mol H_2O m^{-2} hr^{-1}), (g) leaf-specific whole-plant hydraulic conductance (mmol m^{-2} s^{-1} MPa^{-1}), and (h) hydraulic conductivity (g m^{-1} min^{-1} kPa^{-1}), (i) net assimilation rate (µmol CO_2 m^{-2} s^{-1}), (j) electron transport rate (µmol m^{-2} s^{-1}), (k) triose phosphate use (µmol m^{-2} s^{-1}), and (l) mesophyll conductance (µmol m^{-2} s^{-1} Pa^{-1}) at the piedmont field site in North Carolina in 2012. The wild-type control is indicated by a gray triangle, while the two transgenic lines are indicated by circles. Data points are measurements on individual trees (n=12).

5.5 Discussion

Selecting genotypes that maximize carbon sequestration and growth and minimize water use is critically important for the future sustainability of bioenergy production systems (King *et al*., 2013). A previous study found maximum productivity of *P. trichocarpa* in the mountain region of North Carolina (Stout *et al*., in review), indicating that this region is more promising for future biofuel production of this species and similar genera in the southeastern US. This region is cooler and wetter than the piedmont region (Figure 5.1) and therefore more similar to climate conditions in native *P. trichocarpa* habitats. In comparison with other tree crop species being considered for bioenergy production, *P. trichocarpa* ranks as one of the most productive (King *et al*., 2013) due to high A_n (20.3 μmol CO_2 m^{-2} s^{-1}) and g_s (422.4 mmol H_2O m^{-2} s^{-1}) at the mountain site (Figure 5.3a, 5.5a). Maximum aboveground biomass production at this site was 18.3 tons ha^{-1} yr^{-1} for bioenergy systems (Stout *et al*., in review), relative to the recommended yield of at least 25 tons ha^{-1} yr^{-1} (Perlack *et al*., 2005). Aboveground biomass production at the warmer piedmont site was too low (1.3 tons ha^{-1} yr^{-1}) to be economically viable as a SRWC system (Stout *et al*., in review). Productivity at the piedmont site was limited by frequent drought stress, as evidenced by the mean Ψ_{soil} of –2 MPa in July 2012. Even in wild-type trees, A_n (15.3 μmol CO_2 m^{-2} s^{-1}) and g_s (236.3 mmol H_2O m^{-2} s^{-1}) were much lower at the piedmont site than the mountain site (Figure 5.3b, 5.5b). Restricted root growth due to the presence of a plow pan soil layer may have contributed to the frequency of drought stress at the site.

The effect of the genetic transformation on lignin biosynthesis of field-grown trees is site-specific (Stout *et al.*, in review). Initial reductions of stem lignin content of 21 and 37%

were achieved with the insertion of the antisense *4CL* gene in *P. trichocarpa*, and stable lignin reductions of 13 and 18% were maintained after 3 years of growth at the piedmont site (Table 5.1). Another study confirmed that stable lignin reductions of 7–10% could be achieved in transgenic *Populus* after 5 years of field growth, relative to initial lignin reductions of 16–40% (Wang *et al.*, 2012). Contrary to the stable lignin reduction at the piedmont site and to other genetic transformations of *Populus* (Halpin *et al.*, 2007; Wang *et al*., 2012), however, we found that the two transgenic lines of *P. trichocarpa* at the mountain site had the same lignin content and composition as the wild-type control after 3 years of growth (Table 5.1). The wild-type trees at the mountain site had only a small increase in lignin content over time (1.4%, Table 5.1) and did not show any sign of physiological stress, suggesting that stem lignin content of about 23% is adequate for normal plant function of *P. trichocarpa* at sites with low environmental stress. The wild-type trees at the piedmont site had larger increases in stem lignin content (4.4%, Table 5.1), indicating that high lignin content is important in coping with stresses such as drought (Stout *et al*., in review).

Physiological differences in transgenic trees

Genetic transformation by insertion of the antisense *4CL* gene had significant effects on the water relations and physiology of field-grown *P. trichocarpa* trees. Despite large differences in wood chemistry between sites, the transgenic genotypes PT-1 and PT-3 had significantly lower mean Ψ_{leaf}, g_s, E, k_s, and G_t than the wild-type control (Table 5.3, Figures 5.3-5.5). Furthermore, the transgenic trees had lower biophysical and biochemical photosynthetic processes (Table 5.4), A_n (Figure 5.5b), and productivity (Figure 5.2) at the piedmont site,

while foliar nitrogen content (Table 5.3) was lower and mean intrinsic WUE was higher at the mountain site. Decreases in g_s, E, k_s, foliar nitrogen content, photosynthesis, and growth have been reported previously in low-lignin transgenic *Populus* trees (Hancock *et al*., 2007; Coleman *et al.*, 2008; Voelker, 2009; Voelker *et al*., 2010; Stout *et al*., in review). To our knowledge, this is the first report of decreased Ψ_{leaf}, G_t, photosynthetic processes, and increased intrinsic WUE in field-grown low-lignin transgenic trees.

The genetic transformation impaired the water transport capacity of vascular tissues and resulted in decreased hydraulic efficiency (Figure 5.3), confirming our first hypothesis. Decreases in G_t were manifested both as reduced g_s and lower Ψ_{leaf} in transgenic trees at both sites (Figure 5.3). The loss of vascular integrity was particularly evident at the tops of stems, as g_s decreased with increasing height along the stem (Figure 5.4). Hydraulic efficiency of low-lignin transgenic trees was 43–78% of the G_t of wild-type controls (Figure 5.3e,f). A number of changes in plant hydraulics could have occurred to lower the G_t of transgenic trees, such as narrower xylem conduits, decreased ratio of sapwood area to leaf area, increased embolism, and/or decreased hydraulic conductivity. No differences in vessel diameter or anatomy were found between the low-lignin line PT-1 and the wild-type control (Stout, 2011), however. There was also no difference in leaf area or shoot height among genotypes at the mountain site (Figure 5.2a,c). Therefore, decreased G_t of transgenic trees was likely caused by xylem vessel embolism, collapse, blockage by tyloses or phenolics, or some combination of these mechanisms. Two-year-old stems of PT-1 were found to contain more embolized vessels than the wild-type control (Stout, 2011). We observed patches of nonconductive xylem that contributed to the decreased k_s of transgenic stems (Table 5.3).

Other studies have shown that areas of nonconductive xylem in low-lignin transgenic trees contain collapsed vessels and noncollapsed cells blocked by tyloses and phenolic deposits (Coleman *et al*., 2008; Kitin *et al.*, 2010).

As hypothesized, the genetic transformation decreased biophysical and biochemical photosynthetic processes at the piedmont site, including *J*, *TPU*, and g_m (Table 5.4). This resulted in decreased A_n of transgenic trees at the piedmont site (Figure 5.5b). At the mountain site, however, there was no difference in photosynthetic processes or A_n between transgenic and wild-type trees (Table 5.4, Figure 5.5a), as expected if lignin content affects photosynthesis. Lignin biosynthesis processes provide a strong sink for removal of carbohydrates from tree leaves, but accumulation of high levels of starch and soluble sugars can occur in leaves of low-lignin *Populus* genotypes (Coleman *et al.*, 2008). Accumulation of carbohydrates in leaves can repress photosynthesis by decreasing regeneration of ribulose-1,5-bisphosphate, RuBP (Araya *et al*., 2006). Although we did not measure carbohydrate concentrations in leaves, our observations are consistent with photosynthetic limitation caused by a loss of sink strength.

Changes in physiology of transgenic trees at the piedmont site resulted in decreased productivity (Figure 5.2b,d), and lignin quantity was well-correlated with growth (Figure 5.6a,b). The primary cause of low productivity in low-lignin genotypes (Figure 5.2b,d) was water stress, as evident by their extremely stunted growth, desiccation of leaf tips, and lower Ψ_{leaf} relative to wild-type controls (Figure 5.3d). During a temperature-induced drought at the piedmont site in July 2012, reductions in A_n and g_s were greatest in the low-lignin transgenic trees (Figure 5.3b, 5.5b). Stomatal closure in response to low Ψ_{leaf} limits excessive water loss

in plants, but simultaneously restricts carbon gain. Indeed, mean A_n in transgenic trees were 55–65% of rates in wild-type control trees in July 2012 (Figure 5.5b). Photosynthesis of the low-lignin line PT-1 was not only limited by carbon acquisition, but also by decreased *J*, *TPU*, and g_m (Table 5.4). Interestingly, decreased G_t and lower foliar nitrogen concentration had no negative effect on photosynthesis or growth of transgenic genotypes at the mountain site (Table 5.4, Figure 5.2a,c). Differences in specific leaf area (SLA) among genotypes may explain the equivalent productivity, because lower SLA of transgenic trees relative to wild-type trees (R. Marchin, personal observation) can compensate for lower leaf nitrogen on a mass basis.

Differences in physiology of transgenic trees could be partially, but not completely, explained by their lower stem lignin content. At the piedmont site, where stem lignin varied between the genotypes, lignin quantity explained 38–51% of the variation in water relations traits (Figure 5.6). Physiological differences existed at both sites, however, across a range of stem lignin contents of 21.6–23.4% in transgenic lines. Lignin quantity or composition cannot be the cause for differences at the mountain site, since neither trait varied among genotypes after 3 years of field growth (Table 5.1). The mechanism responsible for these physiological differences in transgenic trees at the mountain site is at present unknown, highlighting the need for a better understanding of the effects of genetic transformation on whole-plant function under field conditions.

Water use efficiency

Despite the fact that transgenic trees did not maintain lower lignin content at the mountain site, the genetic transformation resulted in an alternative advantage for its use as a cellulosic biofuel crop – lower water consumption. Variability in WUE among *Populus* genotypes is not correlated with productivity, indicating that highly productive trees can also have relatively high WUE (Monclus *et al*., 2006). The transgenic line PT-1 had significantly higher mean intrinsic WUE than the wild-type control (0.052 vs. 0.047 μmol CO_2 $mmol^{-1}$ H_2O, respectively) without sacrificing productivity. The increase in intrinsic WUE was caused by lower mean g_s of PT-1 throughout the growing season (Figure 5.3a, 5.5a,e) due to the impaired water transport capacity of vascular tissues. Estimated total water savings of this genotype is roughly 1 kg H_2O $tree^{-1}$ day^{-1}, assuming a reduction in transpiration of 1 mol H_2O m^{-2} hr^{-1} and a mean leaf area of 4.73 ± 0.38 m^2. Even a small increase in WUE is advantageous and will help to reduce water stress, since climate change is expected to increase the occurrence of drought and temperature-induced drought stress in the future (Karl *et al.*, 2009; King *et al.*, 2013).

REFERENCES

Araya T, Noguchi K, Terashima I (2006) Effects of carbohydrate accumulation on photosynthesis differ between sink and source leaves of *Phaseolus vulgaris* L. *Plant and Cell Physiology*, **47**, 644-652.

Boerjan W, Ralph J, Baucher M (2003) Lignin biosynthesis. *Annual Review of Plant Biology*, **54**, 519-546.

Braatne JH, Hinckley TM, Stettler RF (1992) Influence of soil water on the physiological and morphological components of plant water balance in *Populus trichocarpa*, *Populus deltoides*, and their F1 hybrids. *Tree Physiology*, **11**, 325-339.

Buckley TN (2005) The control of stomata by water balance. *New Phytologist*, **168**, 275-291.

Chapple C, Ladisch M, Meilan R (2007) Loosening lignin's grip on biofuel production. *Nature Biotechnology*, **25**, 746-748.

Coleman HD, Samuels AL, Guy RD, *et al*. (2008) Perturbed lignification impacts tree growth in hybrid poplar - A function of sink strength, vascular integrity, and photosynthetic assimilation. *Plant Physiology*, **148**, 1229-1237.

DeBell DS (1990) *Populus trichocarpa* Torr. & Gray: black cottonwood. In: Burns RM, Honkala BH (eds) *Silvics of North America: Volume 2, hardwoods*. USDA Forest Service, Washington, DC, pp 570-576.

Fichot R, Barigah TS, Chamaillard S, *et al*. (2010) Common trade-offs between xylem resistance to cavitation and other physiological traits do not hold among unrelated *Populus deltoides* x *Populus nigra* hybrids. *Plant Cell and Environment*, **33**, 1553-1568.

Flexas J, Díaz-Espejo A, Berry JA, *et al*. (2007) Analysis of leakage in IRGA's leaf chambers of open gas exchange systems: quantification and its effects in photosynthesis parameterization. *Journal of Experimental Botany*, **58**, 1533-1543.

Halpin C, Thain SC, Tilston EL, *et al*. (2007) Ecological impacts of trees with modified lignin. *Tree Genetics & Genomes*, **3**, 101-110.

Hancock JE, Loya WM, Giardina CP, *et al*. (2007) Plant growth, biomass partitioning and soil carbon formation in response to altered lignin biosynthesis in *Populus tremuloides*. *New Phytologist*, **173**, 732-742.

Horvath B, Peszlen I, Peralta P, *et al*. (2010) Effect of lignin genetic modification on wood anatomy of aspen trees. *Iawa Journal*, **31**, 29-38.

Hu WJ, Harding SA, Lung J, *et al*. (1999) Repression of lignin biosynthesis promotes cellulose accumulation and growth in transgenic trees. *Nature Biotechnology*, **17**, 808-812.

Karl TR, Melillo JM, Peterson TC (2009) Global Climate Change Impacts in the United States. US Global Change Research Program, Cambridge University Press, New York.

Kaur H, Shaker K, Heinzel N, *et al*. (2012) Environmental stresses of field growth allow cinnamyl alcohol dehydrogenase-deficient *Nicotiana attenuata* plants to compensate for their structural deficiencies. *Plant Physiology*, **159**, 1545-1570.

King JS, Ceulemans R, Albaugh JM, *et al*. (2013) The challenge of lignocellulosic bioenergy in a water-limited world. *BioScience*, **63**, 102-117.

Kitin P, Voelker SL, Meinzer FC, *et al*. (2010) Tyloses and phenolic deposits in xylem vessels impede water transport in low-lignin transgenic poplars: A study by cryo-fluorescence microscopy. *Plant Physiology*, **154**, 887-898.

Koehler L, Telewski FW (2006) Biomechanics and transgenic wood. *American Journal of Botany*, **93**, 1433-1438.

Li L, Zhou YH, Cheng XF, *et al*. (2003) Combinatorial modification of multiple lignin traits in trees through multigene cotransformation. *Proceedings of the National Academy of Sciences of the United States of America*, **100**, 4939-4944.

Li LG, Popko JL, Umezawa T, *et al*. (2000) 5-Hydroxyconiferyl aldehyde modulates enzymatic methylation for syringyl monolignol formation, a new view of monolignol biosynthesis in angiosperms. *Journal of Biological Chemistry*, **275**, 6537-6545.

Monclus R, Dreyer E, Villar M, *et al*. (2006) Impact of drought on productivity and water use efficiency in 29 genotypes of *Populus deltoides* x *Populus nigra*. *New Phytologist*, **169**, 765-777.

Niklas KJ (1992) *Plant biomechanics*. University of Chicago Press, Chicago.

Nobel PS (1999) *Physicochemical and Environmental Plant Physiology*, 2nd edn. Academic Press, San Diego, CA.

Peak D, Mott KA (2011) A new, vapour-phase mechanism for stomatal responses to humidity and temperature. *Plant Cell and Environment*, **34**, 162-178.

Perlack RD, Wright LL, Turhollow AF, *et al*. (2005) Biomass as a feedstock for a bioenergy and bioproducts industry: the technical feasibility of a billion-ton annual supply. USDA and DOE, Oak Ridge, Tennessee.

Schafer JL, Breslow BP, Hollingsworth SN, *et al*. (in review) Enhanced water relations during post-fire recovery of resprouting species. *Plant Ecology*.

Sharkey TD, Bernacchi CJ, Farquhar GD, *et al*. (2007) Fitting photosynthetic carbon dioxide response curves for C_3 leaves. *Plant Cell and Environment*, **30**, 1035-1040.

Shi R, Sun YH, Li QZ, *et al*. (2010) Towards a systems approach for lignin biosynthesis in *Populus trichocarpa*: Transcript abundance and specificity of the monolignol biosynthetic genes. *Plant and Cell Physiology*, **51**, 144-163.

Shope JC, Peak D, Mott KA (2008) Stomatal responses to humidity in isolated epidermes. *Plant Cell and Environment*, **31**, 1290-1298.

Sims REH, Hastings A, Schlamadinger B, *et al*. (2006) Energy crops: current status and future prospects. *Global Change Biology*, **12**, 2054-2076.

Somma D, Lobkowicz H, Deason JP (2010) Growing America's fuel: an analysis of corn and cellulosic ethanol feasibility in the United States. *Clean Technologies and Environmental Policy*, **12**, 373-380.

Stout AT (2011) Ecophysiology and productivity of transgenic decreased-lignin *Populus* for use in short-rotation bioenergy cropping systems. Master's Thesis, North Carolina State University, Raleigh, NC.

Stout AT, Davis AA, Domec JC, *et al*. (in review) Environmental stress affects lignin content and productivity in field-grown *Populus trichocarpa* with altered lignin biosynthesis. *Biomass and Bioenergy*.

Tschaplinski TJ, Tuskan GA, Gebre GM, *et al*. (1998) Drought resistance of two hybrid *Populus* clones grown in a large-scale plantation. *Tree Physiology*, **18**, 653-658.

Tuskan GA, DiFazio S, Jansson S, *et al*. (2006) The genome of black cottonwood, *Populus trichocarpa* (Torr. & Gray). *Science*, **313**, 1596-1604.

Tyree MT, Zimmermann MH (2002) *Xylem Structure and the Ascent of Sap*, 2nd edn. Springer-Verlag, Berlin.

Vance CP, Kirk TK, Sherwood RT (1980) Lignification as a mechanism of disease resistance. *Annual Review of Phytopathology*, **18**, 259-288.

Vanholme R, Demedts B, Morreel K, *et al*. (2010) Lignin Biosynthesis and Structure. *Plant Physiology*, **153**, 895-905.

Voelker SL (2009) Functional decreases in hydraulic and mechanical properties of field-grown transgenic poplar trees caused by modification of the lignin synthesis pathway through downregulation of the 4-coumarate:coenzyme A ligase gene. PhD dissertation, Oregon State University, Corvallis, OR.

Voelker SL, Lachenbruch B, Meinzer FC, *et al*. (2010) Antisense down-regulation of 4CL expression alters lignification, tree growth, and saccharification potential of field-grown poplar. *Plant Physiology*, **154**, 874-886.

Wang HZ, Xue YX, Chen YJ, *et al*. (2012) Lignin modification improves the biofuel production potential in transgenic *Populus tomentosa*. *Industrial Crops and Products*, **37**, 170-177.

Weng JK, Chapple C (2010) The origin and evolution of lignin biosynthesis. *New Phytologist*, **187**, 273-285.

CHAPTER 6

Summary

The climate system on Earth is changing. Evidence of climate change surrounds us – air temperatures and ocean heat content are increasing, the extent of snow and ice is decreasing, sea levels are rising, and extreme climate events (e.g. heavy precipitation events, drought) are more frequent. Temperature in the eastern United States is expected to increase by 2–6 °C by 2100 and drought is projected to become more frequent and severe, yet it is uncertain how terrestrial ecosystems will respond to these climate changes. There are many challenges that our society will face in the coming decades as the climate on Earth changes and world population continues to grow. Conserving biodiversity, increasing carbon sequestration, protecting freshwater stores, and providing energy for 10 billion people are problems that require global solutions. The first step in finding solutions is to improve our understanding of species responses to predicted climate changes. This dissertation uses a physiological approach to analyze plant species responses to increased temperature and drought in North Carolina.

Experimental manipulation of natural ecosystems is arguably the best method for testing how species will respond to the novel climate conditions predicted over the coming century. Field-based warming studies allow us to project plant responses forward to

temperatures for which historical observations offer no comparison. I utilized an experimental warming site in the understory of a temperate oak-hickory forest (Duke Forest, NC, USA) to measure potential effects of climate change on plant phenology, physiology, growth, and reproduction. All large-scale warming manipulations unavoidably alter multiple environmental factors simultaneously, so it is important to realize the limitations of each experimental design. Because open-top chambers were heated at a height of about 50 cm, the forest understory was decoupled from the overstory canopy in our experiment. Chamber structures reduced total irradiance, increased wind, and excluded large herbivores (e.g. deer), although chamberless control plots were present to account for these unintentional effects on plant responses to warming. Mean air temperature inside large open-top chambers was increased by 1.6–5.3 °C above ambient, but heating was uneven throughout the entire width of the chambers. It was necessary to avoid sampling plants near the edge of the chamber, which were not heated above ambient temperatures in some cases. Soil temperature was increased by up to 3 °C at 2-cm depth and 1 °C at 6-cm depth in the warmest chambers (L. Nichols, North Carolina State University, 9 October 2013). Because we did not manipulate water vapor or relative humidity inside the chambers, the heating treatment increased atmospheric vapor pressure deficit (VPD) inside the chambers by 0.16–0.96 kPa. There was no effect of heating on soil water content, which is a distinct advantage for our experiment. Other active (e.g. above-canopy heaters) and passive (e.g. open-top chambers with no active heating) warming experiments reduce soil moisture, which can confound plant responses to warming.

Increasing temperature will have a large impact on the vegetative phenology, reproductive phenology, and biodiversity of temperate forest ecosystems in the future. I measured the effect of experimental warming on the timing of budburst, leaf coloring, flowering, and fruiting in 2011 and compared phenological responses to the colder year 2013. Warming advanced budburst by 5–15 days in four deciduous tree (*Acer rubrum*, *Carya tomentosa*, *Quercus alba*, *Quercus rubra*) and two shrub species (*Vaccinium pallidum*, *Vaccinium stamineum*), while leaf coloring was delayed by 14–20 days in autumn. Warming extended the growing season of the four tree species by 20–28 days. Advances in budburst of diffuse-porous trees were larger than shifts in ring-porous trees, possibly due to more conservative safety mechanisms in ring-porous species for prevention of damage by late-spring frosts. Experimental warming underpredicted advancement in mean budburst by 4-fold relative to interannual temperature variability. I found nonlinear responses of budburst phenology to warming over 2.5 °C and budburst of all species failed to fully track warmer temperatures, however, suggesting that high rates of phenological change observed in the past are unsustainable and will decrease with warming throughout the coming century.

Warming advanced flowering by 6–25 days in three species (*V. stamineum*, *Hieracium venosum*, *Chimaphila maculata*) and delayed reproduction of *Tipularia discolor* by 10 days, but had no effect on three species (*Thalictrum thalictroides*, *Hexastylis arifolia*, *V. pallidum*) that flower in early spring. Chilling or photoperiod requirements likely restrict warming-induced shifts in flowering time in the non-responsive species. Warming of 2 °C resulted in reproductive failure in *C. maculata* when mean May temperature exceeded 21 °C and in *T. discolor* when mean July temperature exceeded 29 °C, suggesting temperature

thresholds that could severely limit the distribution of these species in the future. There were no warming-induced changes in species abundances or community diversity after three years of warming, but these ecosystem-level processes may require longer time periods before any change can be detected.

Winter temperature in the eastern United States has been increasing nearly twice as fast as the annual average, but studies of warming effects on plants have focused on species that are photosynthetically active in summer. The terrestrial orchid *Tipularia discolor* is leafless in summer and acquires carbon primarily in winter. Like many plant species, the optimum temperature for photosynthesis in *T. discolor* is higher than the maximum temperature throughout most of its growing season, and therefore growth should increase with warming. Contrary to my hypothesis, experimental warming negatively affected growth (change in leaf area from 2010 to 2012) and reproductive fitness (number of flowering stalks, flowers, fruits) in *T. discolor*. A warming of 4.4 °C resulted in nearly 60% less growth than under ambient conditions, but is likely due to experimental changes to VPD and not temperature. As a consequence of heating, mean VPD was higher in the chambers, ranging from 0.18–0.53 kPa above controls. Leaf-to-air VPD (D_L) over 1.3 kPa restricted stomatal conductance (g_s) of *T. discolor* to 10–40% of maximum conductance. These results highlight the need to account for changes in VPD when estimating temperature responses of plant species under future warming scenarios.

I investigated the effect of experimental warming of 1.6–5.3 °C and increased vapor pressure deficit (D) of 0.16–0.96 kPa on the growth and physiology of small tree seedlings in the temperate forest understory (Duke Forest, North Carolina, USA). Miniature sap flow

gauges were used to measure transpiration rates (J) of four common deciduous species (*A. rubrum*, *C. tomentosa*, *Q. alba*, *Q. rubra*) throughout the growing season, and these sap flow measurements were then used to estimate seasonal changes in stomatal conductance (g_s) of each seedling. Experimental warming for 3 years increased growth in *C. tomentosa* and *Q. alba* but not the other two tree species. Results suggest that growth of *A. rubrum* and *Q. rubra* was negatively affected by atmospheric drying and decreased annual precipitation over the study period. Plant stomata acclimated to local changes in D_L over time and across the experimental treatment, indicating that stomatal responses to D_L are dynamic within a species or even individual plant. Acclimation of stomata to the experimental treatment resulted in warming-induced increases in g_s and stomatal sensitivity of *Q. alba*. It was unclear if future warming and elevated VPD will increase g_s in the other three species, due to the confounding of temperature and D_L in this experiment. Warming and increased VPD significantly decreased midday leaf water potential while increasing midday transpiration and daily water use, indicating that future climate change will increase the potential for temperature-induced drought stress. Differences among species indicate that the diffuse-porous *A. rubrum* had greater stomatal sensitivity and maintained higher leaf water potential, even under high VPD and drought, than the ring-porous species. Carbon gain in *A. rubrum* will be the most negatively affected by warming and increased evaporative demand in the future, if climate changes occur in the same direction as the experimental manipulation here.

Concerns over energy security and climate forcing from fossil fuel emissions have stimulated interest in development of high-yielding, low-lignin trees for bioenergy. Black cottonwood (*Populus trichocarpa*) has been targeted as a potential bioenergy species due to

its high productivity, but it is not known how transgenically altered lignin biosynthesis will affect water relations. I investigated the physiology of trees growing in short rotation woody cropping systems at two sites in southeastern USA; a mountain site more favorable for growth of *P. trichocarpa*, and a hotter piedmont site that experienced frequent water stress. Maximum productivity was found at the cooler mountain site and resulted from high rates of photosynthesis (20.3 μmol CO_2 m^{-2} s^{-1}) and stomatal conductance (422.4 mmol H_2O m^{-2} s^{-1}). The two low-lignin genotypes had significantly lower mean leaf water potential, stomatal conductance, transpiration, hydraulic conductivity, and leaf-specific whole-plant hydraulic conductance than the wild-type control. The water transport capacity of vascular tissues in transgenic genotypes was severely impaired, which was particularly evident at the top of stems. Productivity was positively correlated to stem lignin content at the piedmont site, and stunted growth of low-lignin trees was caused by (1) stomatal restriction of carbon gain due to water stress and (2) decreased biophysical and biochemical photosynthetic processes. Although there was no difference in lignin among genotypes after 3 years of growth at the mountain site, the transformation resulted in an alternative advantage for potential use in bioenergy systems – lower water consumption. Higher intrinsic water use efficiency of transgenic trees resulted in total water savings of roughly 1 kg H_2O $tree^{-1}$ day^{-1} without sacrificing productivity. Our findings indicate that effects of genetic transformation on field-grown trees are site-specific and highlight the need for a better understanding of the interaction between transgenic alteration of lignin biosynthesis and environmental conditions on whole-plant function.